1976

A review of thermoelectric materials used in radioisotope thermoelectric generators.

Vogt, John F.

Pennsylvania State University

A REVIEW OF THERMOELECTRIC MATERIALS USED IN RADIOISOTOPE THERMOELECTRIC GENERATORS

1976

JOHN F. VOGT

The Pennsylvania State University

The Graduate School

Department of Nuclear Engineering

A Review of Thermoelectric Materials Used In Radioisotope Thermoelectric Generators

A Paper in

Nuclear Engineering

by

John F. Vogt

Submitted in Partial Fulfillment
of the Requirements
for the Degree of

Master of Engineering

November 1976

ACKNOWLEDGMENTS

The author wishes to express his sincere appreciation to Dr. S. J. Fonash, without whose guidance and understanding, completion of this paper would not have been possible. Special credit also due Dr. E. S. Kenney who spent considerable time in reviewing this work and making suggestions which led to notable improvements.

The author also wishes to thank Dr. V. Raag of Syncal Corporation, Mr. N. B. Elsner of General Atomic Company, Mr. D. Peterson of Global Thermoelectric Power Systems, Ltd., and Mr. R. Hannah of Teledyne Isotopes, Inc., for their invaluable assistance in providing current thermoelectric property data and the time they spent in answering many questions.

Finally, the author wishes to express his deepest gratitude to Mr. Victor F. Vogt, without whose influence and encouragement none of this would have been possible.

TABLE OF CONTENTS

TABLE OF CONTENTS (cont.)

LIST OF TABLES

LIST OF FIGURES

LIST OF FIGURES (cont.)

CHAPTER 1

INTRODUCTION

1.1 Radioisotope Thermoelectric Generators

Atomic energy usually calls to mind large concrete-domed nuclear reactors capable of generating hundreds of megawatts of electrical power for the utility industry. In just the last 20 years, however, the atom has been put to much more modest use in a type of electrical power source known as a radioisotope thermoelectric generator (RTG). These devices typically generate a relatively small amount of power--from fractions of a watt to several hundred watts. In this power range, these devices have an interesting and unique advantage over other power sources: they can be designed to operate continuously for periods of time in excess of 10 years without surveillance or an external energy source. Thus there is no need for such things as sunlight, fossil fuels, or air.

A radioisotope thermoelectric generator consists basically of five components: an encapsulated radioisotope heat source, thermal insulation, electrically interconnected thermocouples, a power conditioning device, and a biological radiation shield. The physical arrangement of these components is illustrated in Figure 1.1. Thermal energy generated within the heat source by decay particles colliding with the isotope material is converted into low-voltage DC electrical power by the thermocouples. Thermal losses are reduced by employing insulation to channel the heat flow through the thermoelements. Radiation originating in the heat source from the radioactive decay process often requires the provision of a biological shield (not shown) for personnel protection

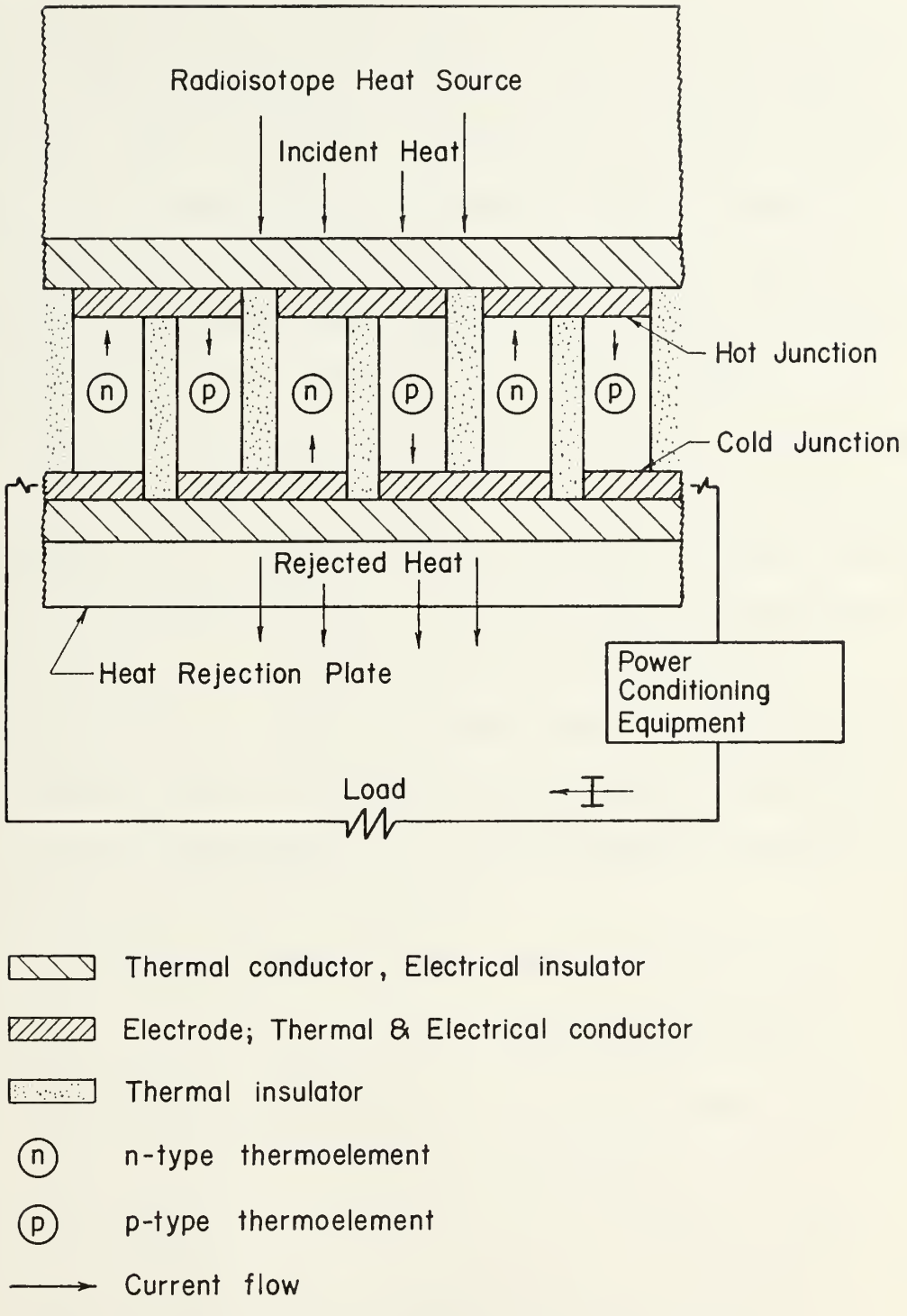

Figure 1.1 Simplified Representation of a Radioisotope Thermoelectric Generator

and power conditioning equipment is normally employed to transform the low voltage produced by the thermoelectric module to a higher potential.

The principal radioisotope fuels used in RTGs are Strontium-90 and Plutonium-238. Both have half-lives sufficient to provide an operating capability of 10 years; however, differences in their radiation and cost result in significant differences in their application. Plutonium-238 has been used extensively in space applications because of its minimum shielding requirements and consequent light generator weight. Strontium-90 is used in terrestrial applications even though heavy shielding is required due to bremsstrahlung production because it can be obtained more economically. Because of its long half-life and radiation characteristics, Plutonium-238 is also used in such biomedical applications as the miniature nuclear batteries used in heart pacemakers.

The thermoelectric elements of an RTG convert the incident heat to useable electrical power. Many different materials have been investigated for use as thermoelements, but only four classes of semiconductor materials have been extensively employed.

1. Bismuth telluride alloys: p-type Bi_2Te_3/Sb_2Te_3
   n-type Bi_2Te_3/Bi_2Se_3
2. Lead telluride alloys: p-type PbTe/SnTe
   n-type PbTe
3. TAGS-85: p-type $(AgSbTe_2)_{.15}/(GeTe)_{.85}$
4. Silicon germanium alloys: n and p-type Si/Ge

Each material has an optimum temperature range over which it should be employed. This can be seen from Figure 1.2 where a material

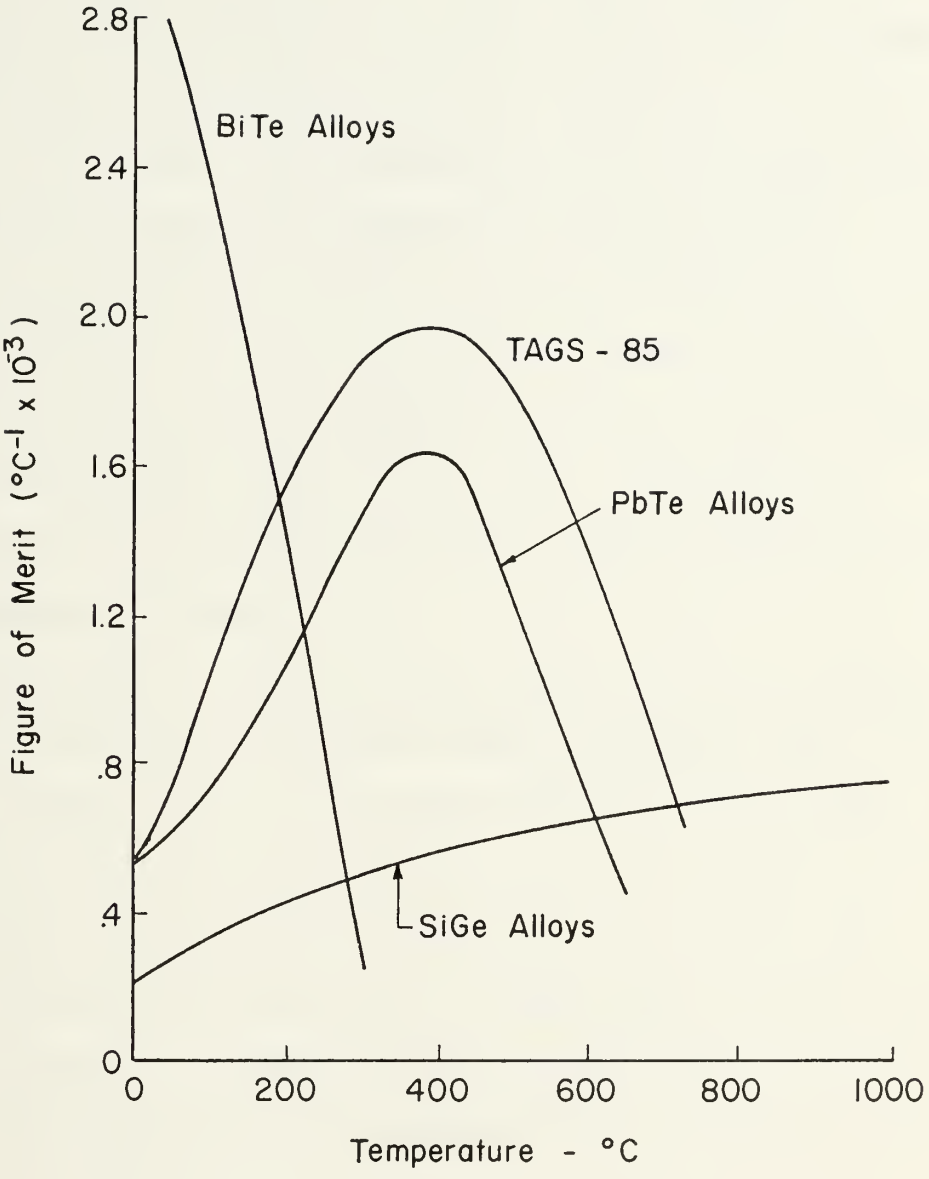

Figure 1.2 A Representative Plot of the Figures of Merit of Commonly Used Thermoelectric Materials

performance parameter called the figure of merit is plotted against temperature for each of the above groups of alloys. Generally speaking, the higher the figure of merit of its thermoelectric materials, the higher the conversion efficiency of an RTG. The plots shown in Figure 1.2 are typical of the behavior of alloys in each group. It can be seen that in low power (~500 mw) applications where the required temperature difference across each thermoelement is small and the hot junction temperature is on the order of 250°C, bismuth telluride alloys result in the best performance. On the other hand, for higher power applications (~100 w) when the hot junction temperature could be as great as 1000°C, silicon germanium alloys give the best results. The importance of proper thermoelectric materials selection in achieving maximum generator performance is evident.

Many advantages can accrue through the use of RTGs over conventional power generating devices when special requirements arise. RTGs provide reliable, long term, unattended operation ideal for remote or inaccessible areas such as outer or dark space, the ocean floor, arctic regions, and the interior of the human body. Their use frees the designer from the worry of limitations normally imposed by such factors as the geographical constraints on commercial power lines, the limited life of chemical batteries, or the availability of sunlight for photovoltaics.

Radioisotope thermoelectric generators have proven ideal for many applications[1,2,3,4]. The SNAP (Systems for Nuclear Auxiliary Power) series of converters is being used extensively to power navigational and weather satellites, deep space probes such as the Viking lander which recently touched down on Mars, and scientific investigating

equipment such as the Apollo Lunar Surface Experiment Package which remained on the moon. Terrestrial applications such as remote weather facilities in the arctic region or isolated microwave repeater stations also are well suited to the maintenance free RTG. Navigational buoys and meterological or oceanographic data collections systems are presently powered by RTGs as well. Radioisotope thermoelectric generators are also being used in implantable devices such as pacemakers and artificial organs that either assist or take over involuntary biological functions. The point is clear--RTGs are and will continue to be used in applications where conventional power generating devices cannot be employed or are impractical.

1.2 Purpose and Scope of the Paper

The purpose of this paper is to review current thermoelectric materials technology relevant to RTGs and to provide a compendium of previously published data on the thermoelectric properties of thermoelement materials in major use today.

Chapters 2 and 3 are devoted to providing a qualitative understanding of the basic physics involved in thermoelectricity and thermoelectric materials selection and to provide the reader with an appreciation of the developments which have led to the present materials technology.

Chapter 4 covers the advantages and disadvantages of each material in major use today. Specifically, problems associated with the fabrication of thermoelectric materials and contacting them to their electrodes will be discussed. After each material is reviewed,

graphical data is presented on its thermoelectric properties for use in RTG design.

CHAPTER 2

THERMOELECTRIC MATERIALS SELECTION BASIC CONSIDERATIONS

2.1 An Introduction to Thermoelectric Effects

2.1.1 Historical Notes

In 1821, Thomas Johann Seebeck noted the deflection of a magnetic needle in the vicinity of a circuit composed of two dissimilar materials in which their junctions were held at different temperatures[5]. Although he did not interpret his observation correctly, Seebeck is generally credited with the discovery of the thermoelectric effect bearing his name in which a voltage is produced across a material in which a temperature gradient is present. Thirteen years later, Peltier found that the passage of current across the junction of two dissimilar materials results in the absorption or generation of heat at the junction[6]. Like Seebeck, Peltier failed to correctly interpret his findings, thinking only that Ohm's Law may not be followed by weak currents. It was several years later that Lord Kelvin (William Thomson) derived a relationship between the two effects based on thermodynamic argument and predicted the existence of a third thermoelectric phenomenon, the Thomson Effect[7]. This effect is characterized by the absorption or generation of heat in a homogeneous conductor where current is flowing in the presence of a temperature gradient.

Even though Lord Kelvin had established the theoretical foundations of thermoelectricity by relating the three effects in terms of thermodynamic principles, it was Altenkirch in the early 1900's who developed the basic theory of thermoelectric power generation and

cooling[8]. His work indicated that materials used in the construction of thermoelements must have high Seebeck coefficients, high electrical conductivities, and low thermal conductivities. It will be seen later that the figure of merit, introduced in Chapter 1, is a combination of these properties. Materials of such quality, however, were not available in Altenkirch's time. It was only with the advent and wide scale use of semiconductors nearly 50 years later that materials with outstanding thermoelectric potential finally became available. It was in the fifties, therefore, that thermoelectricity essentially underwent a rebirth, as manifested by extensive materials research and device development work.

2.1.2 The Seebeck Effect

Consider Figure 2.1, which can be thought of as a portion of one of the thermoelements depicted in Figure 1.1. Here, for illustrative purposes, the material is taken to be a p-type semiconductor and $\Delta T > 0$. Heat flows from left to right in the material via lattice vibrations and the movement of holes, the latter process being driven by the hole flux gradient present in the material. Since the device is open circuited, the flow of holes from left to right cannot continue indefinitely or, in other words, a net current flow cannot be established. What happens is that holes move left to right, driven by the thermal gradient, until a sufficient positive charge builds up at the right end to create an opposing electric field. At this point, the combined actions of the electric field and thermal gradient establish a dynamic equilibrium in which further movement of holes in one direction is offset by movement in the opposite direction. Thus an open circuit

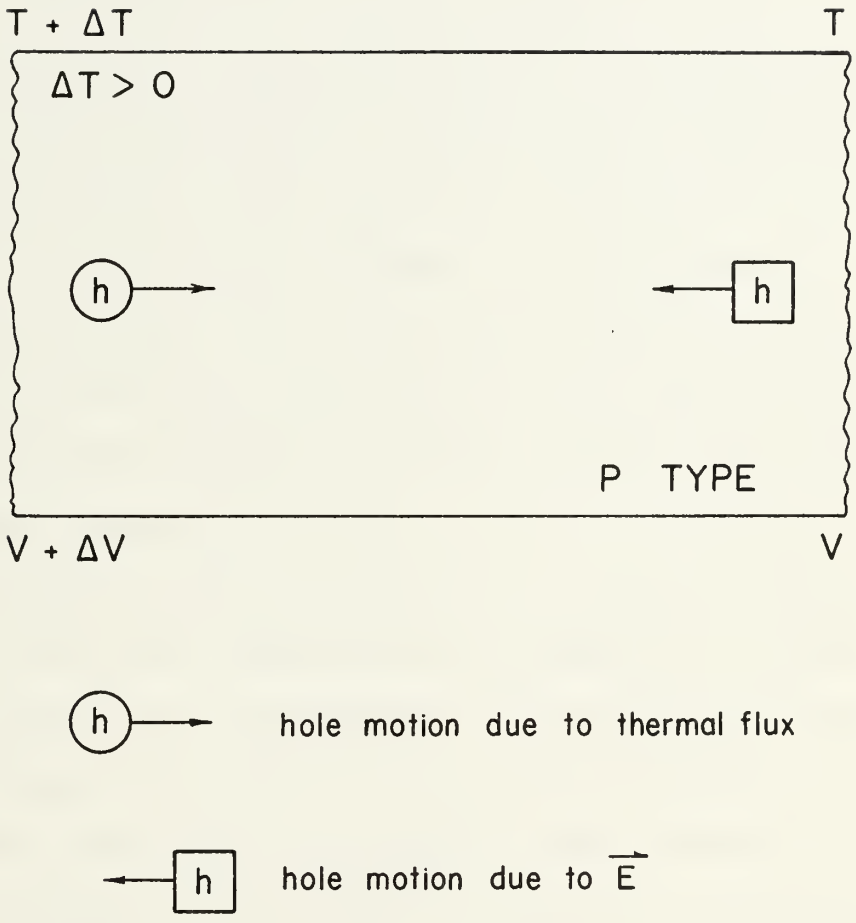

Figure 2.1 The Movement of Charge Carriers in p-type Material when a Temperature Gradient Exists

voltage difference ΔV is established known as the Seebeck potential. This voltage is related to the temperature difference ΔT by the temperature averaged Seebeck coefficient of the p-type semiconductor $\bar{\alpha}_p$:

$$\Delta V = -\bar{\alpha}_p \Delta T \quad * \qquad (2\text{-}1)$$

From examining Figure 2.1, it is obvious that $\Delta V < 0$ and since by convention, $\alpha > 0$ for p-type materials, a negative sign is required in Eq. 2-1 to account for the differing senses of the voltage and temperature gradients. If the material had been a n-type semiconductor or metal where the majority charge carriers are electrons, the situation would be reversed and $\bar{\alpha}_n$ would have to be less than zero in order for the convention established by Figure 2.1 and the relationship expressed in Eq. 2-1 to remain consistent.

When an external circuit is established by connecting the device to a load, a net current will flow as long as the temperature difference is maintained. Hence it is the combined heat and current carrying capabilities of the charge carriers which allow the device to operate. As will be shown later in this chapter, one strives to find a material to use as a thermoelement whose electronic thermal conductivity is large relative

* The precise relationship is $dV = -\alpha(T)\, dT$. This is mentioned here to point out that $\alpha = \alpha(T)$. Since properly averaged values of thermoelectric properties are used in practical calculations, this paper will follow the same practice. Heikes and Ure[9] suggest for $\bar{x} = \bar{\alpha}$ or $\bar{k}$:

$$\bar{x} = \frac{1}{\Delta T} \int_{T_C}^{T_H} x(T)dT \; ; \quad \text{and for } \bar{\rho}: \quad \bar{\rho} = \frac{1}{\bar{k}\Delta T} \int_{T_C}^{T_H} \rho(T)k(T)dT$$

where ρ and k are the electrical resistivity and thermal conductivity, respectively.

to its lattice thermal conductivity. This is because the more charge carriers involved in transporting heat, the higher the Seebeck potential, and the greater the amount of energy delivered to the load rather than through the material's lattice to the heat sink where it would be rejected as waste. Note also that the electrical conductivity of the thermoelectric material should be as high as possible since the more electrical energy is dissipated in the thermoelements, the less power is delivered to the load.

To conclude discussion of the Seebeck Effect, the Seebeck coefficient of a thermocouple such as that illustrated in Figure 2.2 will be defined. When n and p-type thermoelements are placed in series as shown, the voltages established across each due to the temperature difference $T_H - T_C$ are additives since their Seebeck potentials are of opposite polarity. The voltage developed by the couple, V_{AB}, can then be found by adding the contributions of each element:

$$V_{AB} = V_{AC} + V_{CB} = V_{AC} - V_{BC}$$

$$= [-\bar{\alpha}_p (T_C - T_H)] - [-\bar{\alpha}_n (T_C - T_H)]$$

$$= [\bar{\alpha}_p (T_H - T_C)] - [\bar{\alpha}_n (T_H - T_C)]$$

$$= (\bar{\alpha}_p - \bar{\alpha}_n) \Delta T$$

The quantity $(\bar{\alpha}_p - \bar{\alpha}_n)$ is the temperature averaged Seebeck coefficient of a thermocouple consisting of n and p-type thermoelements and hereafter will be designated $\bar{\alpha}_c$. Note that since $\bar{\alpha}_n < 0$, $\bar{\alpha}_c = |\bar{\alpha}_p| + |\bar{\alpha}_n|$.

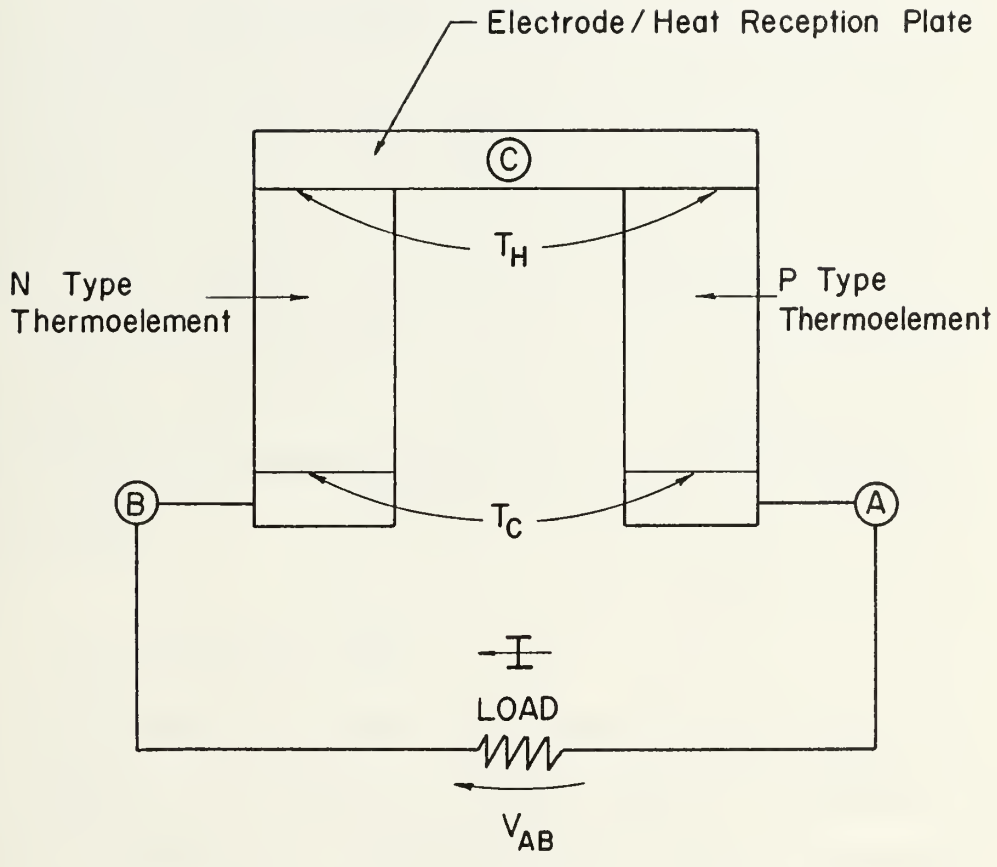

Figure 2.2 A Simple Thermocouple and the Flow of Electrical Energy

Up to this point then, it has been shown that a temperature difference across a thermocouple establishes a voltage difference due to the Seebeck Effect and this potential difference can do useful work when an external circuit is connected.

2.1.3 The Peltier and Thomson Effects

The preceding explanation of the Seebeck Effect and what was gained in discussing the desirable magnitudes of the electrical and thermal conductivities is all the introduction required to begin analyzing the question of what properties one would like a thermoelectric material to have. However, for completeness and because the terms will arise in ensuing sections of this paper, a more detailed explanation of the Peltier and Thomson Effects than was given in Section 2.1.1 will be presented here.

2.1.3.1 Peltier Effect

The current flow across the various interfaces between dissimilar materials in the circuit depicted in Figure 1.1 results in heat liberation or absorption at the junctions as a result of the Peltier Effect. Basically the effect arises because charge carriers approaching the junction in one material are forced into different energy levels in the other material after traversing the junction. As such, energy is either transferred to or taken from the lattice by the charge carriers resulting in heat being generated or absorbed.

For example, if current is flowing from material A to material B as shown in Figure 2.3, the rate at which heat is liberated ($Q_P < 0$) or absorbed ($Q_P > 0$) at the junction is related to the current, I, the

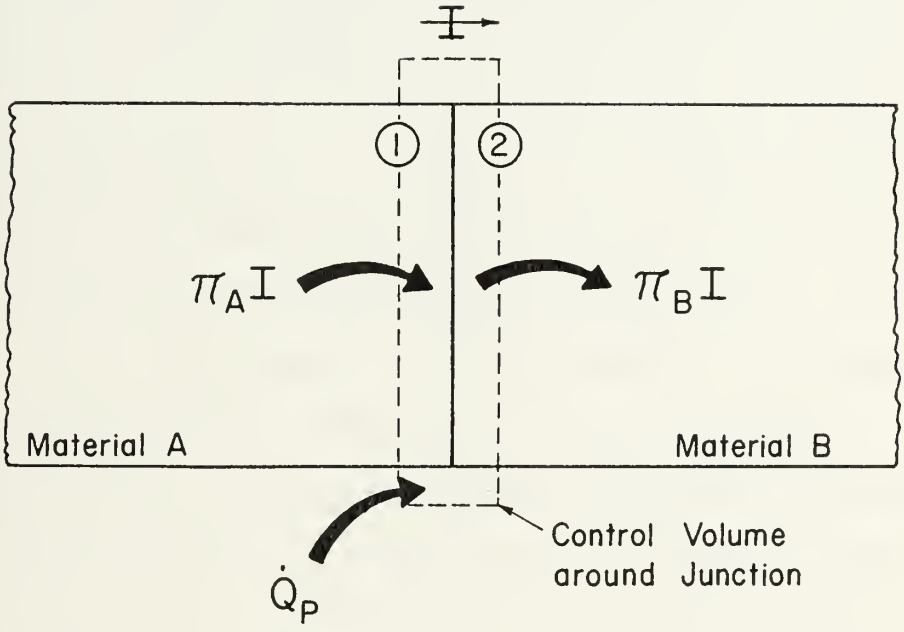

$V_{(1)} = V_{(2)}$ (Assume Ideal Contact)

$T_{(1)} = T_{(2)}$

$\dot{Q}_P > 0 \longrightarrow$ Heat Flow into Control Volume

Figure 2.3 Schematic Representation of the Peltier Effect

Peltier coefficient of material A, π_A, and that of material B, π_B, by the following expression:

$$\dot{Q}_P = (\pi_B - \pi_A)\, I \qquad (2\text{-}2)$$

The coefficients π_A and π_B, like the Seebeck coefficient are functions of temperature and therefore, in Eq. 2.2 they must be evaluated at the temperature of the junction. For p-type materials, $\pi_p > 0$ and for n-type materials and metals, $\pi_n < 0$. The units of π are given as (watts/amp) normally and from a dimensional analysis one can see that π is an indication of the amount of energy each charge carrier possesses. Specifically, π is the average amount of energy possessed by the charge carrier relative to the materials' Fermi Level at a given temperature.

Whether heat is liberated or absorbed at a junction between dissimilar materials depends upon the materials' polarities and the direction the current is flowing. For the thermocouples shown in Figure 1.1, Peltier heat is absorbed at the hot junction at the rate of $(\pi_c)_{T=T_H} I$ and liberated at the cold junction at the rate $(\pi_c)_{T=T_C} I$ where π_c, the Peltier coefficient of the couple, is defined as $|\pi_p| + |\pi_n|$.

2.1.3.2 Thomson Effect

An established axial temperature gradient in a conductor (say one leg of a thermocouple shown in Figure 1.1) which has a current flowing through it, gives rise to heat generation or absorption exclusive of that due to Joule heating. This phenomenon, known as the Thomson Effect, is a bulk solid state occurrence which is caused by

the charge carriers adjusting their energies in the material as they flow along a temperature gradient. As they are forced to acquire different energies due to the changing temperature, they gain energy from the materials lattice or lose energy to it, and this results in heat absorption or generation. The total amount of heat thus liberated or absorbed is called the Thomson heat. Whether heat is liberated or absorbed depends on the relative direction of current flow and the temperature gradient present. For the thermocouple depicted in Figure 2.2, the rate at which the Thomson heat is generated in the thermoelements can be expressed as

$$\dot{Q}_T = \bar{\mu}_c \, I \, \Delta T \tag{2-3}$$

Here $\bar{\mu}_c$ is the temperature averaged Thomson coefficient of the couple, given by $\bar{\mu}_c = \bar{\tau}_p - \bar{\tau}_n$ where τ_p and τ_n are the Thomson coefficients of the p and n-type legs, respectively. The definition of τ for both thermoelements is $\tau_i = T \, d\alpha_i/dT$ where the subscript i pertains either to the n or p-type thermoelement.

2.2 Radioisotope Thermoelectric Generator Performance

2.2.1 Maximum Thermal Efficiency

In attempting to make practical use of radioisotopic thermoelectric power generation, a quantity of great interest is the conversion efficiency for a given temperature difference between the heat source and sink. A derivation of thermocouple efficiency will be outlined in this section as a means of showing its dependency on an important thermoelectric material performance parameter called the figure of

merit. The simplifications discussed below, upon which the derivation is based, are the standard assumptions made[10] and will result in a more direct introduction to the figure of merit concept. None have an important bearing on the conclusion to be drawn regarding the figure of merit and its effect on the device efficiency.

As stated in Chapter 1, radioisotope thermoelectric generators consist of electrically interconnected thermocouples arranged around an isotope heat source.

The first simplification made is to assume that our generator consists of one thermocouple only, as schematically depicted in Figure 2.2. Secondly, the contribution of junctions, the electrode/heat reception plate, and lead wires, to the electrical resistance of the circuit consisting of the thermocouple and external load, will be ignored. Further, it will be assumed that the temperature gradients associated with the thermocouple are wholly axial, that the thermal insulation is a perfect insulator, and that the heat exchanger members at the extremities of the thermocouple possess infinite thermal conductivities. Finally, the Thomson heat generated in the thermoelements will be neglected as the error introduced is only of the order of a few percent at most[11]. Because of the above assumptions, it is clear that the expression for efficiency which will be developed is idealized but, as stated earlier, this will not have any bearing on our conclusion regarding the pertinence of the material figure of merit and its relationship to the device efficiency.

The fundamental expression defining the efficiency of a thermocouple can be expressed as

$$\eta = \frac{V_L I}{\dot{Q}_{in}} \tag{2-4}$$

Here, $V_L I$ is the power delivered to the load and $\dot{Q}_{in}$, the rate at which heat is transferred from the radioisotope heat source to the heat reception plate.

Refer to Figure 2.4. The voltage drop across the load can be written in terms of the Seebeck potential, $\bar{\alpha}_c \Delta T$ and I as

$$V_L = (\bar{\alpha}_c \Delta T - I R_s) \tag{2-5}$$

The current I can be expressed as an arbitrary fraction of the short circuit current,

$$I_{sc} = \frac{\bar{\alpha}_c \Delta T}{R_s}$$

by writing

$$I = f I_{sc} = \frac{f \bar{\alpha}_c \Delta T}{R_s} \tag{2-6}$$

where $0 < f < 1$.

This procedure is recommended by S. Fonash[12] since it will allow one to see how material characteristics affect the device's efficiency regardless of where it is operating on its I-V characteristic (Figure 2.5).

To evaluate $\dot{Q}_{in}$, one writes a heat balance at the hot junction. Heat arriving at the junction consists of $\dot{Q}_{in}$ and $1/2\ \dot{Q}_J = I^2 R_s/2$, one half of the Joule heat generated in the thermoelements[11]. Heat leaving the hot junction consists of the Peltier heat absorbed by the

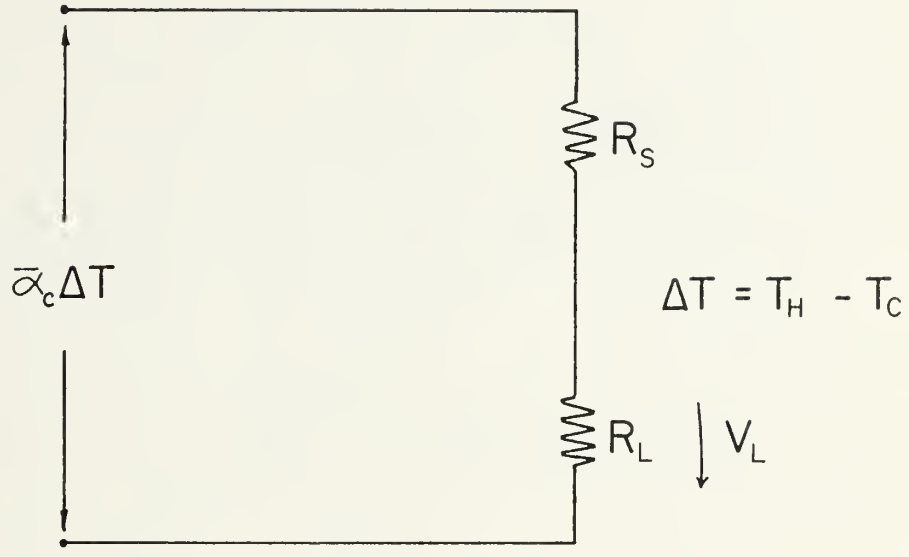

$\bar{\alpha}_c \Delta T$ - Seebeck Potential Developed across Thermocouple

R_S - Electrical Resistance of Thermoelements

R_L - Electrical Resistance of Load

V_L - Voltage Drop Across Load

Figure 2.4 Equivalent Electrical Circuit of Thermocouple Illustrated in Figure 2.2

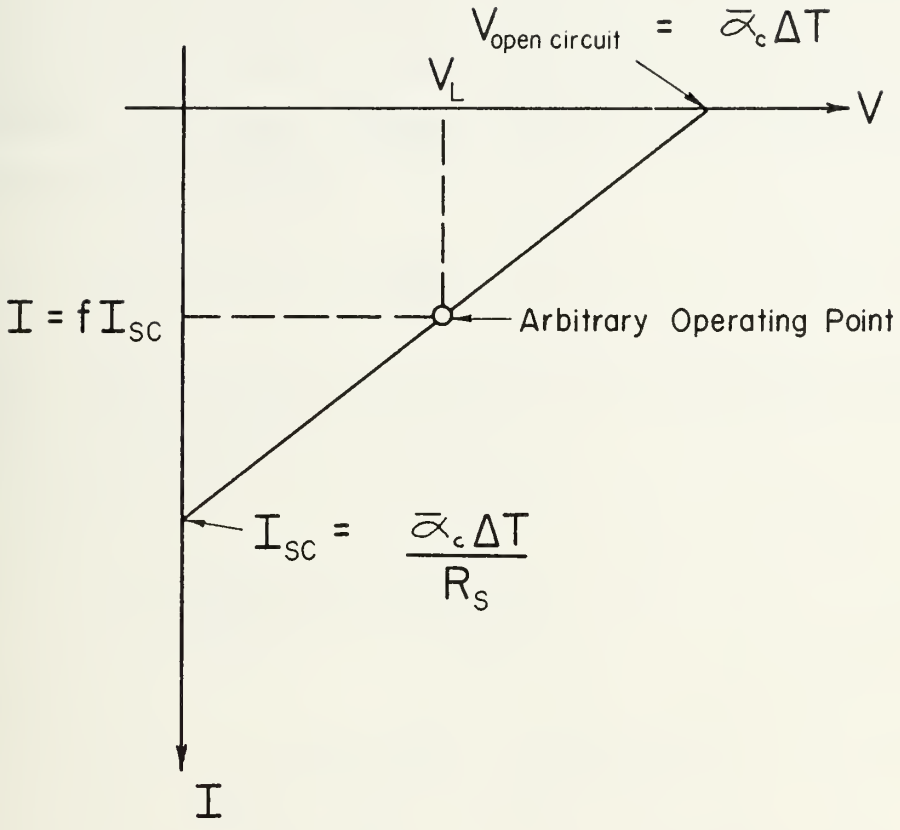

Figure 2.5 Ideal I-V Characteristic of a Thermocouple, Illustrating the Relationship of the Parameter "f" to the Device's Operating Point

charge carriers at that point, $\dot{Q}_P = (\pi_c)_{T=T_H} I \cong \bar{\alpha}_c T_H I$, and the heat transmitted through the thermoelements due to the established temperature difference, $\dot{Q}_K = K \Delta T$. Here, use had been made of Kelvin's second relation, $\pi(T) = \alpha(T) T$, to write $\dot{Q}_P$ in terms of the Seebeck coefficient, $\bar{\alpha}_c$. Also, K is the total thermal conductance of the thermoelements. It follows, therefore, that the rate at which heat enters the thermocouple is given by

$$\dot{Q}_{in} = \dot{Q}_P + \dot{Q}_K - 1/2\dot{Q}_J \tag{2-7}$$

Hence, from equations 2-4 through 2-7 and the expressions developed for $\dot{Q}_P$, $\dot{Q}_K$, and $\dot{Q}_J$, one arrives at:

$$\eta = \frac{\bar{\alpha}_c \Delta T I - I^2 R_s}{\bar{\alpha}_c T_H I + K \Delta T - I^2 R_s/2}$$

or

$$\eta = \frac{\bar{\alpha}_c \Delta T \left(\frac{f \bar{\alpha}_c \Delta T}{R_s}\right) - \left(\frac{f \bar{\alpha}_c \Delta T}{R_s}\right)^2 R_s}{\bar{\alpha}_c T_H \left(\frac{f \bar{\alpha}_c \Delta T}{R_s}\right) + K \Delta T - \left(\frac{f \bar{\alpha}_c \Delta T}{R_s}\right)^2 \frac{R_s}{2}} \tag{2-8}$$

Simplifying, one obtains:

$$\eta = \frac{\Delta T}{T_H} \left\{ \frac{f - f^2}{\left(f - \frac{f^2 \Delta T}{2T_H}\right) + \frac{K R_s}{\bar{\alpha}_c^2 T_H}} \right\} \tag{2-9}$$

where $\bar{\alpha}_c$ is the temperature averaged Seebeck coefficient, K the thermal conductance, and R_s the electrical resistance, all pertaining to the

thermocouple. The latter two quantities are defined by:

$$K = \frac{\bar{k}_n A_n}{\ell_n} + \frac{\bar{k}_p A_p}{\ell_p} \tag{2-10}$$

and

$$R_s = \frac{\bar{\rho}_n \ell_n}{A_n} + \frac{\bar{\rho}_p \ell_p}{A_p} \tag{2-11}$$

where k is the thermal conductivity; ρ, the electrical resistivity; A, the cross-sectional area; and ℓ, the length. The subscripts refer to each thermoelement.

It can be seen from examining Eq. 2-9 that the maximum value of the thermal efficiency is limited to the Carnot efficiency. The expression in the brackets is strongly dependent on the properties of the materials used in each thermoelement due to the term $K R_s/\bar{\alpha}_c^2$, and hence one can begin to see how important materials selection is in achieving maximum RTG performance.

2.2.2 The Figure of Merit of a Thermoelectric Material

At the beginning of the preceding section it was stated that a quantity of prime interest in the practical application of radioisotope thermoelectric power generation was device efficiency. It has been shown that for given source and sink temperatures, regardless of the devices' operating point, its efficiency is strongly materials dependent. It is fair to say, then, that the practical application of RTGs is, to a large degree, dependent on the selection of materials whose properties result in maximizing the bracketed term of Eq. 2-9. Early

investigators recognized this fact and found it convenient to characterize the thermoelectric potential of a material by defining a figure of merit.

Note in Eq. 2-9 that one grouping of variables, $K R_s/\bar{\alpha}_c^2$, contains all the material properties upon which η depends. Assuming all other variables constant, when the inverse of this grouping is maximized, the efficiency is maximized. Hence, a materials figure of merit for the couple, $Z_c = \frac{\bar{\alpha}_c^2}{K R_s}$, can be defined as an indication of the worth of the combined thermoelements. It can be shown that for given thermoelement materials, the lengths and cross-sectional areas of the elements can be chosen to maximize Z_c[11]. After this is done, it is found that:

$$(Z_c)_{\text{optimum geometry}} = \frac{\bar{\alpha}_c^2}{\left[(\bar{\rho}_n \bar{k}_n)^{1/2} + (\bar{\rho}_p \bar{k}_p)^{1/2}\right]^2} \qquad (2\text{-}12)$$

Using the figure of merit of a thermocouple as an indication of the work of a single material is unsatisfactory since, obviously, the couple is composed of two different materials. Hence, the figure of merit of a single material is defined as

$$Z = \frac{\alpha}{\rho k} = \frac{\alpha^2 \sigma}{k} \qquad (2\text{-}13)$$

where α is the materials Seebeck coefficient; σ, its electrical conductivity; and k, its thermal conductivity, all evaluated at the temperature in question. The combination of the figures of merit of individual n and p-type materials into the figure of merit of a thermocouple defined by Eq. 2-12 must make use of the following relationship:

$$(Z_c)_{\text{optimum geometry}} = \left[\frac{Z_n^{1/2} + \beta Z_p^{1/2}}{1 + \beta}\right]^2$$

where

$$\beta = \left[\frac{\bar{\rho}_p \bar{k}_p}{\bar{\rho}_n \bar{k}_n}\right]^{1/2}$$

$$Z_n = \frac{(\bar{\alpha}_n)^2}{\bar{\rho}_n \bar{k}_n}$$

$$Z_p = \frac{(\bar{\alpha}_p)^2}{\bar{\rho}_p \bar{k}_p}$$

Note that if the change in β is small relative to a corresponding change in Z_n and Z_p, maximizing the latter two quantities maximizes $(Z_c)_{\text{optimum geometry}}$, and hence the thermocouple's efficiency. This would be true for any operating point and any temperature range over which the thermocouple may be working. It is conceivable that a situation could exist where maximizing Z_n and Z_p would not maximize $(Z_c)_{\text{optimum geometry}}$ due to the effect of β, so one must be cautious about generalizing on the ultimate results of selecting the highest Z_n and Z_p materials to form a thermocouple. Practically speaking though, the maximum couple efficiency is obtained when Z_n and Z_p are maximized and hence thermoelectric materials research is involved with finding materials that possess large values of Z. Of course, they must also have the mechanical, metallurgical, and thermal characteristics imposed by practical designs and be compatible with the temperature range of operation, but at this point we seek only to identify those with high figures of merit.

2.3 Selecting Materials with Large Z

From the preceding discussion, it is apparent that the suitability of a thermoelectric material is largely determined by its figure of merit. It might have been guessed at this point, in view of the previous analyses based on n and p-type materials, that semiconductors must be the best materials. This is, in fact, the case and this section will explain why. It will also be shown that even among semiconductors, certain conditions must be met to attain high values of Z.

2.3.1 Why Semiconductors?

The figure of merit of a material was defined in Section 2.2.2 as:

$$Z = \frac{\alpha^2 \sigma}{k} \tag{2-13}$$

Obtaining a large value of Z obviously depends on the interrelationship of the variables α, σ, and k. Each of these variables and what they depend upon will be discussed below and by analyzing their dependencies, we will be able to identify those materials most suitable for thermoelectric power generation.

The Seebeck coefficient can be expressed as[13]:

$$\alpha = \pm \frac{k}{e} \left[(5/2 + s) + \ell n \frac{2(2\pi\, m_e k\, T)^{3/2}}{n\, h^3} \right] \tag{2-14}$$

where k is the Boltzman constant; e, the electronic charge; s, a variable dependent upon the scattering mechanisms present in the crystal; m_e, the carrier effective mass; T, the absolute temperature; h, Planck's constant; and n, the carrier concentration in carriers per

unit volume. This relationship is based upon Maxwell-Boltzman statistics and in the strict sense, applies only to nondegenerate semiconductors. Degenerate semiconductors and metals follow Fermi-Dirac statistics and a different expression for α would result. In either case however, Eq. 2-14 correctly illustrates that as the carrier concentration n increases, the Seebeck coefficient decreases and for our present purposes that is sufficient. Note that since the Seebeck coefficient decreases with increasing n, so does Z.

The electrical conductivity of a metal or extrinsic semiconductor is defined as

$$\sigma = n\ e\ \mu \tag{2-15}$$

where μ is the carrier's mobility. The mobility varies with temperature, lattice periodicity, and other material characteristics which effect a charge carrier's mean free path such as grain boundaries. Note in this case as the carrier concentration increases, the conductivity increases and therefore Z increases.

For metals, the thermal conductivity is almost entirely electronic. That is, the vast majority of the heat conducted is via the electrons rather than the lattice structure. From Wright[14], the thermal conductivity is

$$K = \left(\frac{L\ k^2}{e^2}\right)\ \sigma\ T \tag{2-16}$$

where $\frac{L\ k^2}{e^2}$ is the Lorentz member for metals: 2.45×10^{-8} watt-ohm/°K^2. Note that as n increases, σ increases, K increases, and hence Z decreases.

For semiconductors, the thermal conductivity consists of two components:

$$k = k_e + k_L \tag{2-17}$$

The electronic component, k_e, accounts for the heat transported by the charge carriers and hence is a function of n. The lattice component, k_L, accounts for the conductivity of the lattice and is not a function of n but rather various material characteristics which will be discussed in detail later. In section 2.1.2 it was stated that the ratio of the electronic to lattice thermal conductivities should ideally be as large as possible. This was to minimize wasted heat flow. Maximizing the figure of merit further requires that their sum be as small as possible. In most semiconductors, even those heavily doped, the lattice component is much greater than the electronic component[15]. Hence the only way to satisfy both constraints is to make k_L as small as possible.

Sufficient information is available at this point concerning α, σ, and k to determine what class of materials--insulators, semiconductors, metals--is best suited for thermoelectric power devices. Of all the variables upon which these three properties depend, the carrier concentration n is most significant. Its value ranges from near zero (insulator) to $10^{22} cm^{-3}$ or higher (metals) and intermediate magnitudes can be obtained with semiconductors.

No other variable upon which α, σ, or k depends can have such a wide range of values. It makes sense then to consider how $Z = \frac{\alpha^2\sigma}{k}$ varies with n. In Figure 2.6[10], representative curves are plotted for the Seebeck coefficient, electrical conductivity, thermal conductivity, and the resultant figure of merit versus n, the extrinsic carrier

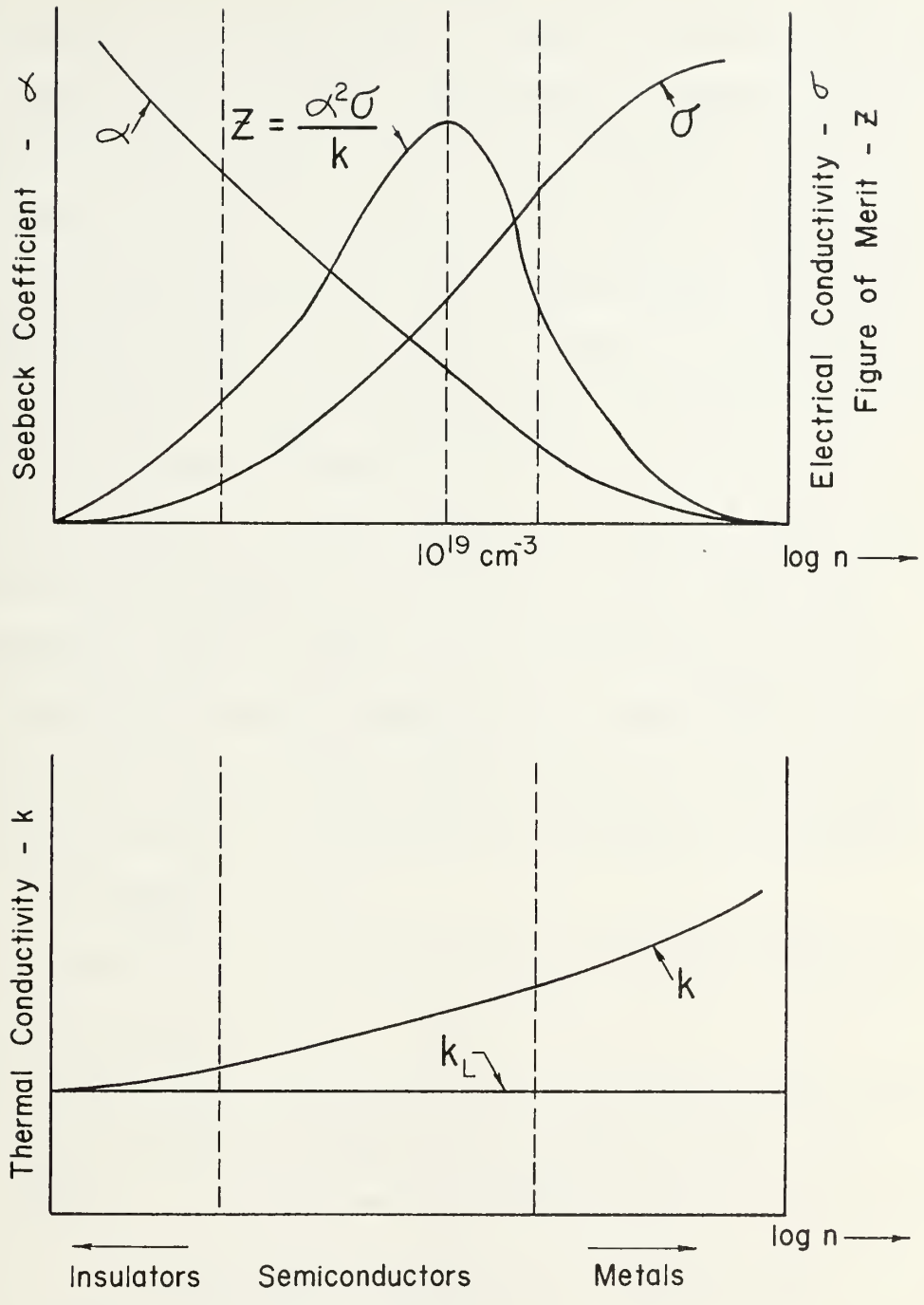

Figure 2.6 A Schematic Representation of How α, σ, k, and Z Vary with the Concentration of Extrinsic Charge Carriers

concentration. Note that neither extremely large nor small values of n are desirable. In the former case, α tends to zero and in the latter case, σ tends to zero. Because of this behavior, a maximum value of Z must occur for some value of n between the two extremes. The value 10^{19} cm^{-3} shown in Figure 2.6 is representative only. The exact value of n which will maximize the value of Z for a given material and temperature depends upon the values of s, m_e, T, μ, and k. It has been found that for the ranges of these variables normally encountered, the optimum value of n lies between 10^{18} and 10^{21} cm^{-3}.[10]

Note that Figure 2.6 has been divided into three sections. In the insulators and metal regions, $n < n_{opt}$ and $n > n_{opt}$, respectively. In the semiconductor region, however, n can be made to have any value desired through proper doping. Therefore, the figure of merit obtainable with insulators and metals will be less than that of optimally doped semiconductors and hence the latter class of materials is the one considered for thermoelectric use.

As an example of the meager performance of metallic thermocouples, consider the following.

A thermocouple with one leg manufactured of bismuth and the other nickel operates between the temperatures of 500°K and 277°K. The average values of α, σ, and k over this temperature range are given as:[2]

	$\bar{\alpha}$(μv/°K)	$\bar{\sigma}$(ohm-cm)$^{-1}$	$\bar{k}$(watt/cm°K)
Bismuth	-75	8.6×10^3	.08
Nickel	-18	1.5×10^5	.87

Assuming the geometry of the thermoelements has been optimized, Z_c is found from Eq. 2-12 to be 1.09×10^{-4}. For the case in which the

thermocouple is delivering maximum power to the load, f = .5, and the efficiency is found from Eq. 2-9 to be .6%. This value is more than an order of magnitude less than that obtained with certain extrinsic semiconductors.

2.3.2 Maximizing the Figure of Merit of Semiconductors

It was shown above that neither metals nor insulators are worthwhile thermoelectric materials when compared with properly doped semiconductors. As stated previously, however, even among semiconductors there are some which have higher values of Z at a given temperature than others. In this section it will be shown why.

Goldsmid[15] has found that in order to maximize the figure of merit of a semiconductor at a given temperature, two things must occur. The carrier concentration n must be optimized to maximize $\alpha^2\sigma$ and the largest possible value of the quantity

$$F = \frac{\mu m_e^{3/2}}{k_L} \tag{2-18}$$

must be obtained.

The existence of an optimum value of n stems from its relationship with the Seebeck coefficient and electrical conductivity. This idea was introduced in the last section to show why metals and insulators are not worthwhile thermoelectric materials. Here we will discuss how the optimum value of the carrier concentration is determined in practice.

As shown previously, when n increases from zero, α decreases and σ increases. The term $\alpha^2\sigma$ thus passes through a maximum as n becomes increasingly large. Since $k \approx k_L$ and $k_L \neq k_L(n)$, $Z = \frac{\alpha^2\sigma}{k}$ also has a

maximum corresponding to some value of n. In principle, given the material and temperature range of interest, values of the doping level (impurities/unit volume) could be calculated which would result in the optimum carrier concentration at every temperature in that range. This would be done by substituting the values of s, μ, m_e, and T into Eqs. 2-14 and 2-15, writing $\alpha^2\sigma = \alpha^2\sigma(n)$ and then $Z = Z(n)$. The optimum carrier concentration for the given temperature would be found from solving $\frac{dz}{dn} = 0$ for n_{opt} and then the required doping level could be calculated. The problem which arises is that since the material operates over a continuous range of temperatures, the doping level must also vary continuously from one end to the other if the material is to contain the optimum number of carriers throughout its length. This, however, in addition to being difficult to accomplish, is of little practical value because between the materials' fabrication and its final use in a device, it is subjected to a variety of time and temperature conditions which tend to modify the concentration of the dopant and therefore upset any previously introduced gradient in the material[13].

Another problem which arises is that the value of s, the scattering "constant" appearing in the expression for α, and the exact dependence of α on n at the high doping levels employed are uncertain[15] and hence, the values of n_{opt} obtained via an analytical optimization procedure would be approximate anyway.

In practice, the best doping level for a given material is determined empirically. First, the approximate upper and lower bounds on n_{opt} are determined analytically by assuming what is necessary and performing the optimization calculations. This gives one an idea of where to begin. Then, by doping different samples of the material to

various concentrations within the calculated range and measuring the thermoelectric properties (α, σ, k) of each sample as a function of temperature, the doping level which results in the largest values of Z over the temperature range of interest is determined.

The fact that $F = \mu m_e^{3/2}/k_L$, the grouping of variables introduced by Eq. 2-18, must be maximized in order to maximize Z, can be seen by comparing Eqs. 2-14 and 2-15 with the definition of Z:

$$Z = \frac{\alpha^2 \sigma}{k} \tag{2-13}$$

Recall that $Z = Z(s, m_e, T, n, \mu, k_L)$. For a given value of F, an increase in s is an obvious advantage but the range over which s can vary is small[15]. Further, the optimum value of n is determined only after a candidate material has been selected. Hence, for a given temperature, F is just a convenient independent parameter of the remaining variables upon which Z depends. Even though μ normally is a function of n and hence one might question the independence of F, Goldsmid[15] has found that in spite of the relatively high electron or hole concentrations in the semiconductors used for thermoelectric applications, the scattering of carriers by ionized impurities is seldom observed.

To maximize F one must locate a semiconductor in which the mobility and effective mass of the charge carriers are high and the lattice thermal conductivity is low. High mobilities are most easily obtained in the intermettalic compounds of medium atomic weight elements, indium antimonide being a good example[16]. On the other hand, low lattice thermal conductivities are found in heavier elements such as bismuth telluride. It might appear that a conflict has arisen, but according

to Wright[17] it has been found empirically by comparing a wide range of semiconductor materials that the product $\mu m_e^{3/2}$, while by no means a constant, shows only an unsystematic and not very large variation compared to k_L. Hence, one must look initially for materials with small lattice thermal conductivity. A rule which, so far, has found widespread application, states that for a group of similar crystals the lattice thermal conductivity decreases with increasing atomic weight (or, for compounds and alloys, mean atomic weight)[18]. The lattice thermal conductivity can also be reduced by introducing into a materials' lattice through alloying, another substance (either element or compound) which crystallizes in a similar lattice and has approximately the same lattice constant. The distortion of the basic lattice by the added substance is then relatively small and is limited to crystal regions in direct contact with the impurity atoms. Such localized distortions reduce k_L, but μ is not significantly affected because lattice periodicity is not greatly altered[16].

In general then, it can be said that among semiconductors those compounds or, better yet, alloys of high mean atomic weight will possess the highest figures of merit and hence are the most suitable materials for thermoelectric power conversion devices.

2.4 Other Considerations in Selecting Thermoelectric Materials

The validity of the figure of merit as a prime indication of the usefulness of a thermoelectric material has been established above. There are, however, other factors which must be considered.

The temperature range over which a thermocouple is designed to operate is extremely important in determining the material to be used.

Consider the behavior of the materials illustrated in Figure 1.2. For applications in which the hot junction temperature is low, say less than 200°C, the bismuth telluride alloys give the best performance. As the hot junction temperature is increased, however, a point is reached where they can no longer be used because of their decreasing figure of merit and another material must be selected. The same thing eventually happens to that material and so on. The thing which limits the useful operating range of a material is the temperature at which its figure of merit begins to decrease and the factor which determines this temperature is known as intrinsic behavior. Intrinsic behavior occurs in extrinsic semiconductors when the temperature is such that the number of minority carriers in the material approaches the number of majority carriers. The smaller the energy gap (the energy required to produce an electron-hole pair) of the material, the lower the temperature at which electron-hole pairs begin to be produced and hence the lower the temperature at which intrinsic behavior has an effect on the properties α, σ, and k. An increasing presence of intrinsically generated carriers reduces the Seebeck coefficient, increases the thermal conductivity, and hence causes the figure of merit to decline[9]. Therefore, the temperature at which intrinsic behavior has the effect of decreasing the figure of merit depends upon the energy gap of the material. We can conclude from this that the temperature range over which a RTG is designed to operate will limit the selection of thermoelectric materials to those with a compatible energy gap. Otherwise, the efficiency of the device will suffer because of an unnecessarily low average value of Z.

Other material factors to be considered are mechanical and metallurgical in nature. Low linear thermal expansion coefficients are desirable to minimize internal stress buildup which could lead to fracturing and large decreases in σ. Furthermore, the materials must be of sufficient strength to be used in a practical design and they must be metallurgically stable so that strength, thermoelectric, and electrical properties do not degrade significantly over time. Brittleness is a problem frequently encountered.

Materials which oxidize readily must be avoided if possible. This is necessary because it is well known that oxides have low electrical conductivities in general, and therefore, through the life of a device, as more oxide is formed, Z decreases and the performance degrades. Chemically stable materials in other respects are required as well.

Finally, sublimation of a thermoelectric material at the hot junction of a device is a frequent problem. In this respect the ability of a material to withstand high temperatures is a definite advantage. Recall also that higher temperatures imply higher Carnot efficiencies and thus even though a material might have lower values of Z over its operating range, if its useable temperature range extends to higher temperatures, its use could result in higher device performance.

2.5 Summary

In this chapter it has been shown that the performance of a radioisotope thermoelectric generator is related to the figure of merit of the materials utilized in its thermoelements. It was concluded that optimally doped semiconductor alloys of high mean atomic weight possess the highest Z of all materials studied to date. Therefore, we would

expect to find that the thermoelectric materials presently used would be compounds or alloys of elements in groups II-B, III-A, IV-A, V-A, and VI-A of the periodic table.

The problem which has been encountered in thermoelectric materials research is that there are numerous elements which can be tried and in most cases, materials consist of at least three--two forming a semiconductor compound or alloy, and a third acting as the dopant. Additionally, the atomic ratio of the constituent elements in a given alloy is variable. This leads to a great many possibilities so that the probability of obtaining the "ideal" material, if there is one, by the trial and error techniques employed is rather remote. As we shall see in the next chapter, many materials have been investigated but no one material has been found which significantly outperforms the rest.

CHAPTER 3

THE EVOLUTION OF PRESENT-DAY THERMOELECTRIC MATERIALS

3.1 Introduction

Obtaining electrical power from heat was one of the first applications of thermoelectricity attempted. The idea was soon abandoned, however, because of the low efficiency metallic thermocouples early scientists were forced to use. Some small devices, however, were constructed. Peltier used a metallic thermocouple as a current source in some of his research and Ohm employed one in the work which led to the law bearing his name. But because of inherently low conversion efficiencies, due basically to their low Seebeck coefficients, metallic thermocouples have only been practically applied in the area of temperature measurement.

With the advent of semiconductors and the practical application of solid state theory in the late 1940's and early 1950's, interest in employing thermoelectric phenomenon for the direct conversion of heat to electricity was revived. Researchers began studying extrinsic semiconductors as potentially high performance materials for thermoelectric power devices since these materials offered the possibility of Seebeck coefficients up to several orders of magnitude greater than those of metals. Even though it was found that conversion efficiencies were only on the order of 10%, this was high enough for applications such as those discussed in Chapter 1.

Between about 1950 and 1965 virtually all thermoelectric materials research was devoted exclusively to finding materials with a high figure

of merit. In Table 3.1 the major results of this work are summarized. For comparison, Table 3.2 lists some properties of common metals and intrinsic semiconductors. Note that in Table 3.1 the materials have been arranged into three groups according to their maximum operating temperature. This temperature is a function of the materials' energy gap and/or melting point and serves as an indication of when intrinsic behavior has caused a significant decrease in the figure of merit or when the material can no longer be safely employed without fear of melting. Note also that the bismuth telluride alloys possess the highest figures of merit. The lead telluride alloys and "TAGS-85" have lower figures of merit and the silicon germanium alloys along with the remainder of the group I materials have the lowest figures of merit of all. The extent of the range of useful operating temperatures, however, is reversed for the three groups. Because the conversion efficiency of a thermocouple can be approximated by $\eta = (1/4)Z_c\Delta T$, it is apparent that the extent of the range of useful operating temperatures is as important to the performance of a thermocouple as is the figure of merit of its thermoelectric materials. It is thus found that the performance available from RTGs using materials from the three groups over their respective temperature ranges is not unduly different[4].

In most RTG designs, the hot junction temperature increases as the required power output increases. Since each group of materials listed in Table 3.1 spans a different range of useful operating temperatures, it follows that each will normally be associated with a certain range of output power. In general, group I materials are employed above about 10 watts, group II materials from about 100 mw to about 50 watts, and group III materials up to about 500 mw. However,

Table 3.1

Selected Properties of Some Thermoelectric Materials

Material	Type	E_g (ev)	α (μv/°C)	σ $(\text{ohm-cm})^{-1}$	k (w/cm-°C)	Z_{max} ($°C^{-1}$)	Temp. (°C)	Max. Oper. Temp. (°C)	Ref.
				Group I					
MnTe(99m/o) NaTe(1m/o)	p	.9	320	44	.012	3.8×10^{-4}	930	1130	9
$CeS_{1.38}$	n	--	250	55	.010	3.96×10^{-4}	1100	1130	19
CeS(+Ba)	n	--	--	--	.01	8×10^{-4}	930	1030	2
Si(63a/o) Ge(37a/o)	n	.94	271	453	.039	8.6×10^{-4}	800	1000	13
Si(80a/o) Ge(20a/o)	n	.98	239	820	.048	9.7×10^{-4}	1000	1000	13
Si(63a/o) Ge(37a/o)	p	.94	260	417	.044	6.5×10^{-4}	810	1000	13
Si(80a/o) Ge(20a/o)	p	.98	283	369	.047	6.3×10^{-4}	870	1000	13
				Group II					
PbTe + PbI_2(.1m/o)	n	.3	149	1200	.021	1.27×10^{-3}	300	630	9
PbTe + Na(1a/o)	p	.3	205	500	.017	1.22×10^{-3}	250	630	9
PbTe(75m/o) SnTe(25m/o)	n	--	195	449	.011	1.6×10^{-3}	610	630	2
PbTe(50m/o) PbSe(50m/o)	n	--	--	--	.018	1.3×10^{-3}	430	630	20
InAs(90m/o) InP(10m/o)	n	.45	181	1333	.059	7.3×10^{-4}	730	830	9

Table 3.1 (cont.)

Material	Type	E_g (ev)	α ($\mu v/°C$)	σ $(ohm\text{-}cm)^{-1}$	k (w/cm-°C)	Z_{max} ($°C^{-1}$)	Temp. (°C)	Max. Oper. Temp. (°C)	Ref.
Sb_2Te_3	p	--	130	2000	.029	1.2×10^{-3}	--	--	15
$AgSbTe_2$	p	.6	242	237	.007	1.9×10^{-3}	375	630	10
GeTe	p	--	157	1667	.045	9.2×10^{-4}	570	730	9
GeTe(95m/o) Bi_2Te_3(5m/o)	p	--	200	807	.019	1.7×10^{-3}	480	630	9
"TAGS": $AgSbTe_2$(15m/o) GeTe(85m/o)	p	--	194	833	.016	1.95×10^{-3}	400	530	21
				Group III					
Zn(34.6a/o) Sb(64.3a/o)-Sn(1a/o) Ag(.1a/o)	p	.6	220	461	.018	1.26×10^{-3}	185	330	9
Bi_2Te_3	n	.15	210	1000	.020	2.3×10^{-3}	27	180	15
Bi_2Te_3	p	.15	190	1000	.020	1.8×10^{-3}	27	180	15
Bi_2Te_3(50m/o) Sb_2Te_3(50m/o)	p	--	183	1333	.015	3.0×10^{-3}	0	250	9
Bi_2Te_3(25m/o) Sb_2Te_3(75m/o)	p	--	210	1000	.013	3.5×10^{-3}	27	250	10
Bi_2Te_3(80m/o) Bi_2Se_3(20m/o)	n	.25	200	914	.015	2.5×10^{-3}	27	300	9
Bi_2Te_3(75m/o) Bi_2Se_3(25m/o)	n	.28	178	868	.013	2.2×10^{-3}	97	300	10

Table 3.1 (cont.)

Notes:

1. The values in columns 4, 5, 6, and 7 pertain to the temperatures given in column 8.

2. The thermoelectric property data given for silicon-germanium alloys is initial. These properties change with time as explained in Chapter 4.

3. Only primary references are given.

Table 3.2[2,9]

Thermoelectric Properties of Some Metals
And Intrinsic Semiconductors

Material	α $\mu v/°C$	σ $(ohm\text{-}cm)^{-1}$	k watt/cm-°C	Z_{max} $°C^{-1}$
Copper	+2.5	5.9×10^{5}	3.96	9.3×10^{-7}
Nickel	-18	1.5×10^{5}	.87	5.6×10^{-5}
Bismuth	-75	8.6×10^{3}	.08	6×10^{-4}
Germanium	200	1000	.636	6.3×10^{-5}
Silicon	200	500	1.133	1.8×10^{-5}
Indium Arsenide	157	2000	.081	4.9×10^{-4}
Indium Antimonide	155	1800	.088	6×10^{-4}

Note: The values of α, σ, and k are those which exist at the temperatures where Z_{max} occurs.

a word of caution is appropriate at this point since design approaches vary. Depending on the design, a higher power output does not necessarily imply a higher hot junction temperature. For example, a 2 kw RTG designed by Westinghouse[22] operates at a hot junction temperature of 541°C and employs PbTe alloys in its thermoelectric module. On the other hand, a 150 watt RTG developed under the Multi-Hundred Watt[23] program operates at a hot junction temperature of 1000°C and employs silicon germanium alloys. Hence, the real key to determining the best materials to employ is the temperature range over which the device is designed to operate. In general though, the relationship between device power output and materials employed which was given above applies to most RTGs constructed to date.

3.2 Historical Data

The modern history of thermoelectric materials research began in 1947 when M. Telkes[24], after making a comprehensive survey of materials available at that time, found that the best p-type material was zinc antimonide, ZnSb. When the compound contained small quantities of tin and silver to increase the mobility and obtain optimum doping, respectively, its maximum figure of merit was found to be about $1.3 \times 10^{-3}/°C$ (Table 3.1). This is some two orders of magnitude larger than that obtained with metals as can be seen by a comparison with the values of Z_{max} given in Table 3.2.

Relying on the knowledge that as the atomic weight of an element or mean atomic weight of a compound increases, k_L decreases, and hence the figure of merit increases, researchers initially studied the semiconductor compounds Bi_2Te_3 and PbTe. Goldsmid and Douglas[25] first

reported on n and p-type Bi_2Te_3 in 1954 and Ioffe[26,27] published several articles on PbTe in the mid 1950's. Another high mean atomic weight compound, Sb_2Te_3, was also investigated in the 1950's by Airapetyants and Efimova[28]. In each case, the figure of merit proved to be significantly larger than that of metals. Note from Tables 3.1 and 3.2, for example, that $Z_{max} = 2.3 \times 10^{-3}/°C$ for n-type Bi_2Te_3, whereas $Z_{max} = 9.3 \times 10^{-7}/°C$ for copper.

The next advance came with the use of alloys of high mean atomic weight semiconductor compounds. Recall from Chapter 2 that the lattice thermal conductivity of a semiconductor material is reduced when alloying the material with another substance whose atoms have a similar valence electron structure but different atomic weights. This observation was initially proposed by Ioffe, et al.[29] and was verified through the investigation in the late 1950's and early 1960's of various solid solutions such as Sb_2Te_3 in Bi_2Te_3, SnTe in PbTe, PbSe in PbTe, and Bi_2Se_3 in Bi_2Te_3. It was found that the lattice thermal conductivity falls, in many materials, until about 50% of one kind of atom is replaced by another. For example, alloys of Bi_2Te_3 and Sb_2Te_3 have minimum values of k_L near 65m/o Sb_2Te_3[18] and alloys containing PbTe and PbSe have minimum k_L near 50m/o PbSe[17]. With foreign atom concentrations of this magnitude, in some cases not only is k_L reduced, but μ changes as well. Hence the alloy composition which minimizes k_L does not necessarily maximize Z and it becomes a matter of selecting that composition which results in the largest value of μ/k_L. Note in Table 3.1 the significant improvement in the figure of merit of Bi_2Te_3 (25m/o)--Sb_2Te_3 (75m/o) over that of p-type Bi_2Te_3. This increase in gained by the reduction of k ($k \cong k_L$). Similar results can be seen to occur for other alloys containing Bi_2Te_3 and PbTe.

Other materials listed in Table 3.1 also exemplify that an increase in Z can be gained through the addition of foreign atoms. The maximum figure of merit of InAs as shown in Table 3.2 is $4.9 \times 10^{-4}/°C$ but when 10% of the arsenic is replaced by phosphorus, Z increases to $7.3 \times 10^{-4}/°C$. Similarly if 5m/o Bi_2Te_3 is alloyed with 95m/o GeTe the figure of merit of GeTe is increased by 85%. And when 15m/o $AgSbTe_2$, which has an extremely low k_L, is alloyed with 85m/o GeTe to produce what is known as "TAGS-85," the figure of merit is increased even further to a value of $1.95 \times 10^{-3}/°C$. Admittedly, the decrease in k_L gained by alloying is not the only factor which is producing higher figures of merit since α and σ are also varying, but the above examples clearly indicate that better thermoelectric materials are obtained by alloying one high mean atomic weight semiconductor compound with another.

In the United States, perhaps the greatest stimulus to the development of radioisotope thermoelectric generators and hence thermoelectric materials, was the need for small, reliable, electrical power supplies in satellites and other spacecraft. In 1956 the old Atomic Energy Commission initiated a plan involving private industry to design and build RTGs for space and terrestrial uses. This plan became known as the SNAP (Systems for Nuclear Auxiliary Power) program. As of 1972, sixteen distince SNAP RTG designs had been developed. Corliss and Harvey[1] present a detailed review of this program up through SNAP-21 in their book, Radioisotopic Power Generation. The main contributions of this program to thermoelectric materials research was in the development of higher Z PbTe alloys, a new class of materials for high

temperature use based on Si/Ge alloys, and a high performance p-type material known as "TAGS-85." The PbTe alloys and "TAGS-85" have already been mentioned, but Si/Ge alloys have yet to be discussed.

As indicated in Table 3.2, silicon and germanium, individually, are of no value for thermoelectric applications because of high thermal conductivities. Alloys of the two elements in the range of 20-40% Ge, however, result in a tremendous decrease in k and a usable, although relatively small value of Z. These alloys are practical in certain applications because their relatively large energy gap of ~.9 ev lends them to high temperature operation (1000°C) and hence the Carnot efficiency obtainable is higher than that using materials from the other two groups. Thus, even though their figures of merit are somewhat smaller, the overall efficiency which results from their use is comparable to that achieved by the other materials.

The thermoelectric materials most widely used in current radioisotope thermoelectric generators are:

1. High Temperature (T_C-1000°C) Applications[30]
   n and p-type Si/Ge alloys
2. Intermediate Temperature (T_C-630°C) Applications[21]
   n-type PbTe
   p-type PbTe/SnTe alloys
   p-type TAGS-85
3. Low Temperature (T_C-330°C) Applications[31]
   p-type Bi_2Te_3/Sb_2Te_3 alloys
   n-type Bi_2Te_3/Bi_2Se_3 alloys.

The main reason that these materials have received widespread use is that they possess the highest figures of merit of all studied materials in their respective temperature range. Research has continued in the development of still higher Z materials but the bulk of the effort since the mid 1960's has been devoted to improving the performance of RTGs which use these materials. Much of this effort has concerned itself with solving problems associated with joining electrical contacts to the thermoelements and eliminating the degradation of material performance at the hot junction caused by high temperature and material incompatibility.

In the next chapter, the materials listed in the preceding paragraph will be examined, their thermoelectric properties presented, and the major problems encountered in utilizing each in RTGs will be discussed.

CHAPTER 4

RTG THERMOELECTRIC MATERIALS: PRESENT TECHNOLOGY

4.1 Introduction

This chapter reviews the presently most widely used thermoelectric materials in radioisotope thermoelectric generators. These materials were listed by useful temperature range at the conclusion of the preceding chapter. After initial discussion concerning material fabrication, dopants, electrode contacting methods, and operational advantages and disadvantages, graphical thermoelectric property data is presented for each material. Whenever possible, this data is given as a function of both time and temperature. For those materials listed under the low and intermediate operating temperature ranges, only initial property data is given since any changes which occur as a function of time are mainly a result of factors which are significantly influenced by RTG design. That is, changes in the thermoelectric properties of these materials stem mainly from such design dependent items as oxidation, sublimation, and "poisonings" by other materials employed in the thermoelectric module. Therefore, since it is impossible to generalize about the operating environment (design) each material may be subjected to, the only practical alternative is to present the "as-fabricated" or initial thermoelectric properties only. The situation with the high temperature, silicon-germanium alloys, however, is different. In their case, the cause of time dependent properties is not influenced by design variations, but is related to a metallurgical reaction which occurs in the material irrespective of operating environment. Its effects have

been extensively studied, are well understood, and the resulting change in thermoelectric properties has been quantified. Hence for the silicon-germanium alloys, data can be given as a function of time and temperature with the assurance that it is applicable to all designs regardless of operating environment.

4.2 High Temperature Thermoelectric Materials

4.2.1 Silicon-Germanium Alloys

4.2.1.1 Introduction

It is generally accepted that of all possible RTG systems which operate at hot junction temperatures on the order of 1000°C it is those which utilize silicon-germanium alloys as thermoelements that best combine the desirable qualities of high performance, good reliability, and low weight[32]. The main reason for their superiority over the other materials listed in group I of Table 3.1 is their higher figure of merit.

The alloys of silicon and germanium were first investigated in this country as promising thermoelectric materials in the early 1960's[33,34]. Since that time, devices employing silicon-germanium alloys have been constructed for use in terrestrial as well as aerospace environments and have proven to be extremely reliable sources of electrical power. The largest thermoelectric power system for space application developed to date used silicon-germanium alloys and was successfully launched in 1965 (SNAP-10A)[2]. More current applications include RTGs developed under the Multi-Hundred Watt (MHW) Program[23]. Under this program, two versions of the MHW RTG are planned for use. The first is intended for deployment in earth orbital missions and

the second more advanced version is being developed for outer planetary missions. The basic design produces 150 watts of electrical power and weighs 80 pounds. It uses a Pu-238 heat source and has a design life of 10 years.

Selected data on the silicon (78a/o)/germanium (22a/o) alloy is included in Table 4.1.

Table 4.1

Selected Data on the Si(78a/o)/Ge(22m/o) Alloy[30,35]

Solidus Temperature	1290°C
Liquidus Temperature	1400°C
Density	3.5 g/cm^3
Thermal Expansion Coefficient	5×10^{-6}/°C
Tensile Strength	5,000 psi
Compressive Strength	150,000 psi

4.2.1.2 Alloy Compositions Employed

Silicon-germanium alloys used in thermoelectric energy conversion typically consist of 70 ± 10a/o Si and 30 ± 10a/o Ge, the composition range over which lattice thermal conductivity is minimized. The alloys which have been investigated most are silicon (63a/o)/germanium (37a/o), silicon (78a/o)/germanium (22a/o), and silicon (80a/o)/germanium (20a/o). Initially, the silicon (63a/o)/germanium (37a/o) alloy was employed. This was because of a closer match between its linear thermal expansion coefficient and that of the electrode materials available at the time.

After compatible electrodes were developed, however, the latter two alloys were used since their average figures of merit over the useful temperature range (27°C-1000°C) are larger. More will be said about electrodes and the problems which arise in their selection in section 4.2.1.5. Other advantages of the higher silicon content alloys include[32]: a closer match between the thermoelectric properties of the n and p-type materials, and a smaller change in thermoelectric properties as a function of operating time. The more closely matched thermoelectric properties of the n and p-type materials of each of the higher silicon content alloys result in nearly equal sized thermo-elements when the geometry of each is optimized for maximum thermocouple efficiency. For reasons of symmetry, this results in a thermocouple which is easier to construct and is more rugged. Finally, since the properties of the higher silicon content alloys degrade less with time, their performance is more stable and there is a smaller decrease in output power and efficiency over a given mission lifetime.

4.2.1.3 Fabrication Techniques

Any method employed to fabricate silicon-germanium alloys should be able to achieve a uniform distribution of constituent atoms in the desired proportions. Further, the resultant alloy should have sufficient strength to withstand the stresses arising from the expansion and contraction which occurs during its use and in the case of space applications, the accelerations experienced during launch, in-flight maneuvers, and landing.

A homogeneous distribution or true alloy of silicon and germanium atoms is desired to minimize the material's lattice thermal conductivity

and to preclude subsequent changes in k_L when the alloy is operating in an RTG. The reasons behind this statement can be seen as follows. Alloys of silicon and germanium used in thermoelectric applications have lattice thermal conductivities over an order of magnitude lower than either silicon or germanium by themselves (see Tables 3.1 and 3.2). This, however, applies only to a true alloy of the elements. If, instead, the fabricated material is a mixture which exhibits varying concentrations of silicon and germanium from nearly pure silicon to pure germanium, the lattice thermal conductivity will not be as low as that of the true alloy. Furthermore, it a true alloy is not attained during fabrication and the material is then exposed to temperatures such as those near the hot junction of an operating thermocouple (600°C-1000°C), the degree of inhomogeniety and hence the lattice thermal conductivity will decrease with time due to the diffusion of constituent atoms or what Raag[36] calls "enhanced alloying." Therefore, to preclude unnecessarily high values of k_L after material fabrication and enhanced property changes during operating time, it is necessary that the fabrication technique employed be able to maximize the uniformity of silicon and germanium atoms in the alloy.

Various fabrication methods, resulting in either single of poly-crystalline silicon-germanium alloys, have been investigated. They include:

1. Melt grown single crystal alloys
2. Vacuum cast poly-crystalline alloys
3. Vacuum cast, zone-leveled, poly-crystalline alloys
4. Vacuum hot pressed poly-crystalline alloys.

The most commonly used technique at present is vacuum hot pressing (the process itself will be explained later in this section). The other methods were abandoned in favor of vacuum hot pressing because they were either basically impractical or achieved less desirable results. Melt grown single crystals are difficult to grow in useable sizes[37], require extremely slow pulling rates[35], and are more expensive to produce than the poly-crystalline alloys.

Vacuum casting, a technique in which a molten mixture of the silicon and germanium is cast in a mold under vacuum, is not employed because producing homogeneous alloys requires an immediate quench of the entire melt. This is an impossible task for any sizable amounts of alloy due to its low thermal conductivity[38]. Furthermore, the alloy resulting from the vacuum casting technique consists of individual crystals which are large compared to those in alloys produced by vacuum hot pressing. For this reason, vacuum cast alloys fail along grain boundaries and imperfections in their crystals under stresses which have no effect on vacuum hot pressed materials[35]. Vacuum casting followed by zone-leveling* eliminates much of the problem of a non-uniform distribution of silicon and germanium atoms in the alloy but does not improve its mechanical strength.

Vacuum hot pressing is an alloy fabrication technique used in powder metallurgy. In this method, cast ingots of the silicon-germanium

*The term zone-leveling denotes a group of zone melting techniques whose aim is to produce a uniform, or level, distribution of solute in an ingot of solvent. Zone melting techniques pass a molten zone along the length of an ingot via RF heating, for example, to control the distribution of soluble impurities or solutes in crystalline materials[39].

alloy and dopant are ground into a fine powder which is pressed at various combinations of temperature and pressure until through atomic diffusion, the initial inhomogeneities are essentially eliminated. The process is completed by immediately cooling the pressed material with, for example, helium. In one report[40], the density of the resulting alloy was 99% of theoretical and the silicon to germanium ratio did not vary more than 2% from the desired value throughout. Unfortunately, measured thermal conductivity data was not provided, but according to Raag[35], with compositional variations of this order, there would be an insignificant difference between the actual thermal conductivity and that of the true alloy. Alloys produced by the vacuum hot pressing technique, then, not only have greater mechanical strength than those produced by other methods, but also can be made very uniform.

4.2.1.4 Dopants Employed and Associated Problems

Pure silicon-germanium alloys are intrinsic materials and as such are of no value in thermoelectric energy conversion. In order to increase the carrier concentration to the level required to optimize the figure of merit, it is necessary to dope the alloys with an impurity of sufficiently high solid solubility. Since the solid solubility of an impurity in a silicon-germanium alloy is primarily determined by the compatibility of its atomic size and electronic structure with that of the silicon and germanium atoms, elements from groups III-A and V-A of the periodic table are particularly attractive dopants. Group III-A elements, having one less outer electron than is required to form complete bonds with neighboring silicon and germanium atoms, serve as

acceptor impurities and therefore result in a p-type alloy. Group V-A elements have one more electron than is needed and hence act as donor impurities to produce n-type materials.

Impurities other than those from groups III-A and V-A, such as elements of groups II-A and VI-A, can also serve as dopants in silicon-germanium alloys. But because of considerably lower solid solubilities, the carrier concentrations generally obtained with dopants from other groups of the periodic table fall far short of those needed to maximize the figure of merit[13].

The acceptor impurities from group III-A which have been investigated are boron, aluminum, and gallium, while the donor impurities considered from group V-A include antimony, arsenic, and phosphorus. For silicon-germanium alloys employed in RTGs and the temperature range over which they are operated (300°K-1300°K) the optimum carrier concentration lies in the range 10^{20}-10^{21} cm^{-3}.[13] As each atom of group III-A or V-A elements supplies one carrier, it is therefore necessary to have 10^{20}-10^{21} impurity atoms per cubic centimeter in solution with the alloy. However, the solid solubilities of the above dopants, over all temperatures that the alloys are employed, range from approximately 10^{19} to 3×10^{20} atoms per cm^3 and increase in the sequence: antimony, aluminum, gallium, arsenic, phosphorus and boron[13,35]. Boron and phosphorus have maximum solid solubilities in silicon-germanium alloys of approximately 4×10^{20} atoms/cm^3[35] at 1100°C and 1.5×10^{20} atoms/cm^3[13] at 1000°C, respectively. But even these are not sufficiently soluble to remain in solution over all operating temperatures (27°C-1000°C) when introduced into the alloy in the desired concentration of 10^{20}-10^{21} atoms/cm^3.

This is because their solubilities rapidly decrease with decreasing temperature. However, since boron and phosphorus have the greatest solubilities, they are used as p and n-type dopants, respectively, in all silicon-germanium thermoelectric materials produced.

It is apparent from the above that because of the limited solid solubilities of boron and phosphorus, the theoretically possible efficiency of thermocouples using silicon-germanium alloys cannot be obtained, Furthermore, at the doping levels which are actually employed ($\sim 10^{20}$ atoms/cc), the alloy is supersaturated at certain temperatures in its operating range (that is, at certain positions in the thermoelement) and the excess boron and phosphorus precipitate within the material. The rate and extent to which precipitation occurs are dependent upon the temperature and degree of supersaturation. At temperatures near the hot junction (1000°C), there is little supersaturation, diffusion of the excess dopant atoms proceeds rapidly, and the precipitation process goes to completion relatively fast with only a small amount occurring. At low temperatures, such as those near the cold junction (27°C-200°C), supersaturation is greatest but excess dopant atom diffusion occurs so slowly that precipitation, again, amounts to little--even over a period of 12 years[32]. It is at intermediate temperatures, in the range of 300°C-600°C for phosphorus doped alloys and 700°C-950°C for boron doped alloys, that significant precipitation occurs. Here the combined actions of sufficiently high temperature and supersaturation result in considerable precipitation over an extended length of time (>12 years).

The time decreasing dopant concentration due to the precipitation process explained above, and hence the time decreasing carrier concentration manifests itself in time dependent thermoelectric properties for

silicon-germanium alloys. As explained in Chapter 2, as the carrier concentration decreases, the electrical conductivity decreases and the Seebeck coefficient increases. Therefore, these are the changes we would expect to see in a silicon-germanium thermocouple with increased operating time. It has been shown that the decrease in σ dominates the increase in α, even though the latter term is squared in calculating Z, and hence the net effect is a decrease in the figure of merit and the thermocouple's efficiency with increased operating time[41]. This effect on Z is completely independent of what may occur due to changes in thermal conductivity, as the latter is strictly a function of the quality of the alloy fabrication process, whereas the precipitation effects described above occur in all alloys regardless of production technique (or operating environment).

It may not have been immediately obvious why precipitation has to occur at all. It was stated earlier that it was due to the doping levels actually employed, but why use doping levels which lead to dopant precipitation, a decrease in the carrier concentration, and associated problems? The answer to this question will be explained in terms of what happens with phosphorus doped alloys. A similar argument also applies to boron.

Precipitation in phosphorus doped silicon-germanium alloys comes about in the following manner. Since an insufficient number of phosphorus atoms can remain in solution with a silicon-germanium alloy to permit optimum doping at all temperatures, the best possible performance of the material is obtained when the dopant concentration has its maximum permissible value at every point in the material, or in other words, over all operating temperatures. This suggests that in order

to maximize the materials' performance, the dopant concentration between the hot and cold junctions should exactly equal its solid solubility at the corresponding temperature. This way the material is not supersaturated with dopant at any point and the maximum possible carrier concentration is also present. As discussed in Chapter 2, however, maintaining a given doping concentration gradient is impossible and thus the best solution to the problem is impractical. What can be done however, is to introduce sufficient dopant uniformly in the alloy such that its concentration equals its solid solubility at the hot junction temperature. In this way the maximum dopant concentration is also attained at all lower temperatures since solubility decreases with decreasing temperature. But even though this has been achieved, another problem has been created. Since the dopant concentration employed equals the solid solubility at the hot junction temperature and solubility decreases with decreasing temperature, at all lower temperatures the lattice will be supersaturated with phosphorus, and precipitation will occur over time. As mentioned previously, this causes the figure of merit to decrease with time. Conversely, if an amount of dopant is introduced uniformly into the alloy equal to its solid solubility at the cold junction temperature, supersaturation will not exist, precipitation will not occur, performance will not degrade with time, but the material will no longer be doped to its maximum allowable extent throughout and hence its figure of merit will be less over all time.

In summary, the dopants used in p and n-type silicon-germanium alloys are boron and phosphorus, respectively. Neither have sufficient solid solubility over all operating temperatures to permit optimum

doping and in attempting to maximize the figure of merit of the material, precipitation occurs in operating thermoelements due to these solubility limitations. Precipitation reduces the number of dopant atoms in solution with the alloy over time and hence, the carrier concentration. This has the effect on the thermoelectric properties α, σ, and Z of causing them to be time dependent for silicon-germanium alloys.

Eventually, these properties reach values commensurate with the solid solubility (i.e., allowable doping level) at each point between the hot and cold junctions. Although α increases and σ decreases with time, the net effect is a decrease in Z and the efficiency of thermocouples utilizing silicon-germanium alloys decreases with increased operating time.

4.2.1.5 Operational Considerations

Silicon-germanium alloys are quite insensitive to their operating environment. Oxygen has no effect on their thermoelectric properties and therefore devices utilizing these alloys do not require hermetic sealing, at least for the purpose of eliminating oxidation. Also, at the temperatures which these alloys are employed (<1000°C), sublimation is not a problem. Therefore, RTGs employing silicon-germanium alloys can be operated at atmospheric pressure or in vacuum without the need of specially designed features to control thermoelement sublimation[4].

As stated previously, thermoelectric materials and their junctions with electrodes must be capable of withstanding stresses which arise

from expansion and contraction occurring during their use, and in the case of space applications, the accelerations experienced during launchings, in-flight maneuvers, and landings. Relative to other thermoelectric materials, silicon-germanium alloys have fewer problems in this area as they are less brittle and have higher tensile strength (compare data in Tables 4.1 and 4.2). Furthermore, they can be metallurgically bonded to both the hot and cold junction electrodes[35]. As a result, complex and bulky spring and piston mechanisms are not necessary to maintain silicon-germanium thermoelements in compression or hold them in place at the hot junction as is required for other materials such as lead telluride alloys.

Concerning electrodes, tungsten and certain silicon alloys have proven to be excellent materials for contacting to silicon-germanium alloy thermoelements[4]. The most current RTG design utilizing silicon-germanium materials [silicon (78a/o)/germanium (22a/o)], the Multi-Hundred Watt (MHW) converter, employs an alloy of silicon (95a/o)/molybdenum (5a/o) as the hot junction electrode and tungsten as the cold junction electrode. Tungsten is best employed in conjunction with the silicon (63a/o)/germanium (37a/o) alloy due to the close match of their thermal expansion coefficients[32]; however, it can also be used with the MHW alloy if a layer of silicon (63a/o)/germanium (37a/o) alloy is placed between the electrode and thermoelement to act as a "mating" device. The silicon (95a/o)/molybdenum (5a/o) alloy mentioned above can be used as an electrode with any silicon-germanium thermoelectric material.

At temperatures greater than 600°C, tungsten oxidizes rapidly and also diffuses into the thermoelement, if allowed[2,4]. These effects

limit the useful life of a metallurical bond at the hot junction between tungsten and silicon-germanium thermoelements to less than 5000 hours[4]. Because of this, if tungsten is to be used at the hot junction, the device must be hermetically sealed and a diffusion barrier, such as graphite, installed between the tungsten electrode and silicon-germanium thermoelement. Silicon alloy electrodes, however, can be operated at a temperature of 1000°C, in air or vacuum, and without a diffusion barrier[10]. Hence they are much more practical hot junction electrode materials from design, fabrication, and cost standpoints. As an example of the silicon alloys' durabilities, the silicon (95a/o)/molybdenum (5a/o) alloy has been found to possess a useful operating life in excess of 10 years, in air, at a temperature of 1000°C[2].

4.2.1.6 Thermoelectric Property Data[42]

This section presents the thermoelectric properties of the silicon (78a/o)/germanium (22a/o) alloy. Although other alloys were discussed in section 4.2.1.2, this alloy is the most widespread silicon-germanium material presently in use. For example, it is being employed in the Multi-Hundred Watt RTG intended for use in NASA's outer planetary exploration program.

Figures 4.1 and 4.2 give the electrical resistivity and Seebeck coefficient as functions of time and temperature for the n-type silicon (78a/o)/germanium (22a/o) alloy. The corresponding data for the p-type alloy is presented in Figures 4.5 and 4.6. The n-type material is doped with phosphorus at approximately 1.5×10^{20} atoms/cm^3 and the

p-type material is doped with boron at approximately 2.5 x 10^{20} atoms/cm^3. As expected, both properties increase with time due to dopant precipitation.

The time and temperature dependence of thermal conductivity for this alloy is shown in Figures 4.3 and 4.7 for the n and p-type alloys, respectively. The effects of "enhanced annealing" (section 4.2.1.3) are apparent at temperatures in excess of 600°C as evidenced by the decrease in thermal conductivity with time. Thus, the samples used here (hot pressed, prepared by RCA) obviously had a non-uniform distribution of silicon and germanium atoms after fabrication was completed.

The electrical resistivity, thermal conductivity, and Seebeck coefficient data have been combined in Figures 4.4 and 4.8 to give the figure of merit as a function of time and temperature.

The experimental data upon which the electrical resistivity and Seebeck coefficient plots are based was obtained from isothermally annealed samples of the silicon (78a/o)/germanium (22a/o) alloy under test for approximately 18,000 hours. The thermal conductivity data was obtained from other samples under test for approximately 12,000 hours. A complete discussion of the methodology employed in obtaining these properties as a function of time is contained in works of Raag[36,42].

4.3 Intermediate Temperature Thermoelectric Materials

4.3.1 Lead Telluride Compounds and Alloys

4.3.1.1 Introduction

The lead telluride materials are the most commonly used thermoelectric materials over the temperature range 27°C-630°C. As

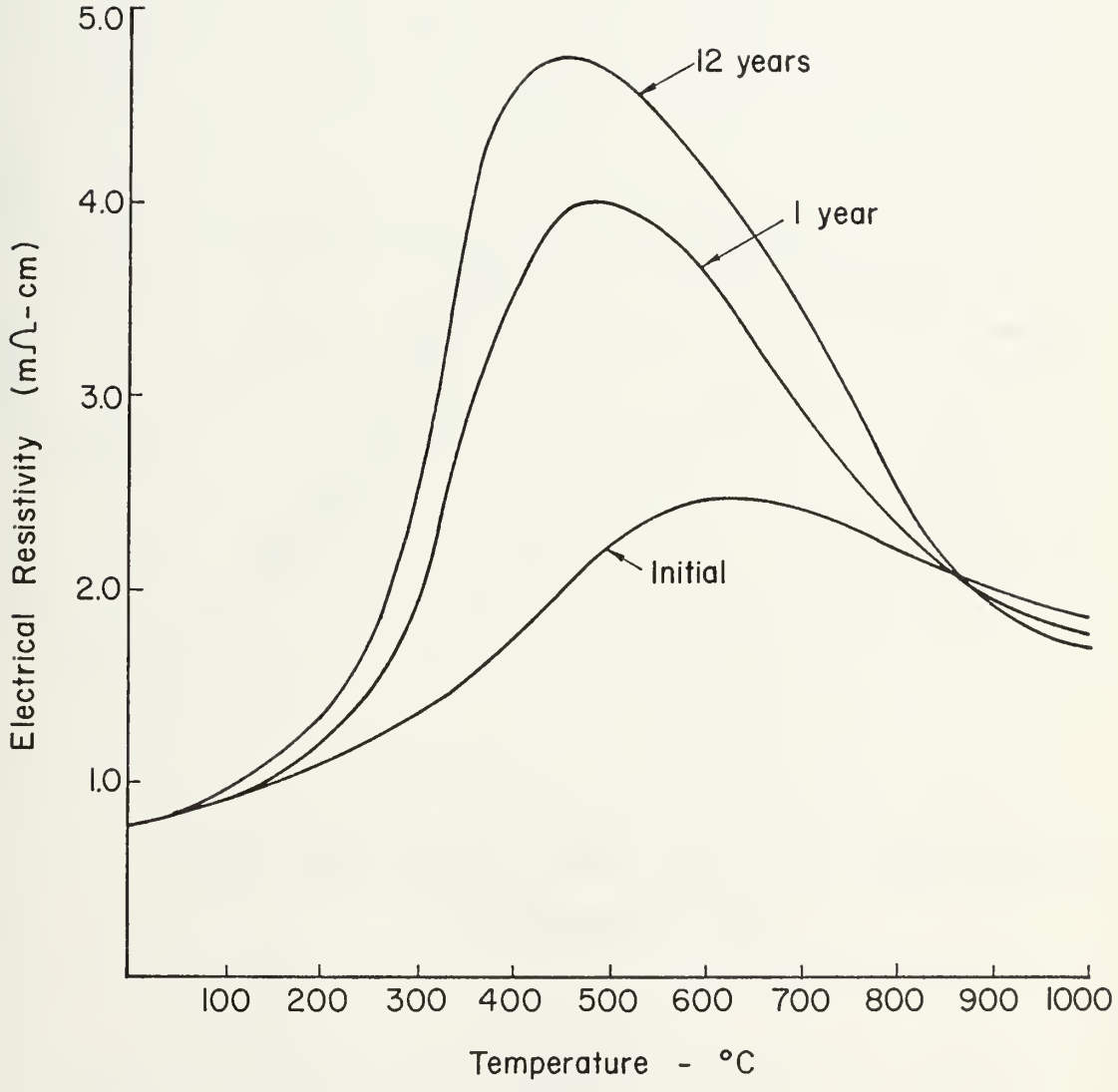

Figure 4.1 Electrical Resistivity of n-type Si(78a/o)/Ge(22a/o) Alloy

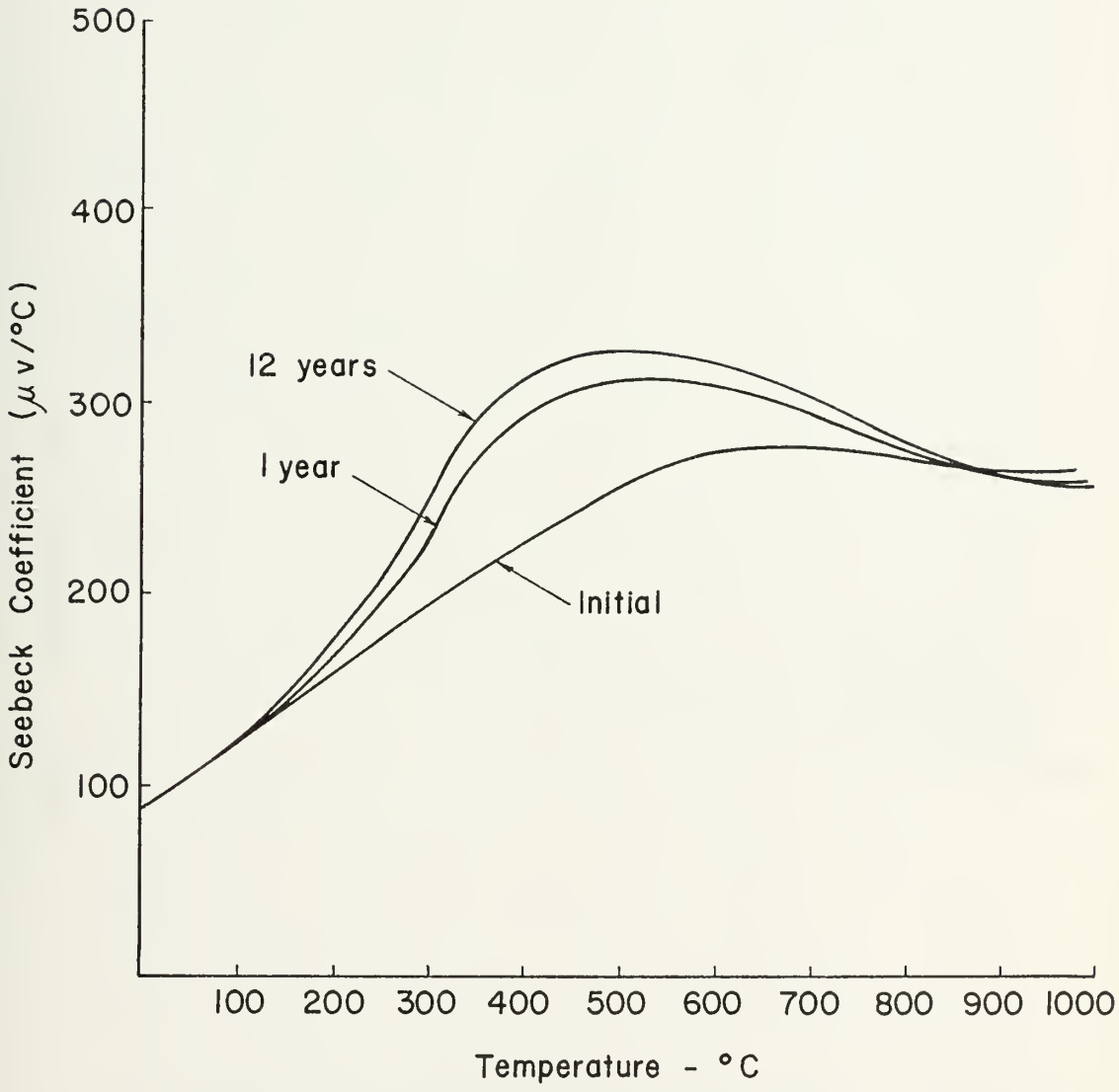

Figure 4.2 Seebeck Coefficient of n-type Si(78a/o)/Ge(22a/o) Alloy

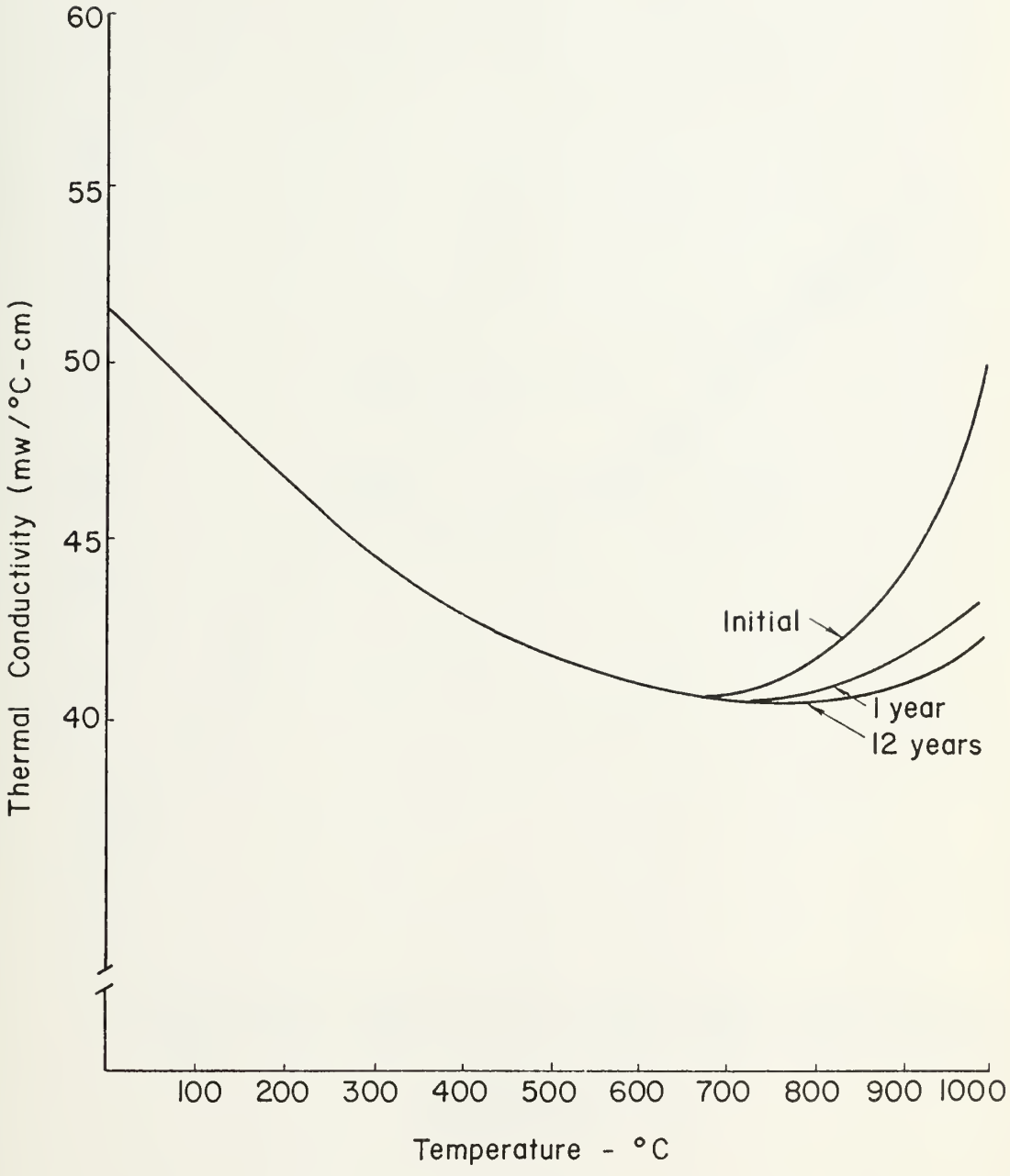

Figure 4.3 Thermal Conductivity of n-type Si(78a/o)/Ge(22a/o) Alloy

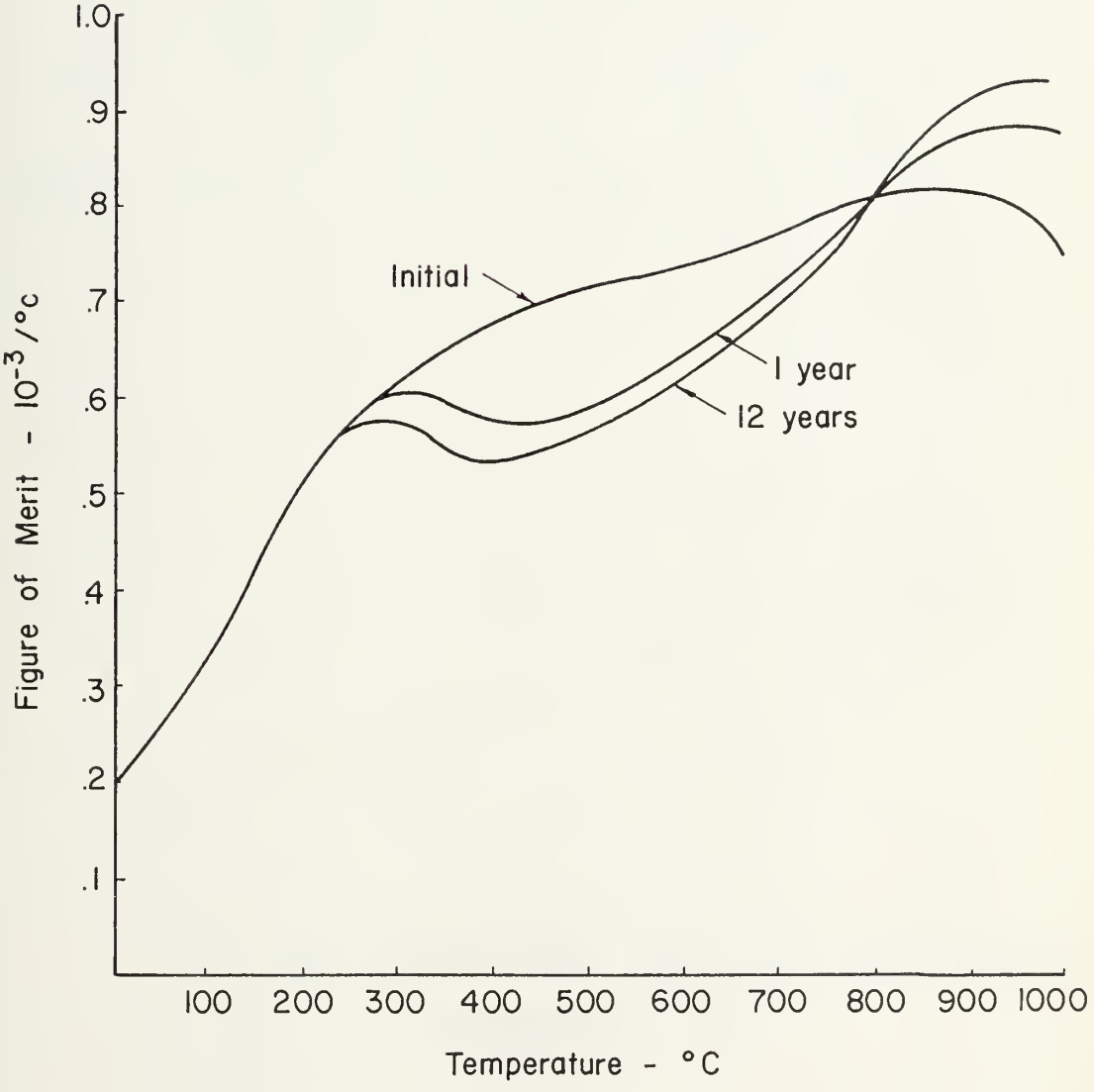

Figure 4.4 Figure of Merit of n-type Si(78a/o)/Ge(22a/o) Alloy

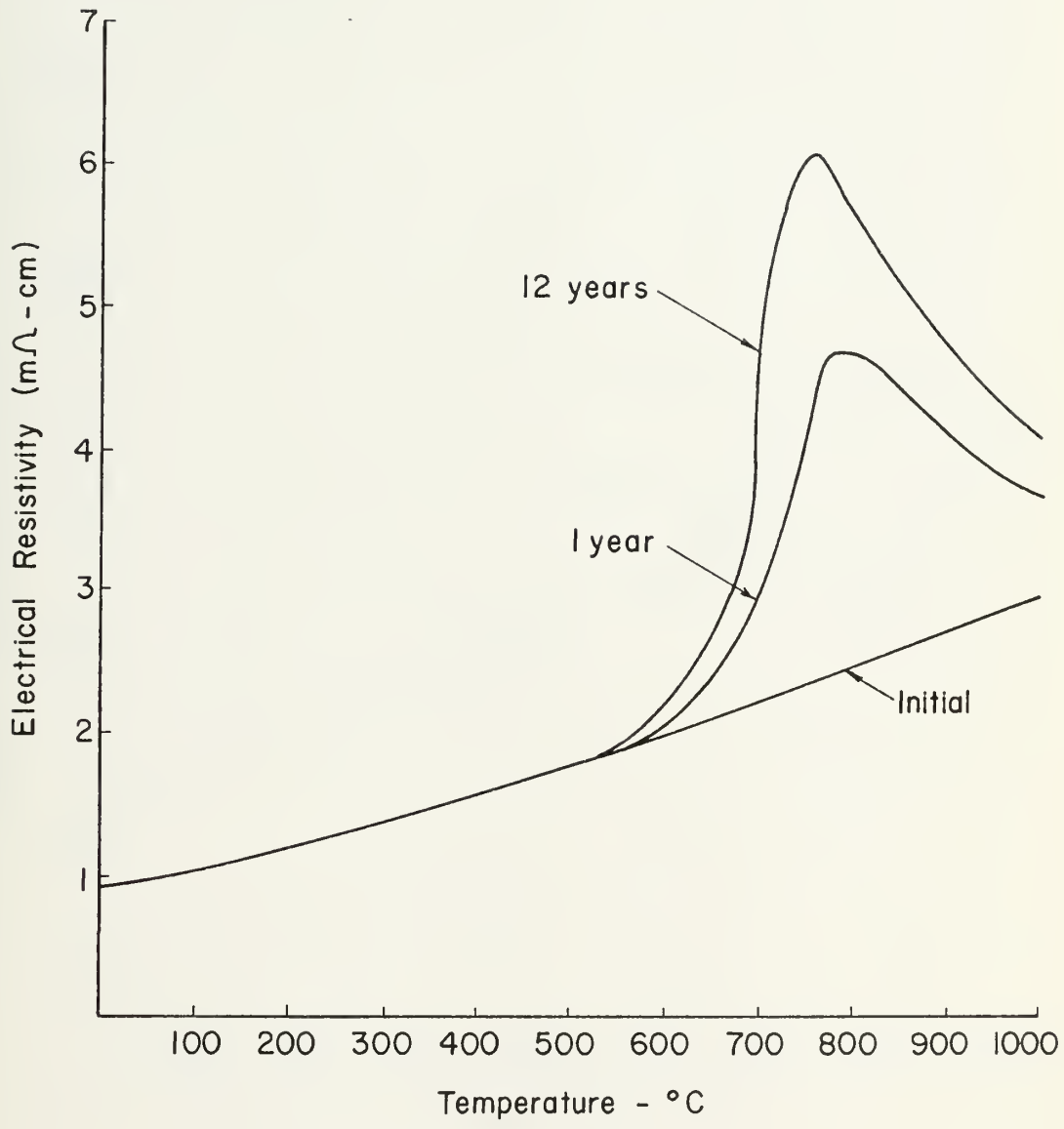

Figure 4.5 Electrical Resistivity of p-type Si(78a/o)/Ge(22a/o) Alloy

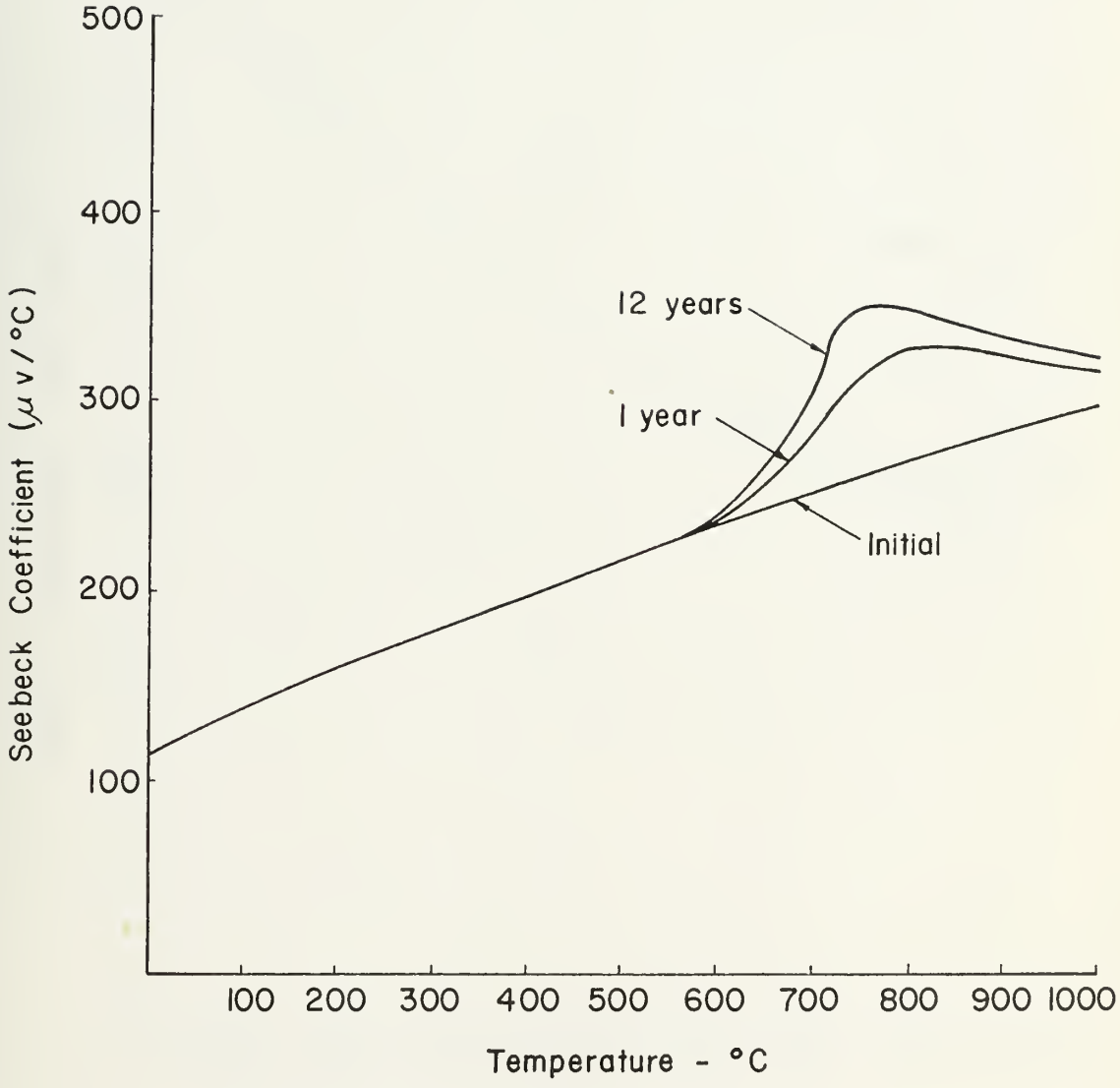

Figure 4.6 Seebeck Coefficient of p-type Si(78a/o)/Ge(22a/o) Alloy

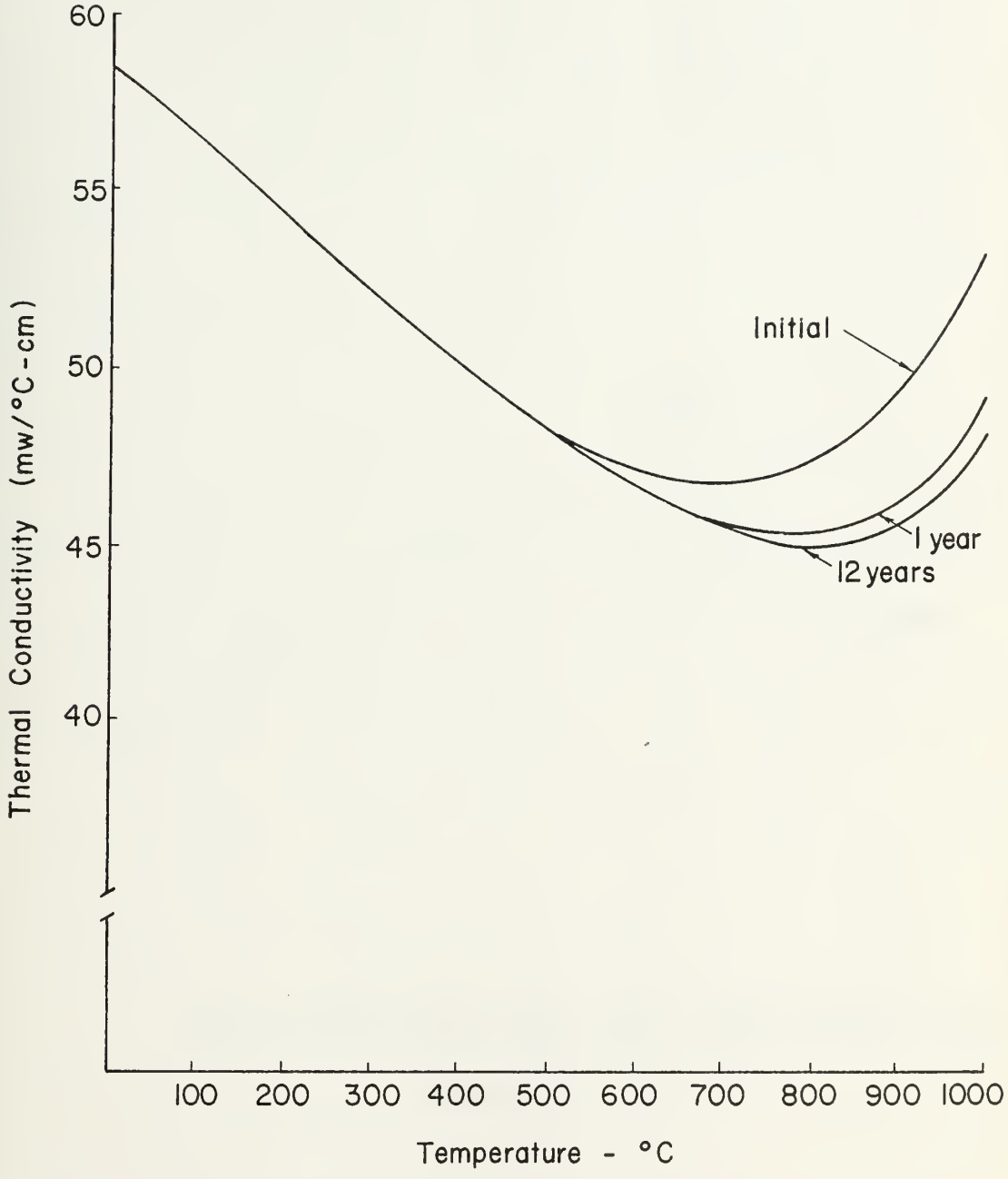

Figure 4.7 Thermal Conductivity of p-type Si(78a/o)/Ge(22a/o) Alloy

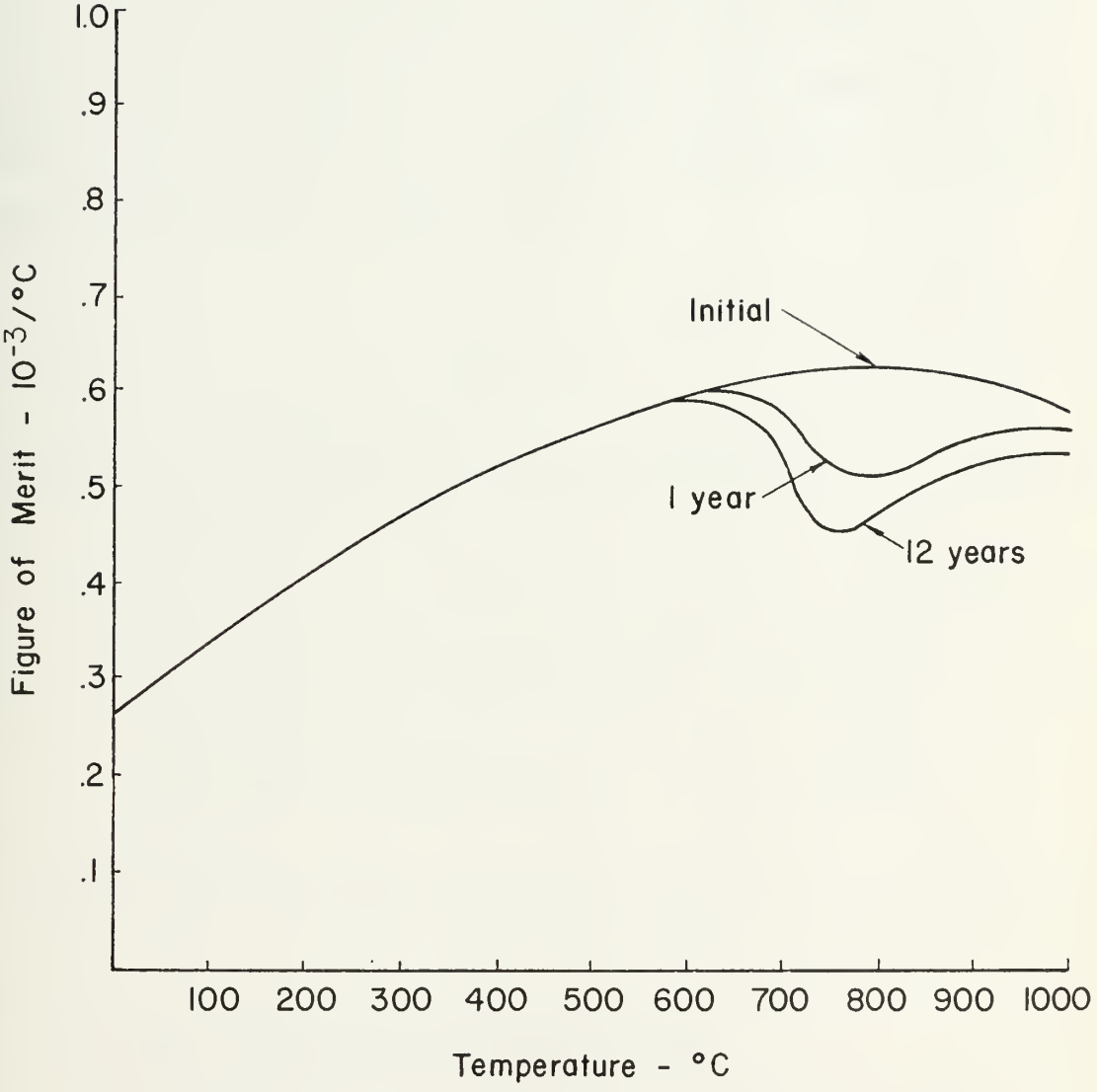

Figure 4.8 Figure of Merit of p-type Si(78a/o)/Ge(22a/o) Alloy

mentioned in Chapter 3, they were initially investigated in the mid-1950's and then extensively used in space applications. In fact, all U.S.A.-flown radioisotope thermoelectric generators, namely SNAP-3, 9A, 19, 19 (Pioneer), 19 (Viking), and 27 were assembled with lead telluride materials as either the n or p-type thermoelements or both. In this section, a review of these materials will be given including thermoelectric property data on those most widely employed. Selected physical data is also included in Table 4.2.

Table 4.2

Selected Data on n or p-type PbTe[30]

Melting Point (°C)	922
Density (g/cm^3)	8.3
Thermal Expansion Coefficient ($°C^{-1}$)	18×10^{-6}
Tensile Strength (psi)	1,000
Compressive Strength (psi)	10,000

4.3.1.2 Material Fabrication; Dopants

As with the silicon-germanium alloys, lead telluride materials are prepared using powder metallurgy techniques rather than by casting. Materials having essentially the same thermoelectric properties can be produced by either method but powder metallurgy processes result in materials of superior mechanical strength[17]. As discussed previously, this is most important as thermoelectric materials are

generally quite brittle. The fabrication techniques commonly employed are vacuum hot pressing or cold pressing and sintering. The latter is a procedure whereby cast material is ground into a fine powder, compacted, and then heated until the individual particles are sufficiently fused. Vacuum hot pressing was described in section 4.2.1.3. The details of either fabrication procedure as pertains to the lead telluride materials could not be ascertained, as manufacturers consider this information proprietary[43,44].

PbTe and its alloys with other elements such as tin are inherently intrinsic and hence must be doped in order to obtain extrinsic carrier concentrations sufficiently large ($\sim 10^{20} cm^{-3}$) for thermoelectric applications. Excess lead or tellurium can be incorporated within the PbTe lattice to produce n or p-type material, respectively. However, due to solid solubility limitations, the concentration of charge carriers which can be gained in this manner is an order of magnitude too small[9]. In order to increase the charge carrier concentration, one must introduce other dopant atoms. In PbTe, one has the freedom of substituting for either Pb or Te to accomplish this. That is, either Pb or Te can be replaced by an element whose atoms have either a greater or lesser number of valence electrons. Depending on which is the case, n or p-type material is produced. For example, possible donor impurities are PbI_2, $PbBr_2$, Bi_2Te_3, and GeTe. Acceptor dopants include Na and K. The n-type materials most commonly employed in thermoelectric applications have an excess of Pb and are doped with PbI_2 while the p-type materials are of excess Te and are doped with Na[30]. A further discussion on the doping of PbTe can be found in Heikes and Ure[9].

4.3.1.3 PbTe Materials Commonly Employed

The lead telluride materials most commonly used in RTGs are n-type PbTe, p-type PbTe, and p-type alloys of PbTe and SnTe. Commercially, the most widely used compositions are those originally manufactured by the 3M Company but now by Global Thermoelectrics[43]. The designations originated by 3M for these materials--2N, 3N, 2P, 3P--are still in use and hence will be employed in this paper.

The 2N and 3N varieties are n-type PbTe with differing concentrations of PbI_2 dopant and excess Pb. The exact doping level and amount of excess lead associated with each material is proprietary[43] but it is known that the resulting carrier concentration is greater in the 3N material. Further, industry sources indicate that 2N is on the order of .005m/o PbI_2 with .055a/o excess lead and 3N is approximately .1m/o PbI_2 with .1a/o excess lead[44]. Because of its higher doping level, the 3N material also possesses a greater extrinsic carrier concentration at any temperature. This raises the temperature where intrinsic behavior causes the figure of merit to decrease with increasing temperature (see section 2.4) and results in higher values of Z above approximately 360°C (see Figure 4.12). For designs where the cold junction temperature is on the order of 200°C (e.g., space application), the improvement in Z at higher temperatures makes 3N material more attractive from an efficiency point of view.

The 2P material is p-type, Na doped, PbTe with an excess of Te and 3P is also p-type, but an alloy of Pb, Sn, Mn, and Te which is doped with Na. Once again, the precise concentration of elements used in these materials is proprietary and only estimates can be given. In

this respect, 2P is doped at approximately 1a/o Na with 1a/o excess Te and the composition of 3P is on the order of PbTe (48m/o) SnTe (48m/o) MnTe (4m/o) doped with approximately .1a/o Na and .1a/o excess Te[44]. The 3P material, although more undesirable than 2P from the standpoint of maximum figure of merit (Figure 4.16), results in better performance above approximately 450°C, a stronger thermoelement, and less problems with the electrode/thermoelement connection at the hot junction[43]. The reason for the latter is basically as follows. For reliable operation, a 2P thermoelement requires a barrier between it and all electrode materials (e.g., Fe, Mo, Stainless Steel) except tungsten. This is to reduce diffusion of electrode atoms into the 2P material, the subsequent reaction with Te, and the resulting deterioration of the electrode/thermoelement contact and the thermoelectric properties of the 2P material. If tungsten is employed, further contact reliability problems are encountered because its thermal expansion coefficient (5×10^{-6}/°C) is less than a third of that for 2P (18×10^{-6}/°C). With the 3P material these problems are resolved. It can be used with any of the electrode materials mentioned above and does not require a barrier for isolation from the electrode.

4.3.1.4 Operational Considerations

One of the problems which is encountered in the use of lead telluride materials is their relatively poor mechanical strength. For example, from Tables 4.1 and 4.2 one sees that the tensile strength of PbTe is only 1/5 that of silicon-germanium alloys. According to Rouklove[30], it is because of their low tensile strength that PbTe

thermoelements cannot withstand the stresses encountered during operation unless some means are provided to limit these stresses to compression. By far, the most common method of achieving this goal is to install a spring and piston mechanism at the cold junction of each thermoelement. This mechanism loads the element sufficiently in the axial direction to preclude tensile forces from arising and at the same time provides a path for the waste heat. Admittedly, all this adds to the expense of an RTG based on lead telluride materials and also makes it more difficult to fabricate, but it does assist in one method of contacting electrodes which will be explained later in this section.

Two other operational problems which exist for lead telluride materials are sublimation and oxidation. Tellurium sublimes at temperatures in the neighborhood of 430°C. This has two undesirable effects. First, the thermoelement decomposes. Second, the sublimed vapor is liable to condense elsewhere in the system and cause electrical "shorts." Since lead telluride material thermocouples should be operated with $T_H \approx 630°C$ to maximize performance, some means of inhibiting sublimation is required. Above approximately 480°C, lead telluride materials are also susceptible to oxidation. This not only increases the resistance of the thermoelement but has the possibility of "fouling" the electrode and its contact with the thermoelement at the hot junction. This matter must be dealt with as well. Any means of excluding air from the vicinity of the thermoelements and reducing diffusion of atoms from their surface will solve both problems. The method favored by most RTG designs is to encapsulate all thermocouples in a slightly pressurized atmosphere of argon and other inert gases[2,43].

One additional problem area must be discussed before this section can be considered complete--contacting electrodes to lead telluride materials. No standard technique exists for accomplishing this. Different methods are employed depending upon the particular design and the level of success a manufacturer can achieve with a given method (again, the particulars are proprietary). At the cold junction, connections can be made by metallurgical bonding or soldering depending upon the design cold junction temperature. At the hot junction, pressure contacting or, again, metallurgical bonding can be employed[4,16,44]. In metallurgical bonds, the lead telluride thermoelement is heated until just molten at one end and then brought into contact with the electrode material (e.g., iron). Iron is commonly used because its thermal expansion characteristics closely match those of the lead telluride materials[4]. In pressure contacting, one takes advantage of the previously stated fact that the thermoelement must be in compression anyway. For this method, the thermoelement is held in place at the hot junction by a spring loaded mechanism located at the cold junction. This affords sufficient pressure to enable intimate contact between the electrode and thermoelement material.

4.3.1.5 Thermoelectric Property Data[45]

In this section, the initial thermoelectric property data of 2N, 3N, 2P, and 3P lead telluride materials will be presented. The constituents of these materials and their approximate concentrations can be found in section 4.3.1.3. All were cold pressed and sintered.

Figures 4.9 through 4.12 give the electrical resistivity, Seebeck coefficient, thermal conductivity, and figure of merit as functions of temperature for the 2N and 3N materials. The corresponding data for the 2P and 3P varieties are shown in Figures 4.13 through 4.16. Properties of both n-type materials are plotted on the same graphs to simplify comparisons. The same applies to the p-type materials.

4.3.2 TAGS-85

4.3.2.1 Introduction

This section summarizes the characteristics and performance of the thermoelectric material known as TAGS-85 (hereafter simply referred to as "TAGS"). At its conclusion, plots of the Seebeck coefficient, electrical resistivity, thermal conductivity, and figure of merit will be presented. The latter property indicates that TAGS is the most efficient p-type material presently available for use in RTGs operating over the temperature range 27°C-530°C.

4.3.2.2 Material Characteristics

The acronym TAGS is derived from the first letter of each of the material's constituents: tellurium, antimony, germanium, and silver. These elements form a solid solution of $AgSbTe_2$ (15 m/o) and GeTe (85 m/o) which has a solidus temperature of 586°C and a liquidus temperature of 680°C. As far as mechanical properties are concerned, TAGS is considerably better than either the 2P or 3P lead telluride materials. As-cast TAGS has double their compressive strength (~20000 psi), a superior fracture resistance, and a tensile strength which is five

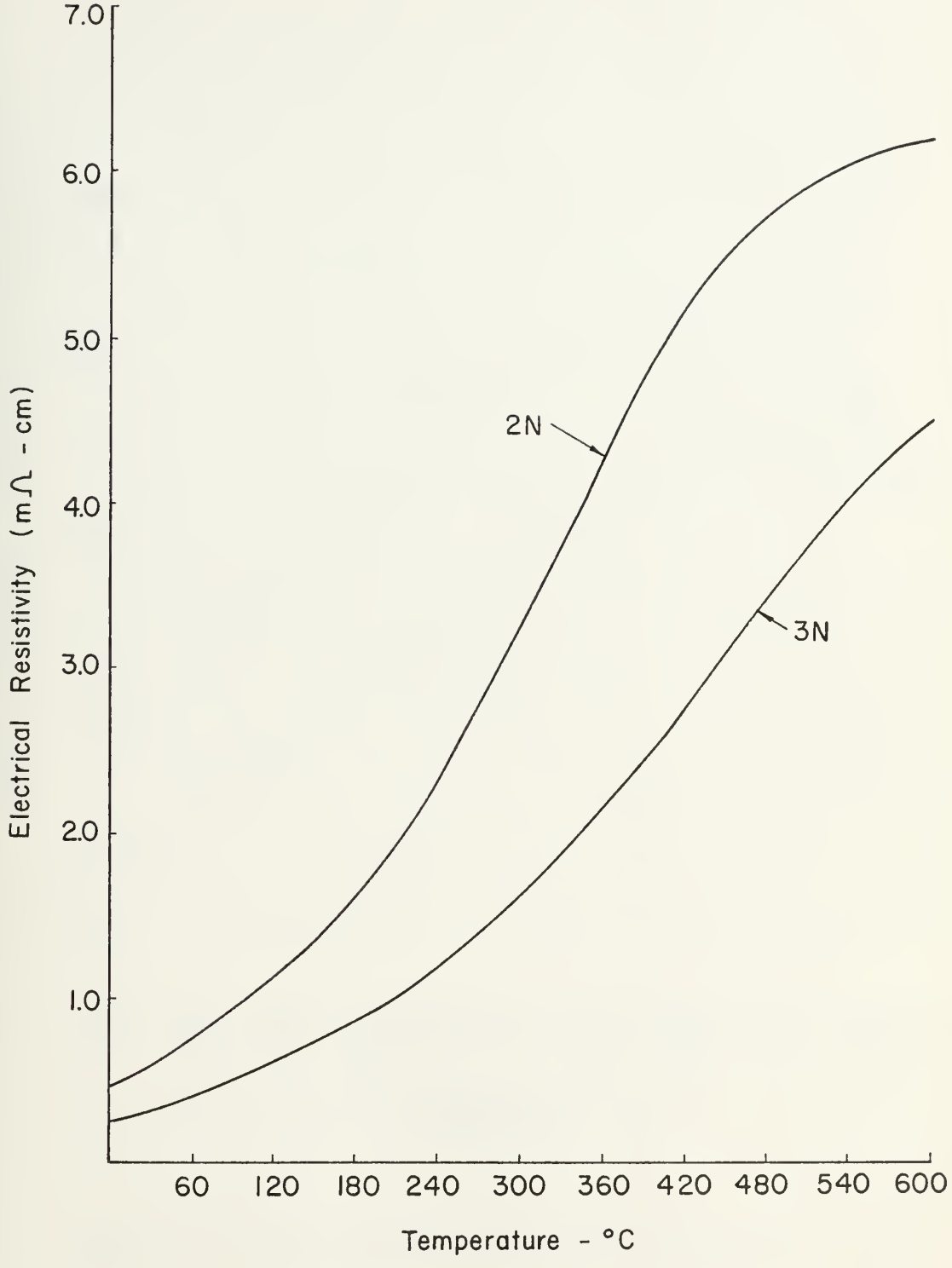

Figure 4.9 Electrical Resistivity of 2N and 3N Materials

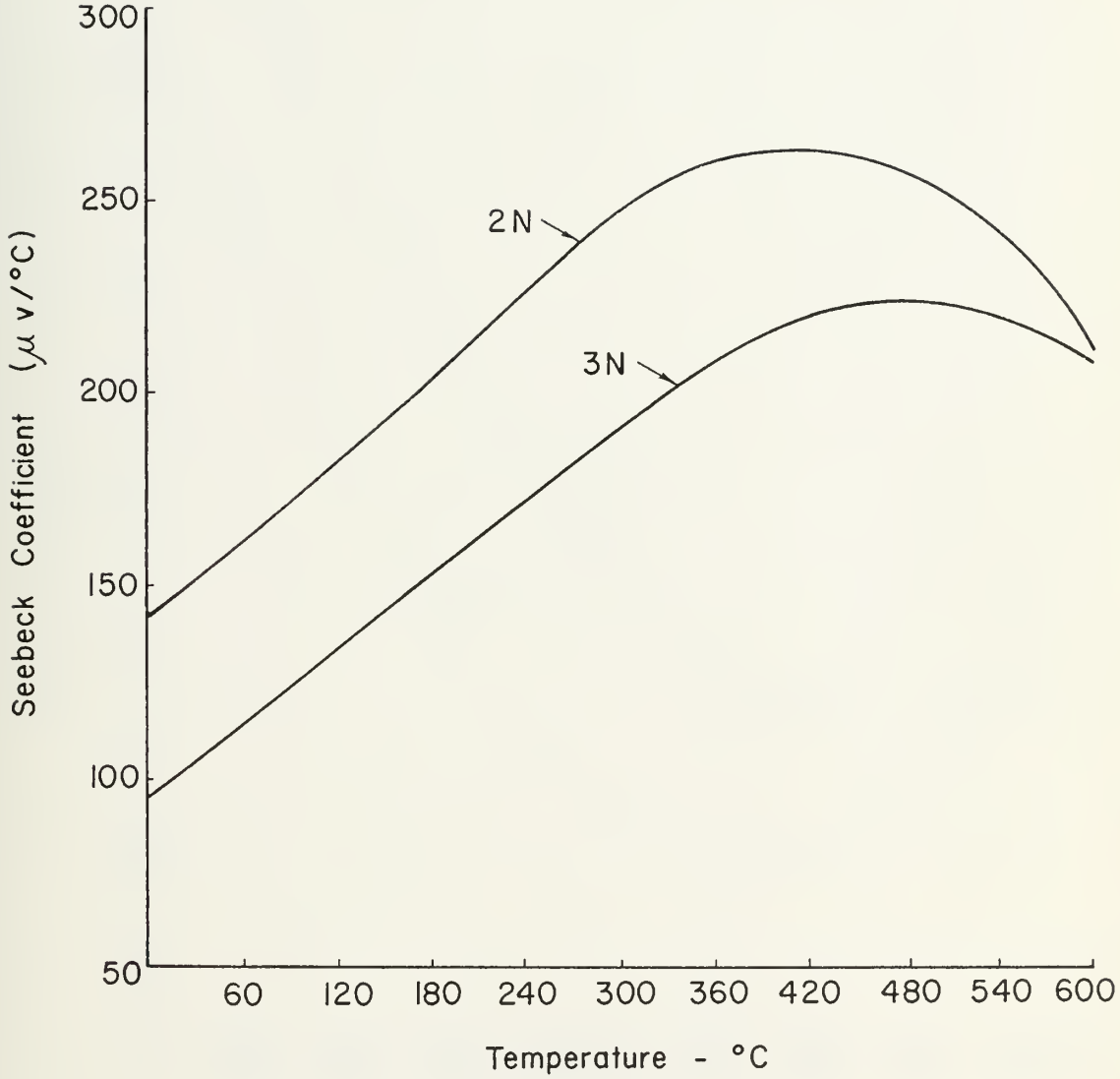

Figure 4.10 Seebeck Coefficient of 2N and 3N Material

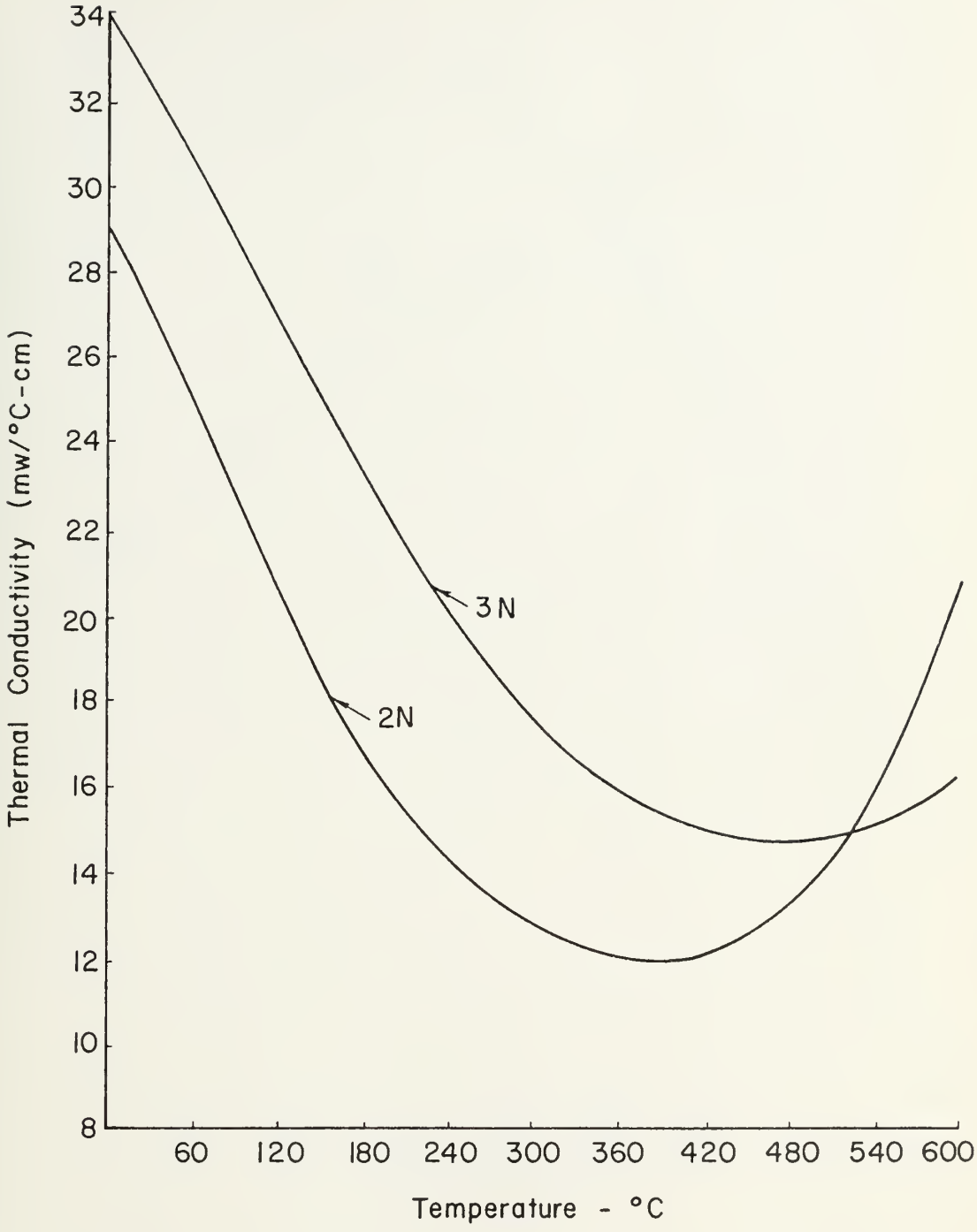

Figure 4.11 Thermal Conductivity of 2N and 3N Materials

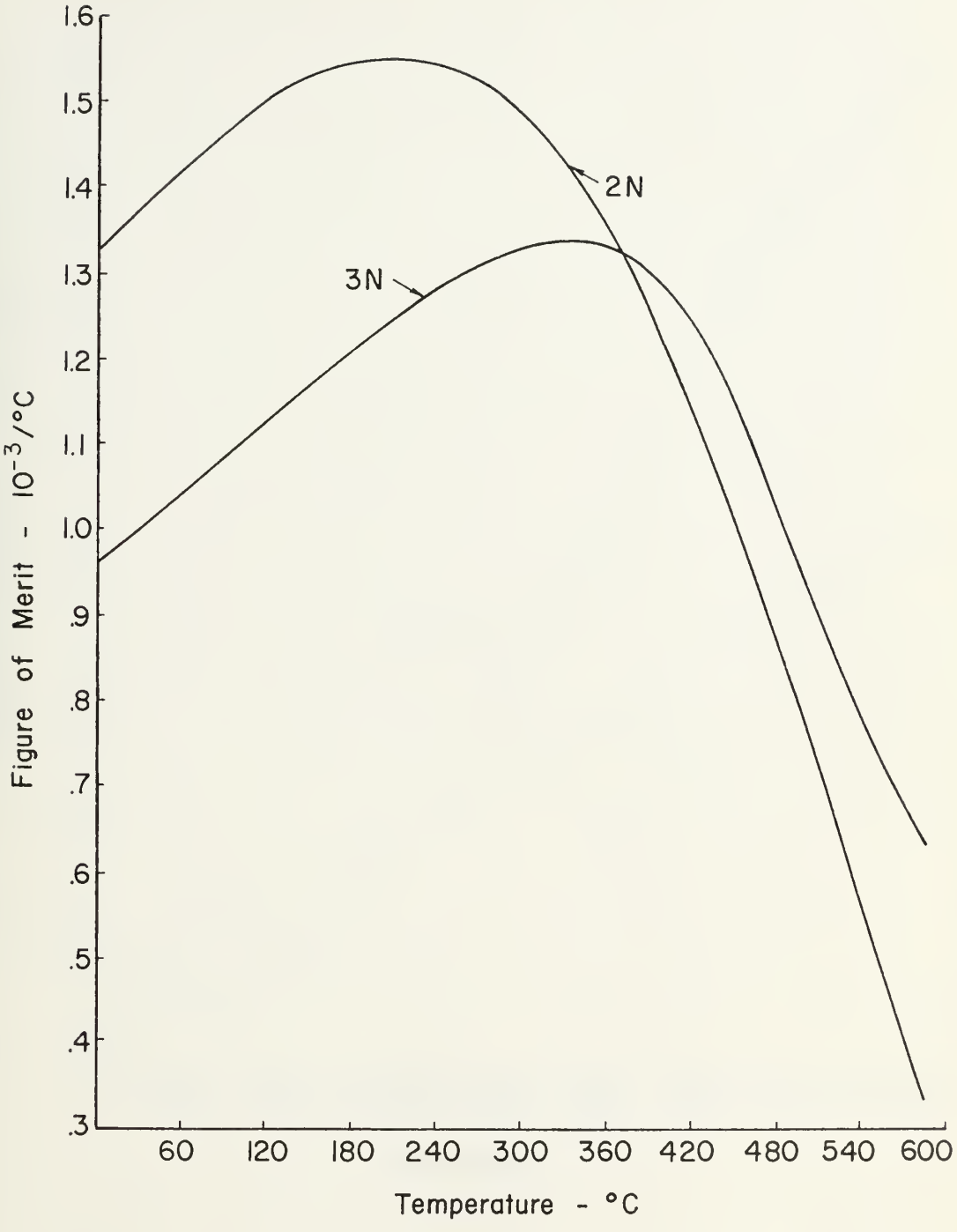

Figure 4.12 Figures of Merit of 2N and 3N Materials

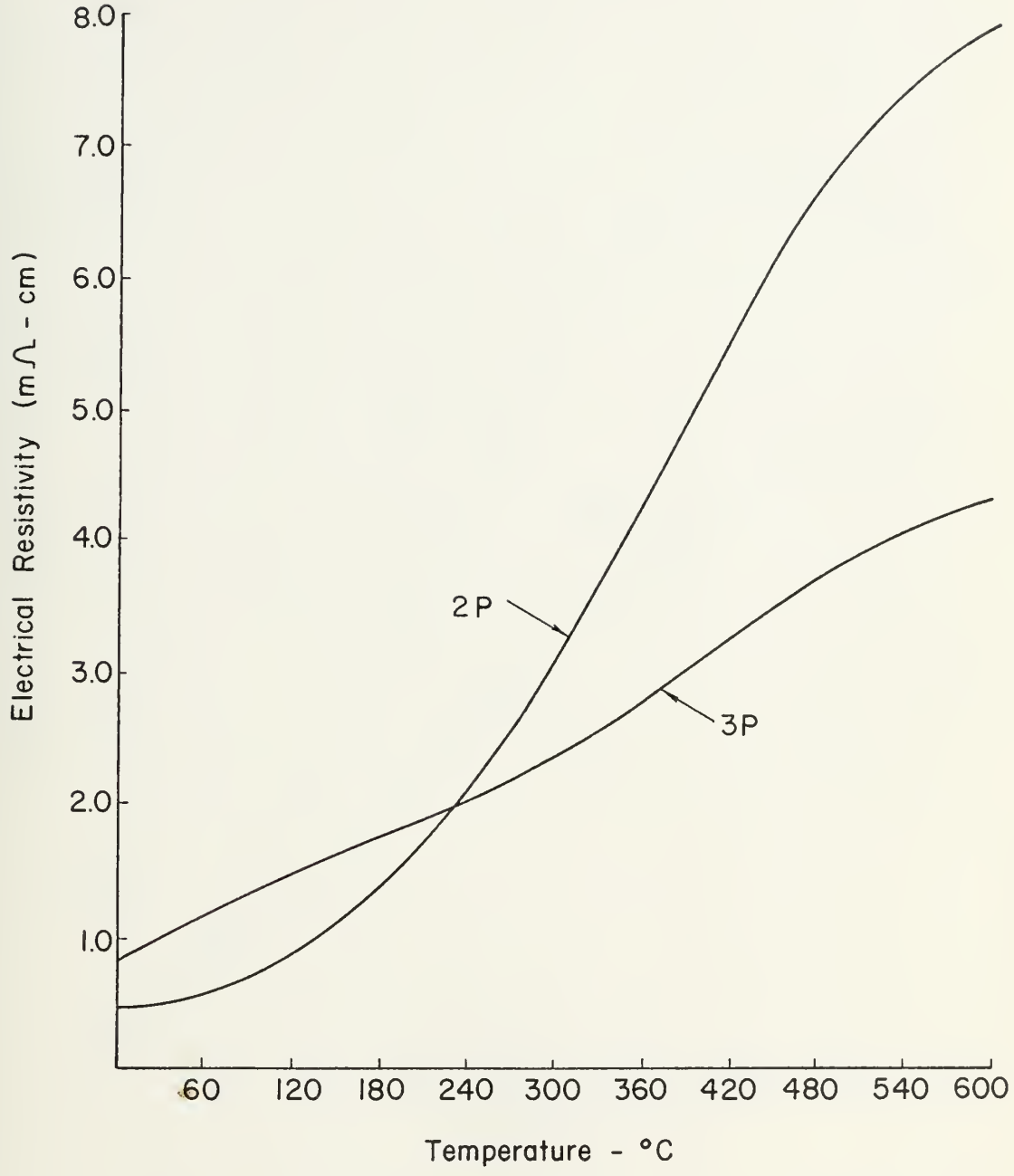

Figure 4.13 Electrical Resistivity of 2P and 3P Materials

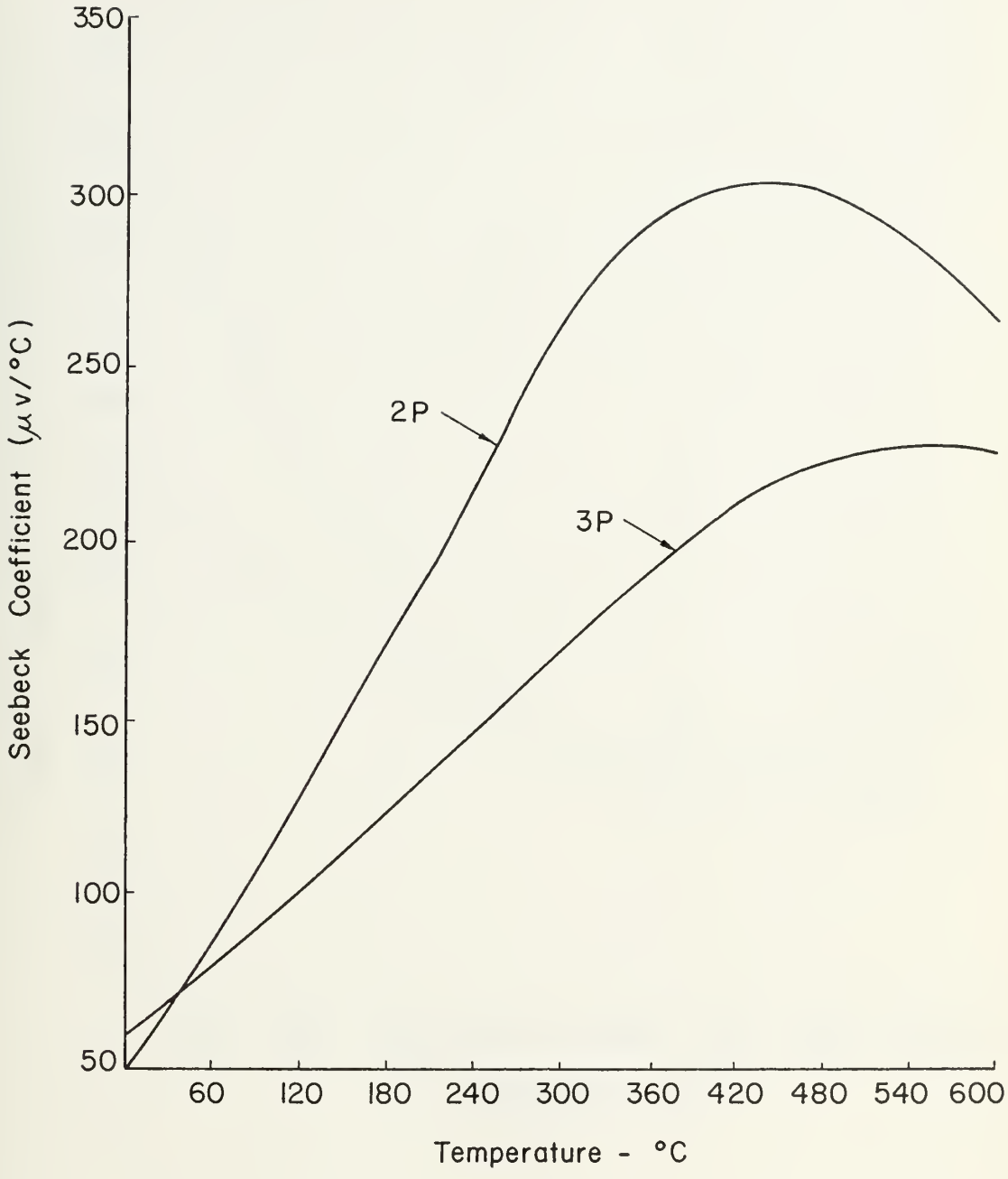

Figure 4.14 Seebeck Coefficient of 2P and 3P Materials

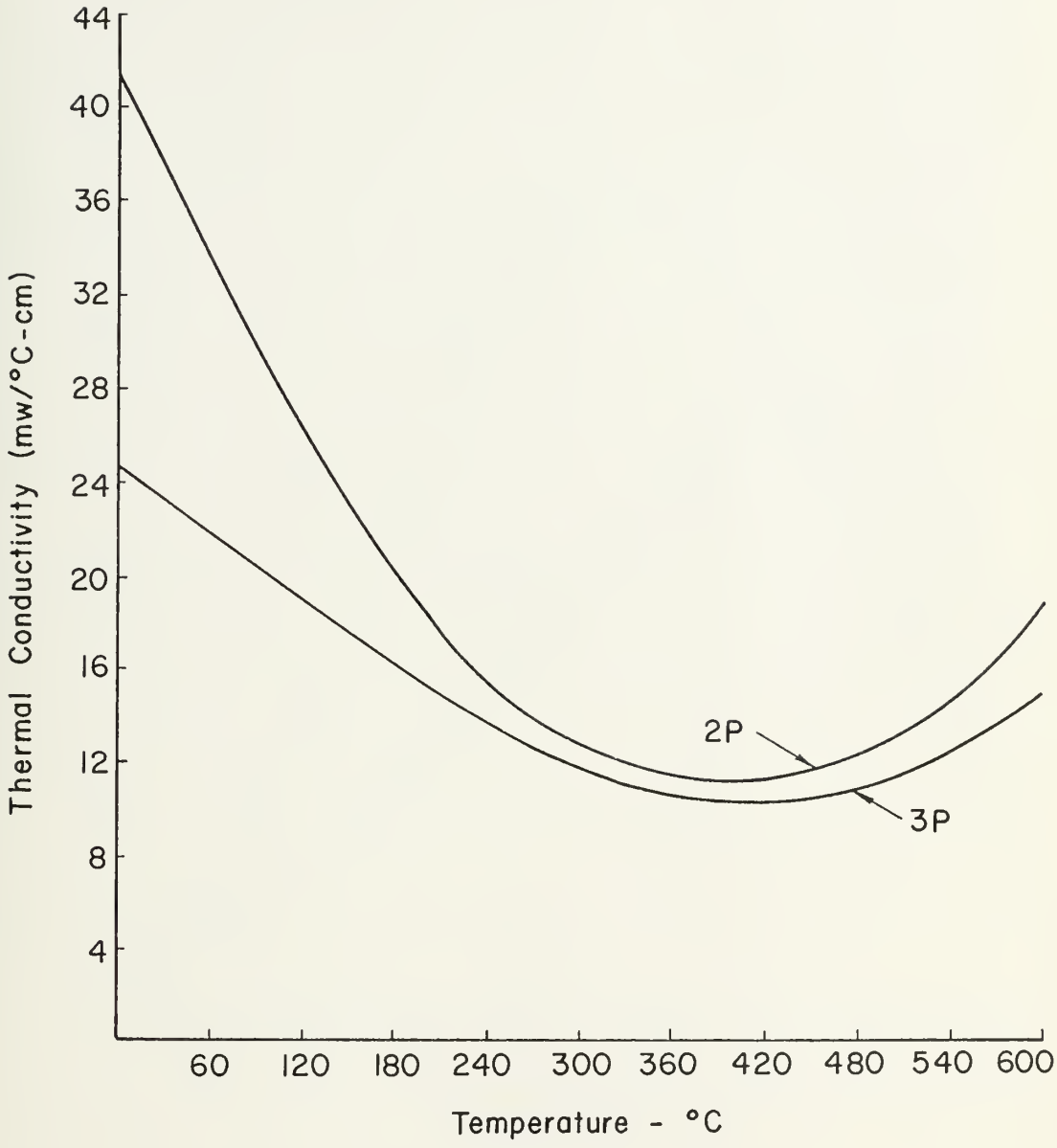

Figure 4.15 Thermal Conductivity of 2P and 3P Materials

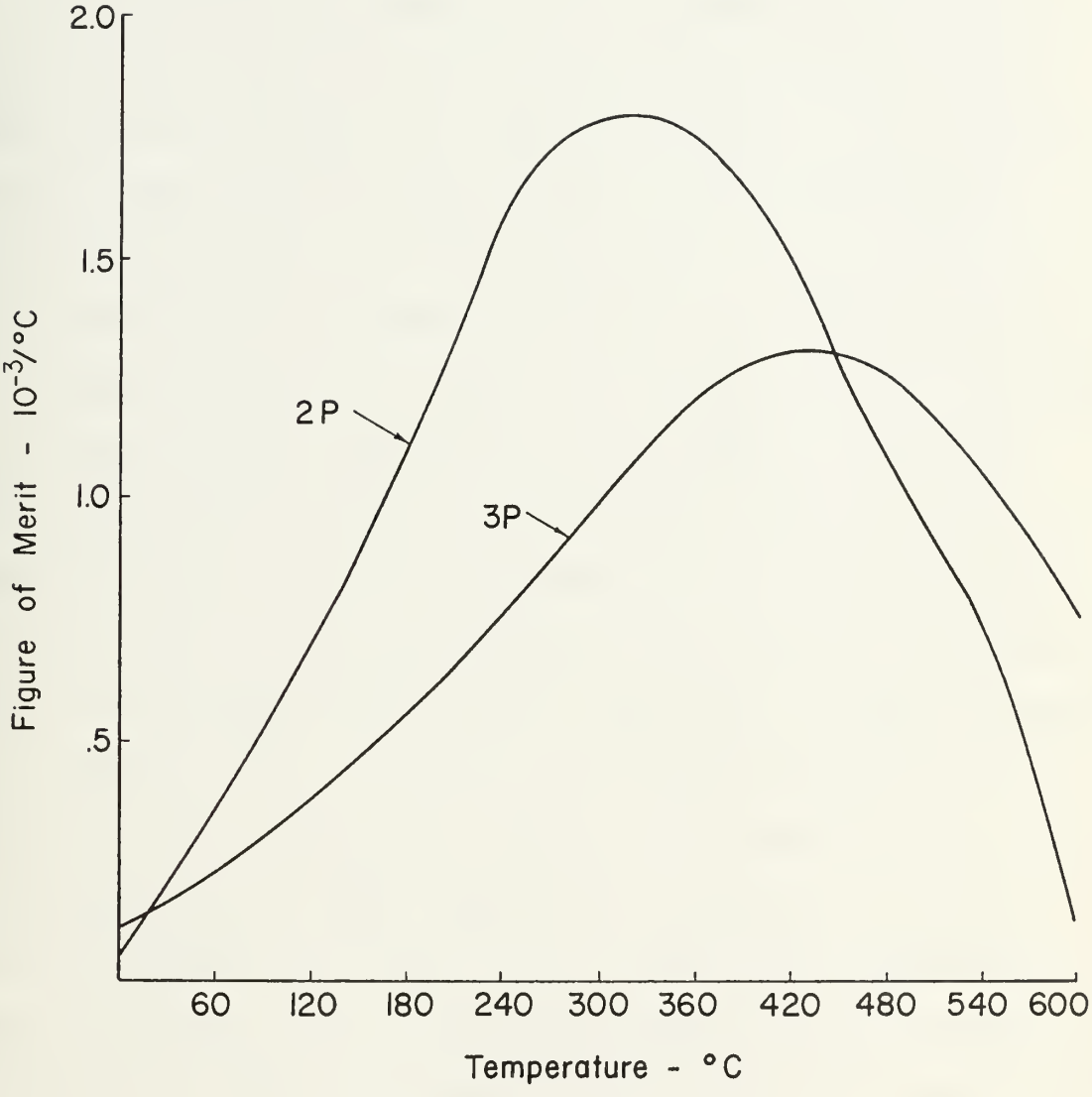

Figure 4.16 Figure of Merit of 2P and 3P Materials

times larger (~5000 psi)[21]. The latter value, as that of the silicon-germanium alloys, precludes the need of compressively loading a TAGS thermoelement while operating in an RTG.

TAGS is an undoped, inherently p-type material which has been manufactured by both casting and powder metallurgy techniques. The company (Teledyne Isotopes, Inc.) which is presently its sole producer uses the former method because it results in better thermoelectric properties (comparative data is not available)[46]. The as-cast structure of TAGS is not homogeneous. It consists of at least four different solid phases, descriptions of which are provided by McGrew[21]. Annealing the material increases homogeneity but slight amounts of individual phases still exist even after prolonged heating. This means that a certain degree of structural non-uniformity is present in the "as-fabricated" material. As mentioned earlier in this chapter, this generally leads to time dependent thermoelectric properties. For TAGS, the result is no different. Since the material continues to be annealed, effectively, while in the temperature gradient of an operating RTG, its metallurgical structure will change with time and hence its thermoelectric properties will change also. Note that these changes will occur irrespective of those caused by sublimation, foreign material contamination, or other "environmental factors" and thus cannot be eliminated through design. However, these "environmental factors" constitute the most significant degradation mechanisms for TAGS[46] and hence the material's performance as a function of operating time depends more upon the design of the RTG and how well it limits sublimation, etc. As discussed in section 4.1, under the circumstances

where the time dependency of the thermoelectric properties is more a function of design than of irreversible changes which occur in the material itself, it is impractical to present these properties as functions of time and therefore only initial data is given here.

4.3.2.3 Operational Considerations

As with the other thermoelectric materials used in the intermediate temperature range, the major problems encountered in the use of TAGS are sublimation, oxidation, and contacting electrodes.

Oxidation can be handled in the same manner as for the lead telluride materials but sublimation cannot. Because TAGS sublimes much more readily, it is necessary to employ additional or more sophisticated methods of sublimation suppression in order to prevent physical deterioration (and accompanying increases in electrical resistance) of the thermoelements and breakdown of the material with subsequent degradation of its figure of merit[47,48]. The techniques investigated thus far include[46]:

1. limiting the material's operating temperature to a value of approximately 405°C. In this way, a pressurized atmosphere alone sufficiently reduces sublimation;
2. surrounding the TAGS thermoelement with an inert material which will satisfactorily inhibit sublimation;
3. coating the material with a substance which will sufficiently decrease the rate of sublimation.

With respect to method (1), the hot junction temperature of the thermocouple may simply be limited to approximately 405°C. However,

this technique is unsatisfactory because the n-type materials (2N or 3N) normally used in conjunction with TAGS operate most efficiently with $T_H > 405°C$. Alternatively, the p-type thermoelement can be segmented[21,46]; that is, constructed of two different thermoelectric materials. In this way, the TAGS material can be located sufficiently far from the hot junction to limit its operating temperature to 405°C. A second material (e.g., SnTe) is then mated to the TAGS segment and spans the temperature range $405°C - T_H$. However, even though the performance of the n-type thermoelement is improved by this technique, that of the p-type element is still less than optimum. This is because in solving the sublimation problem, both techniques limit the temperature of TAGS to a value where the p-type thermoelement is forced to operate at less than maximum efficiency. The reason for this is that no p-type material is presently available which performs as well as TAGS over the range 405°C - 530°C, the latter being the maximum operating temperature of TAGS. Thus when TAGS is used over the range T_C - 405°C rather than T_C - 530°C in order to preclude sublimation, efficiency of the p-type thermoelement is sacrificed. It follows from this that if a means could be discovered which would allow TAGS to be operated up to 530°C without subliming at an unacceptable rate, the full thermoelectric potential of the material could be realized. Methods (2) and (3) listed above represent attempts to achieve this end.

With respect to method (2), at least two schemes have been tried. The first consists of wrapping that portion of the TAGS element or segment subject to sublimation with quartz or glass yarn. Problems were encountered with this scheme, however, because gaps developed between the windings where sublimation could again occur. Another

related technique stacks washers of Mo opacified, quartz paper around the TAGS element at temperature points where sublimation would occur. With this technique, it was found that TAGS could be safely operated up to 530°C.

Method (3), the use of coatings, has the advantages of resulting in a lighter thermoelement and one which is easier to construct. According to one industry source[46], this method is the most successful in limiting sublimation and allowing TAGS to be used at the higher temperatures in its operating range. The compositions of the coatings used are proprietary.

The other operational consideration to be discussed in this section is contacting electrodes. As explained above, TAGS is not always in direct contact with the electrode at the hot junction and therefore, this particular requirement doesn't always exist. However, when the hot junction temperature is on the order of 530°C or lower, one must contact an electrode directly to the TAGS material. In this regard, the type of bond utilized is metallurgical in nature (the specifics are proprietary)[46] and the electrode material may be W or Mo, for example. Stainless steel, iron, or nickel cannot be employed unless a diffusion barrier is placed between the electrode and thermoelement since these materials react strongly with TAGS to degrade its figure of merit. At the cold junction, a connection between TAGS and the electrode is always present. It can be made through a metallurgical bond or by proprietary soldering techniques[46]. Copper is usually employed as the cold junction electrode material.

4.3.2.4 Thermoelectric Property Data[49]

In this section, the initial thermoelectric properties of cast TAGS will be presented. Figures 4-17 through 4-20 give the electrical resistivity, Seebeck coefficient, thermal conductivity, and figure of merit, respectively--as all functions of temperature. Note that the resistivity is less than that of the PbTe materials over most of the temperature range shown and furthermore, it varies by only a factor of two, which is again less than that of the PbTe materials (compare Figures 4.9 and 4.13 with 4.17). This is the reason why TAGS has a significantly better figure of merit.

4.4 Low Temperature Thermoelectric Materials

4.4.1 Bismuth Telluride Alloys

4.4.1.1 Introduction

This section discusses the performance and considerations involved in the use of thermoelectric materials based on bismuth telluride, bismuth selenide, and antimony telluride. Because of their high figure of merit at low operating temperatures (27°C-300°C), alloys of these materials are used in thermoelectric cooling as well as in low power (~500 mw and below) terrestrial and undersea radioisotope thermoelectric generators. As mentioned in Chapter 3, alloys of Bi_2Te_3 and Bi_2Se_3 and those of Bi_2Te_3 and Sb_2Te_3 have proven to be the most efficient n and p-type materials, respectively. For the n-type material, the composition which is presently most widely employed is on the order of Bi_2Te_3 (80 m/o) and Bi_2Se_3 (20 m/o). The p-type material most commonly used is Bi_2Te_3 (25 m/o) and Sb_2Te_3 (75 m/o)[44]. These two

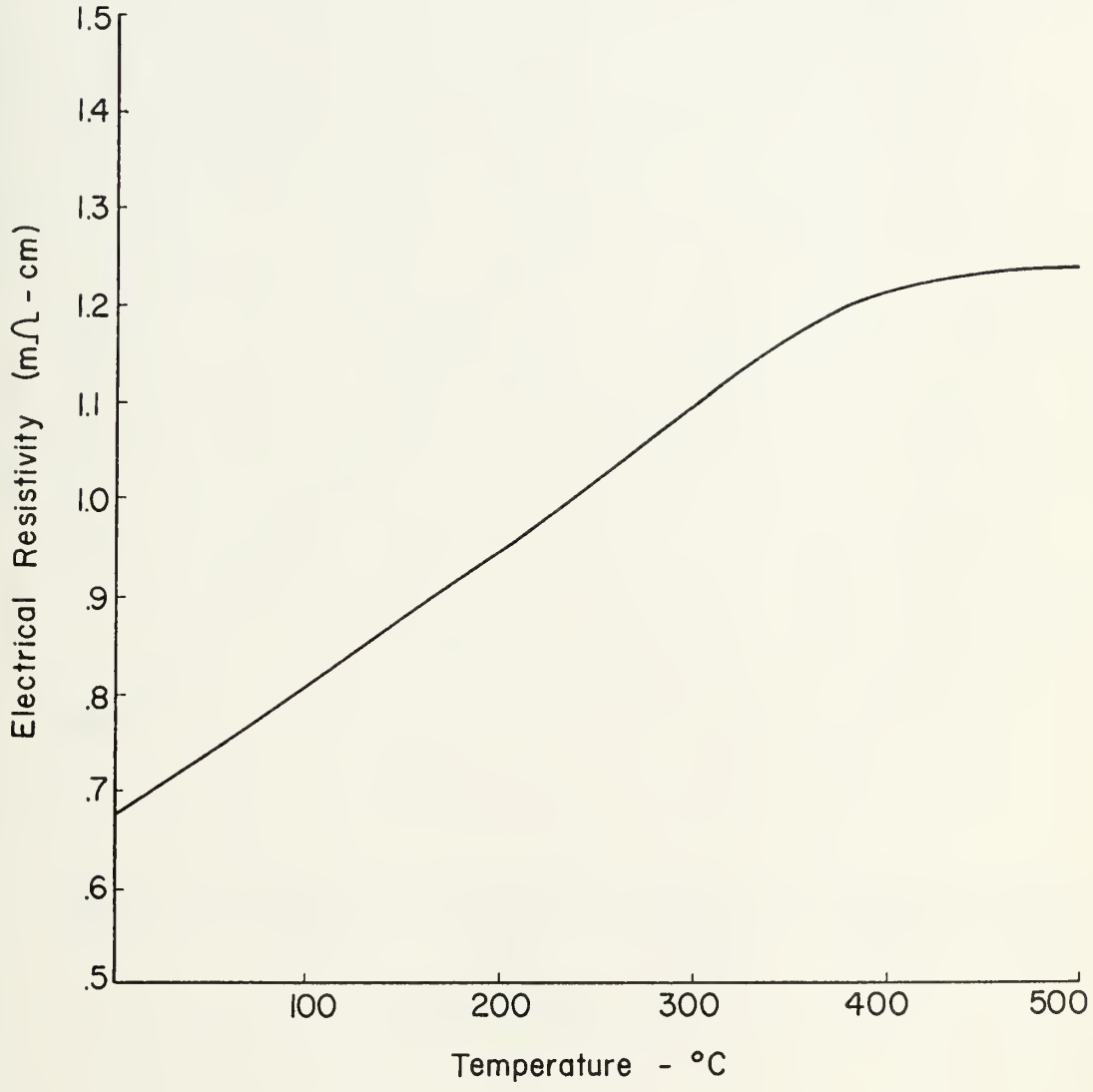

Figure 4.17 Electrical Resistivity of TAGS-85

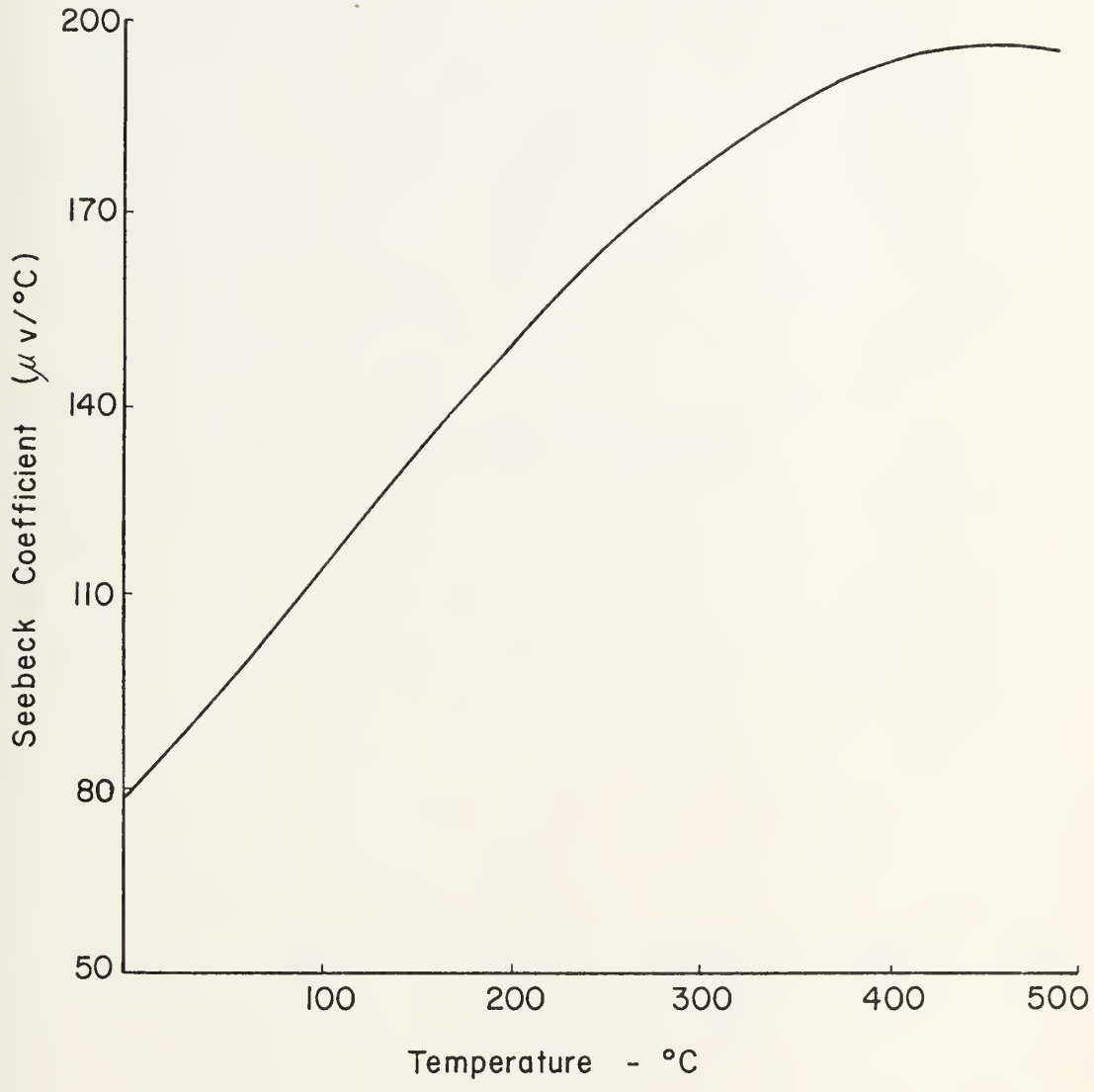

Figure 4.18 Seebeck Coefficient of TAGS-85

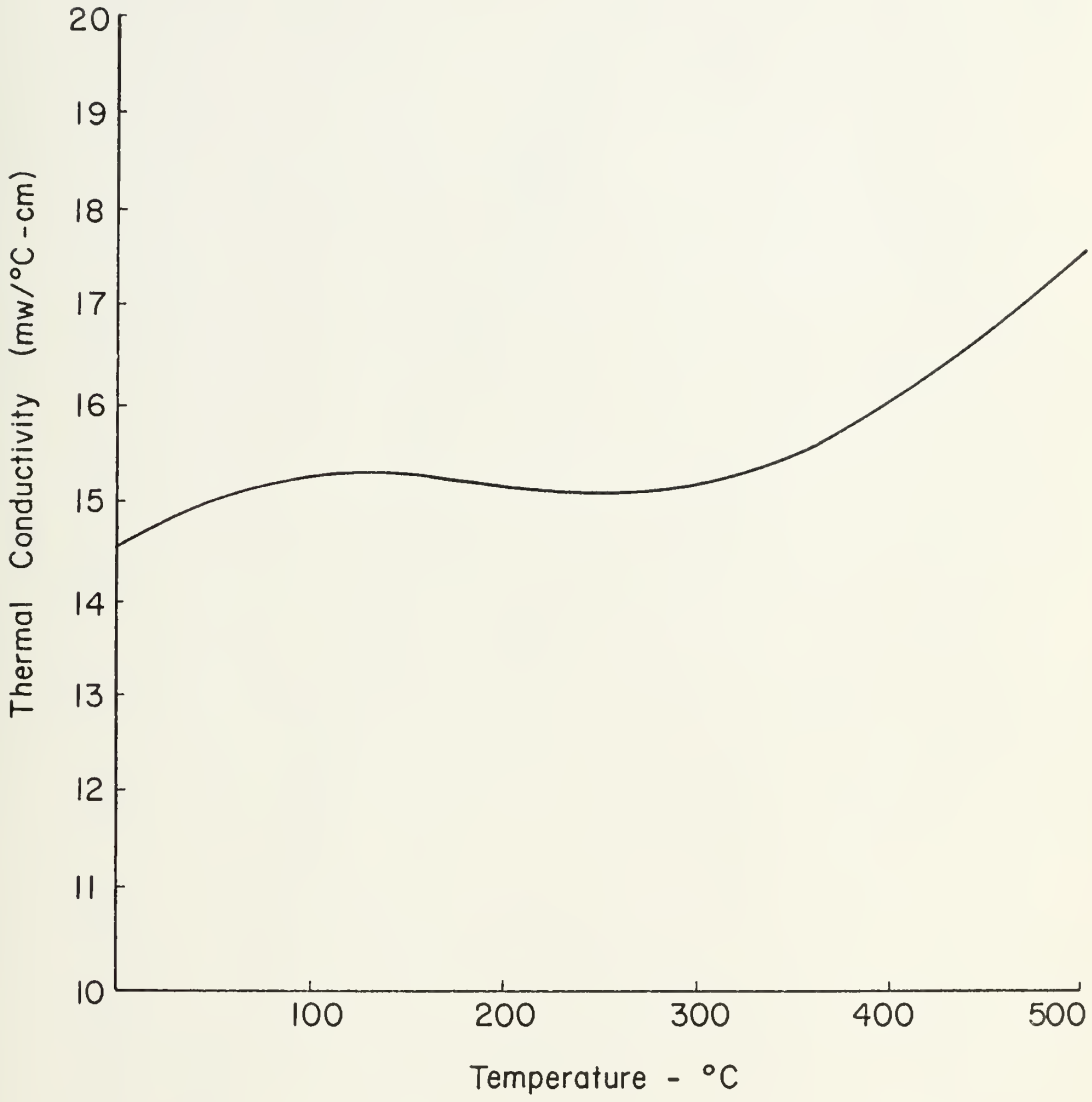

Figure 4.19 Thermal Conductivity of TAGS-85

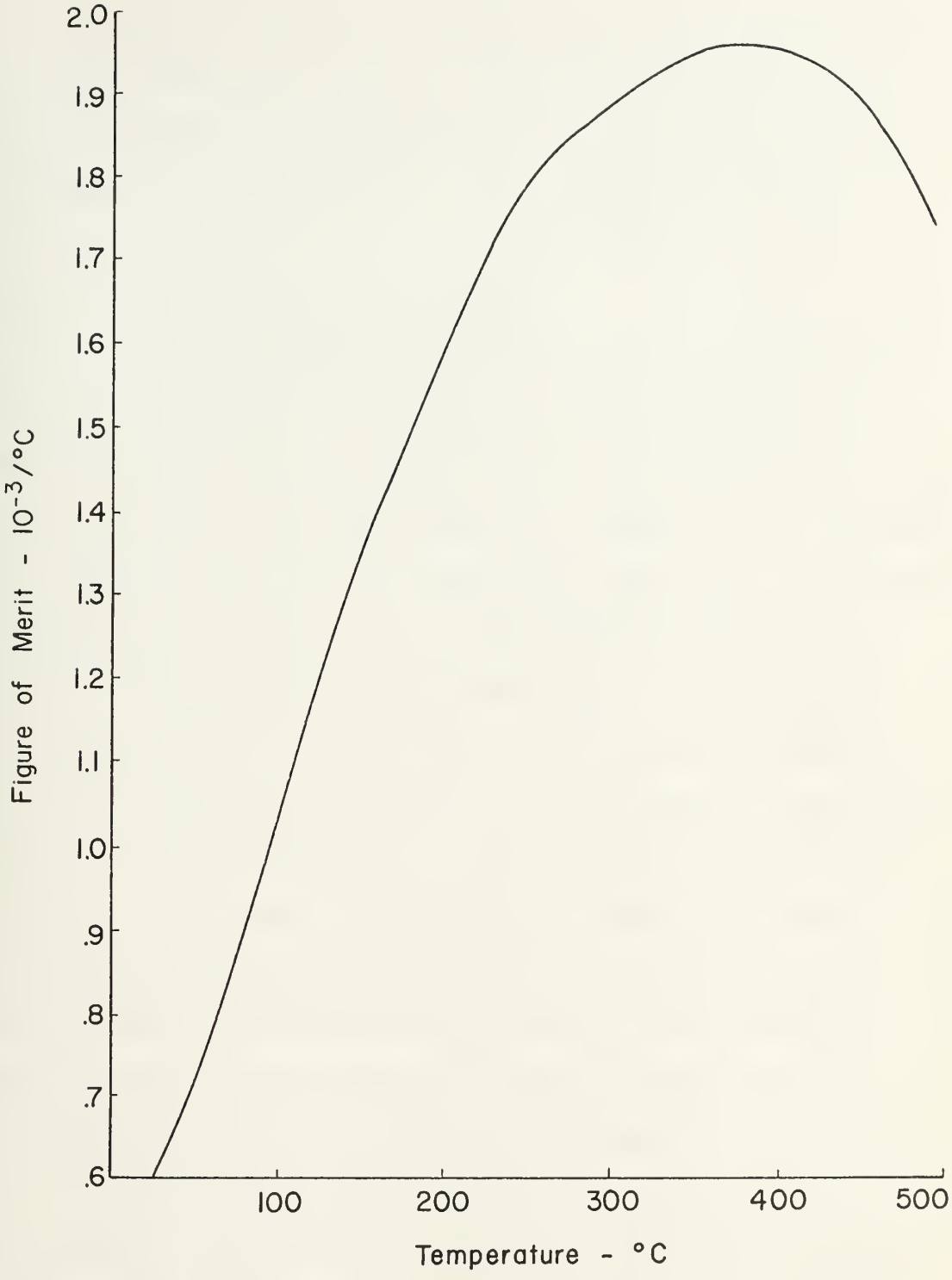

Figure 4.20 Figure of Merit of TAGS-85

alloys are employed to construct thermocouples which perform best at a hot junction temperature of 300°C. The reason why the above alloys are preferred to others is simply that when properly doped, they result in the maximum average figure of merit over the range of 27°C-300°C.

4.4.1.2 Fabrication Techniques

In order to understand the pros and cons of different fabrication techniques, one must understand the anistropic behavior of bismuth telluride crystals. Bismuth telluride has a tetradymite lattice structure in which the Bi and Te atoms are arranged in planar hexagonal layers perpendicular to the "C" crystal axis. Each layer contains only one kind of atom. In the unit cell, the layers are arranged[50]: Te_I-Bi-Te-Bi-Te_I-Te_I-Bi-Te-Bi-Te_I. (The subscript I is a means of identifying adjacent Te layers.) In alloys of Bi_2Te_3 and Sb_2Te_3 or Bi_2Se_3, the antimony and selenium atoms substitutionally replace bismuth and tellurium atoms, respectively. Hence, the same crystalline structure exists. As a result of the weak Van der Waal bonds between the Te_I-Te_I layers, the alloys have anisotropic or directional properties. This anisotropy is manifested in both mechanical and thermoelectric properties. The crystal cleaves very readily between the Te_I-Te_I layers or in other words, in a direction which is perpendicular to the "C" axis. The lattice thermal conductivity of n and p-type alloys is approximately 2.1 times as great parallel to these cleavage planes as when measured at right angles to them[15]. The ratio of the electrical conductivity when measured in a direction parallel to the cleavage planes to that when measured perpendicular to them is 2.7:1 for p-type alloys and 4.7:1 for n-type alloys[15]. Furthermore, even though the

Seebeck coefficient is isotropic for p-type material, in n-type it has a maximum value when measured in the direction of the cleavage planes[15]. It is concluded from the above that the maximum figure of merit will be obtained when the crystal is aligned such that its cleavage planes are parallel to the thermal gradient and the direction of current flow. This is most important in the n-type crystals. It is less so with the p-type, since, for the latter, the anisotropy in the thermal conductivity is nearly compensated for by that in the electrical conductivity. It can be seen from the above that because these crystals cleave very readily, single crystal thermoelements will result in a thermocouple which is very weak mechanically. Because of this problem, fabrication techniques have been directed towards producing polycrystalline alloys whose individual grains are optimally oriented (cleavage planes parallel to current flow). This improves mechanical strength since the grain boundaries inhibit the spread of cleavage cracks. Little change in the figure of merit obtainable with single crystals occurs as long as the individual grains are aligned properly. It should be noted at this point that because of the compensating effects of the anisotropy in their electrical and thermal conductivities, randomly oriented polycrystalline p-type alloys display essentially the same figure of merit as that found in optimally oriented single crystals[50]. Thus, as far as obtaining the best thermoelectric properties is concerned, the method of fabricating p-type thermoelements makes little difference. It is for the n-type alloys, because of the non-compensating effect of their anisotropic thermoelectric properties, that fabrication technique becomes extremely

important if the maximum figure of merit is to be obtained.

The principal methods of fabricating polycrystalline bismuth telluride alloys include vacuum casting with zone leveling, vacuum hot pressing, and Bridgman casting[37]. Vacuum casting followed by zone leveling and vacuum hot pressing were described in section 4.2.1.3. In Bridgman casting, the alloy is produced by encapsulating the elemental materials in a quartz container, then heating the capsule in a furnace at approximately 750°C, followed by mixing the molten mass until a homogeneous melt is obtained. The molten mixture is then directionally solidified by withdrawing the capsule from the bottom of the furnace at a rate of approximately 5mm/min. The resulting ingot or rod is a columnar growth of polycrystalline material.

Because not all of the above methods result in the same degree of cleavage plane alignment or mechanical strength, one must be cautious in choosing the fabrication technique to be employed. For Bridgman casting or vacuum casting with zone leveling, it is found that the individual grains are oriented with their cleavage planes parallel to the ingots' longitudinal axis (the growth direction)[15,37]. Thus thermoelements with the crystal orientation necessary for optimum thermoelectric properties can be easily cut from the resulting ingot. With vacuum hot pressing it has been found that the individual grains tend to rotate into an orientation where their cleavage planes are perpendicular to the pressing direction; however, this does not occur for all grains[44]. Thus it is necessary to align thermoelements prepared from hot pressed material such that the thermal gradient and current flow is perpendicular to the pressing direction. However, since the

individual grains are, to a certain degree, randomly oriented rather than all optimally aligned, the resulting thermoelectric properties will not be as good as those obtained with material prepared by the other two methods. Instead they will be some average between those obtained when the cleavage planes are all properly oriented and when the granular mixture is completely random. On the other hand, vacuum hot pressed material is more resistant to fracturing since the grain sizes obtainable are smaller.

It is impossible to generalize about when to use a particular fabrication technique because the matter is dependent upon the intended application of the RTG. That is, even though the Bridgman cast or zone leveled cast material will result in higher efficiency, it cannot be used in all applications because thermoelement size and strength requirements vary. Its use is generally limited to the larger cross sectional area thermoelements which can be fabricated, installed, transported, and generally "handled" without breakage. To give an idea of when hot pressed materials are used, the guidelines of one manufacturer can be cited[44]. When the RTG is employed in an application which requires thermoelements of cross sectional dimensions on the order of .76mm x .76mm or smaller (e.g., heart pacemaker power supplies, miniature batteries), hot pressed materials are employed. Otherwise, Bridgman cast alloys are used.

To summarize then, because of the anisotropic nature of bismuth telluride alloys, different fabrication techniques result in materials with different thermoelectric and mechanical properties. Alloys prepared by vacuum casting followed by zone leveling or Bridgman casting

result in optimum thermoelectric properties but are relatively weak. Those fabricated by vacuum hot pressing are stronger but do not attain as high a figure of merit. The decision on when to use the different techniques is a function of the RTG application and more specifically the required thermoelement size.

4.4.1.3 Dopants Employed

Neither the Bi_2Te_3 (25 m/o)/Sb_2Te_3 (75 m/o) alloy nor those on the order of Bi_2Te_3 (80 m/o)/Bi_2Se_3 (20 m/o) is basically intrinsic. This is due to the departure from stiochiometry which occurs when the material is fabricated. Undoped alloys of Bi_2Te_3 with Sb_2Te_3 are always p-type, regardless of composition, and those of Bi_2Te_3 with Bi_2Se_3 are p-type for Bi_2Se_3 content between 0 m/o and 30 m/o but n-type otherwise. As already stated, it has been found that the best p-type material for a hot junction temperature on the order of 300°C is Bi_2Te_3 (25 m/o)/Sb_2Te_3 (75 m/o) and the best n-type, Bi_2Te_3 (80 m/o)/Bi_2Se_3 (20 m/o). In view of the above it is obvious that the latter alloy must be doped to become n-type. It turns out that the other alloy must also be doped because its hole concentration is less than optimum (~5 x $10^{19}/cm^3$) when fabricated in the concentration Bi_2Te_3 (25 m/o)/Sb_2Te_3 (75 m/o). A number of acceptor impurities have been investigated for the p-type alloy. They include Cd, Sn, Na, Pb, Se, and excess Te. The most frequently employed are Pb or Se. Many donor impurities have also been considered. They include I, AgI, AgBr, Cu, and CuBr. According to Gordyakova, et al.[51], the figure of merit of the n-type alloys is highest when Cu, or compounds of copper

(principally CuBr), are used as doping agents than when other impurities (e.g., the halogens) are employed. More information on dopants can be found in the literature[9,51].

4.4.1.4 Operational Considerations

Problems encountered in the use of thermoelements fabricated from bismuth telluride alloys include oxidation, sublimation, and contacting electrodes--much the same as with the other thermoelectric materials discussed in this chapter. These alloys are susceptible to oxidation and sublimation at temperatures of approximately 250°C and higher. The adverse affects of each have been identified previously. In order to eliminate oxidation, the thermoelement assembly (module) is encapsulated within an inert atmosphere. The sublimation and electrode contacting problems are handled simultaneously by what has become a standard method of constructing modules consisting of bismuth telluride alloy thermoelements. Previously, electrodes and thermoelements were treated as two separate components and were joined together by soldering. The latter was possible at either junction because of the relatively low operating temperatures involved. Now, the electrode is no longer considered a separate component in the sense that it is fabricated before joined with the thermoelement. Instead, it is formed "in-situ." In this method of thermoelectric module construction[44], the required number of thermoelements are stacked on end, side by side, in their proper orientation to form a cube or parallelopiped array. Between each is a solid insulator (electrical and thermal) of the same height as each thermoelement. The entire assembly is also surrounded by insulation so that

what results looks like an egg crate constructed from insulation with thermoelements positioned in each of the openings. In this way, only the ends of the thermoelements are exposed and after they are capped with electrodes, sublimation no longer poses a problem.

The thermoelements are connected with electrodes in the following manner. A "pattern" or "shield" is positioned so that only the ends of elements which are to be connected and the area between each pair is exposed. (Thermoelements are joined in pairs; see Figure 1.1.) The entire end surface of the assembly then receives a layer(s) of molten electrode material by plasma arc spraying or vacuum deposition, for example. This material solidifies on the unshielded surfaces to form the electrodes which connect the individual thermoelements. In this way, the electrodes are created and connected to the thermoelements in the same process rather than being treated as a separate component and joined to the element through some means such as soldering. Obviously, the material deposited in the above manner must be metallurgically compatible with the bismuth telluride alloys. Tungsten and Mo form sufficiently stable contacts but Fe, Ta, and stainless steel, for example, react with the alloys to form intermettalic compounds at the interface[44]. This results in a brittle region which is susceptible to failure from mechanical shock and thermal cycling. As an example of what materials are actually employed in forming electrodes, one technique[44] plasma sprays a layer of Mo, 2-3 mil thick, over the surfaces to be covered in the manner described above. This is followed by a layer of aluminum approximately 20 mil in thickness. The Mo eliminates materials compatibility problems while the aluminum serves as a good electrical conductor.

4.4.1.5 Thermoelectric Property Data

This section presents the thermoelectric properties of commonly used n and p-type bismuth telluride alloys. The data is based on material samples which were either Bridgman cast or vacuum cast and then zone leveled. Thus, from a fabrication point of view, the properties presented here are optimum. Comparative data for hot pressed materials was not available. Figures 4.21-4.23 give the electrical resistivity, Seebeck coefficient, and figure of merit versus temperature for the p-type Bi_2Te_3 (25 m/o)/Sb_2Te_3 (75 m/o) alloy[52]. The material is doped with 1.75 w/o Se. For this alloy the average figure of merit over the temperature range 25-250°C is approximately 2.5×10^{-3}/°C. Figures 4.24-4.27 present the same data for the Bi_2Te_3 (80 m/o)/Bi_2Se_3 (20 m/o)[9] and Bi_2Te_3 (75 m/o)/Bi_2Se_3 (25 m/o)[44] n-type alloys. The alloy containing 20 m/o Bi_2Se_3 is doped with CuBr (.05 w/o) and the other, with CuBr (.06 w/o).

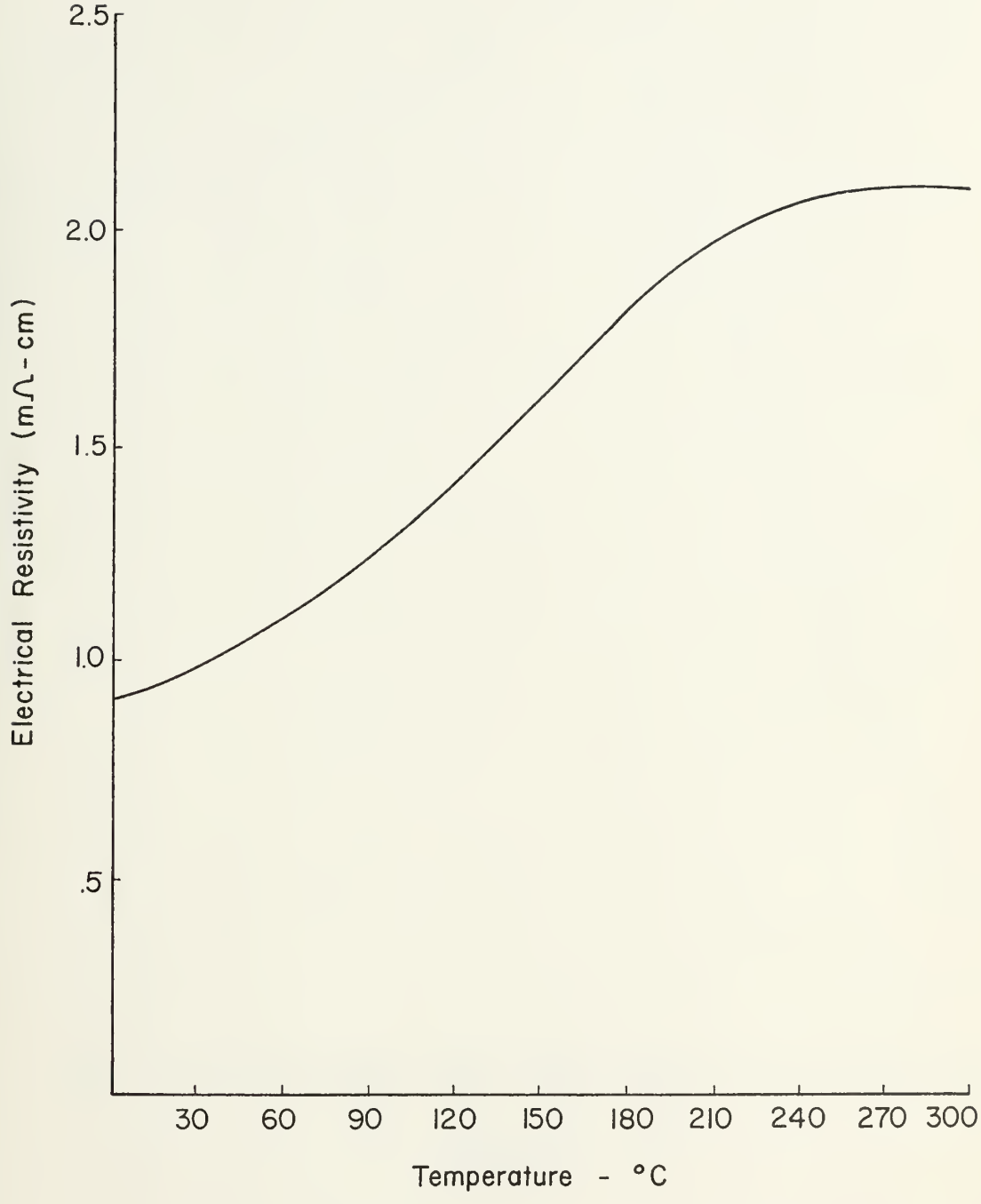

Figure 4.21 Electrical Resistivity of p-type Bi_2Te_3(25m/o)/ Sb_2Te_3(75m/o) Alloy

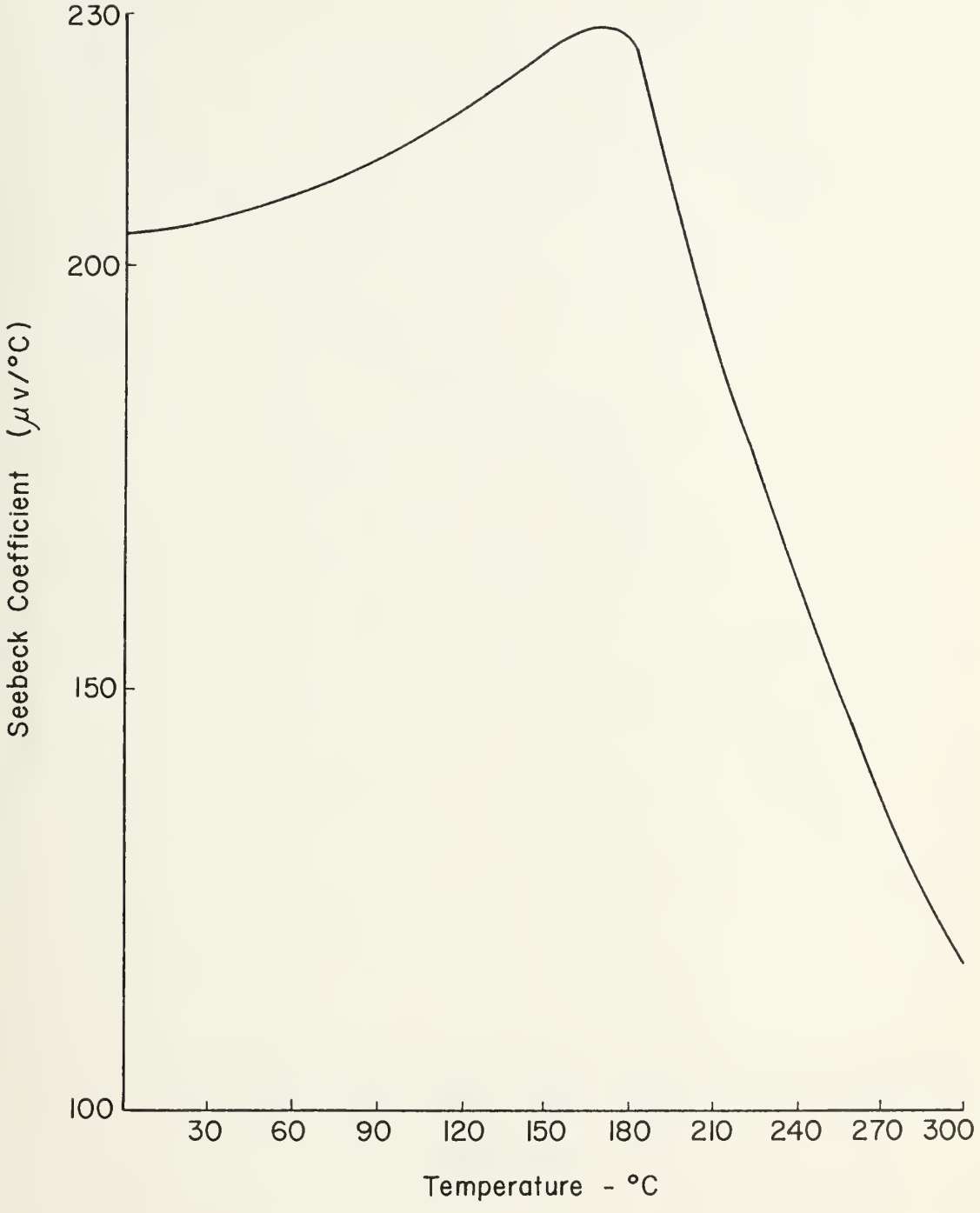

Figure 4.22 Seebeck Coefficient of p-type Bi_2Te_3(25m/o)/ Sb_2Te_3/Sb_2Te_3(75m/o) Alloy

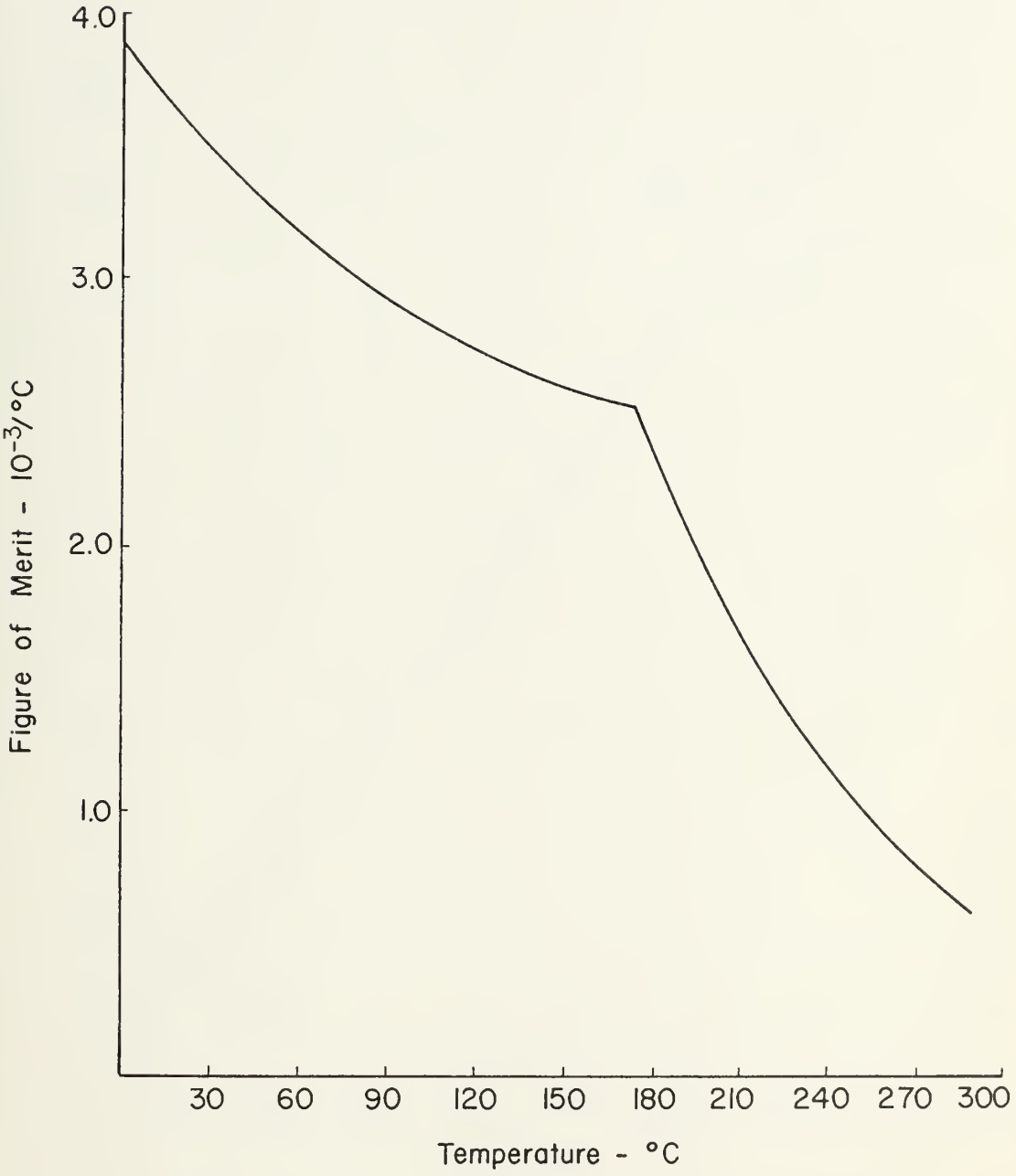

Figure 4.23 Figure of Merit of p-type Bi_2Te_3(25m/o)/Sb_2Te_3(75m/o) Alloy

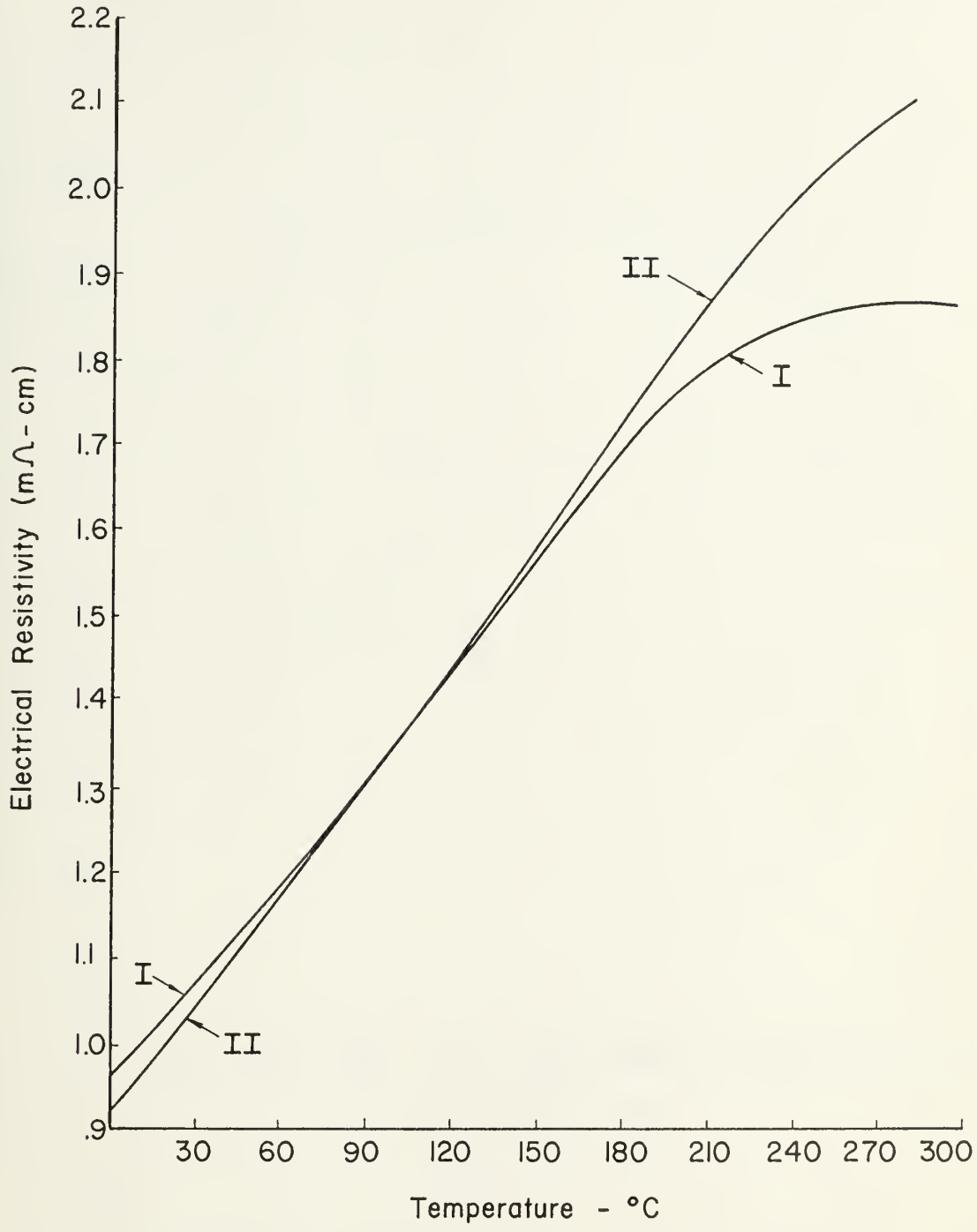

Figure 4.24 Electrical Resistivity of n-type:
(I) Bi_2Te_3(80m/o)/Bi_2Se_3(20m/o) and
(II) Bi_2Te_3(75m/o)/Bi_2Se_3(25m/o) Alloys

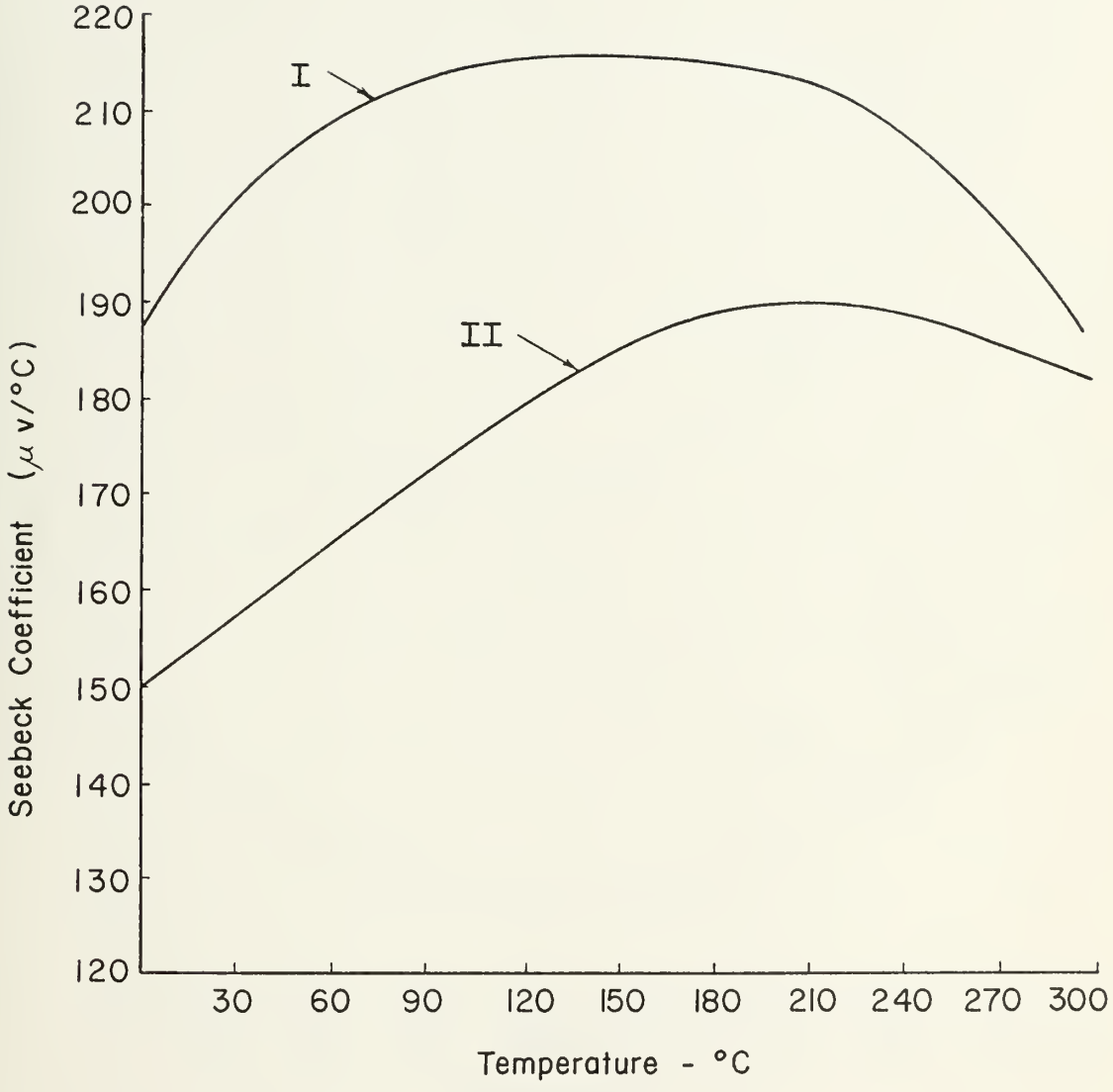

Figure 4.25 Seebeck Coefficient of n-type:
(I) Bi_2Te_3(80m/o)/Bi_2Se_3(20m/o) and
(II) Bi_2Te_3(75m/o)/Bi_2Se_3(25m/o) Alloys

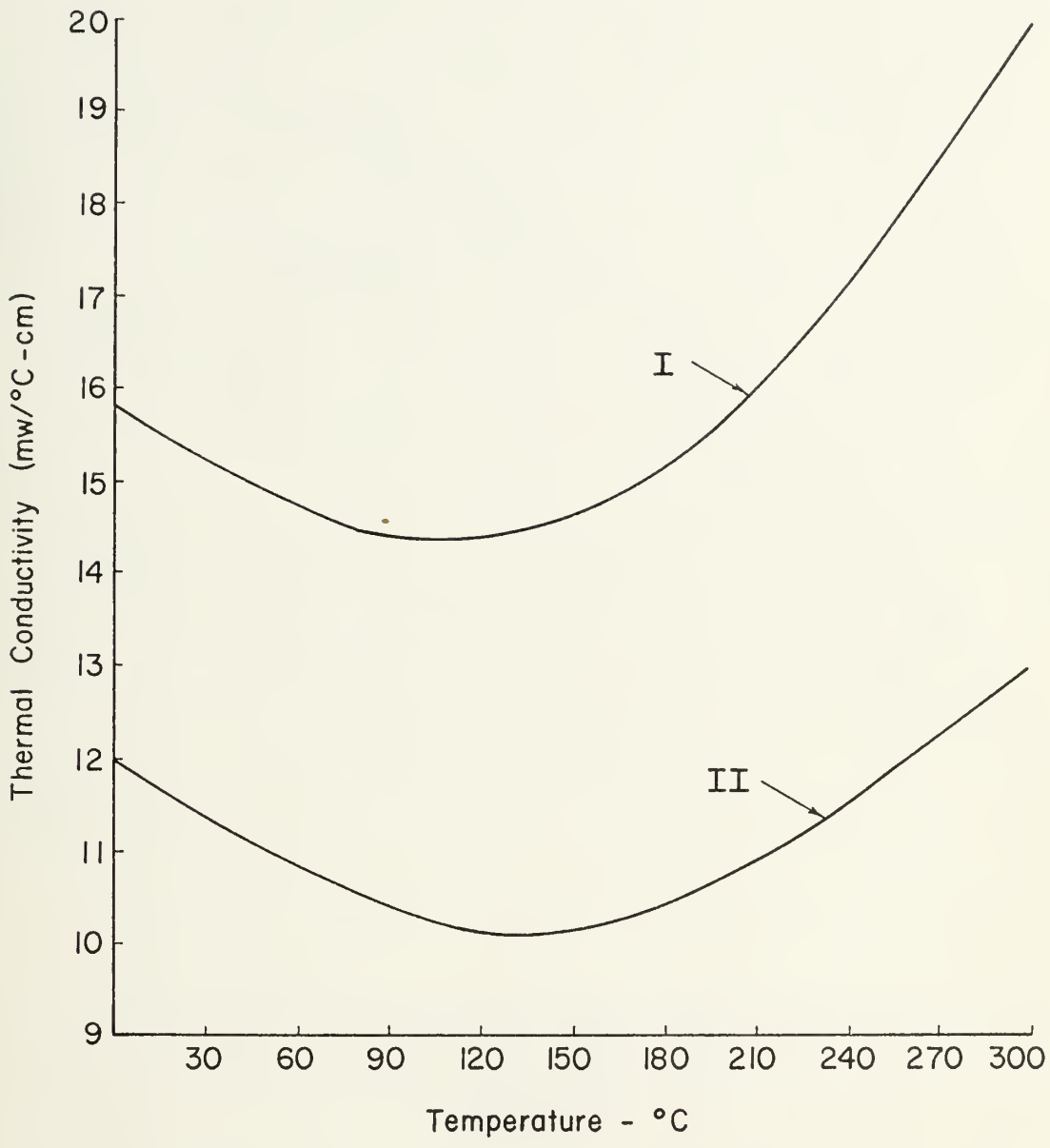

Figure 4.26 Thermal Conductivity of n-type:
(I) Bi_2Te_3(80m/o)/Bi_2Se_3(20m/o) and
(II) Bi_2Te_3(75m/o)/Bi_2Se_3(25m/o) Alloys

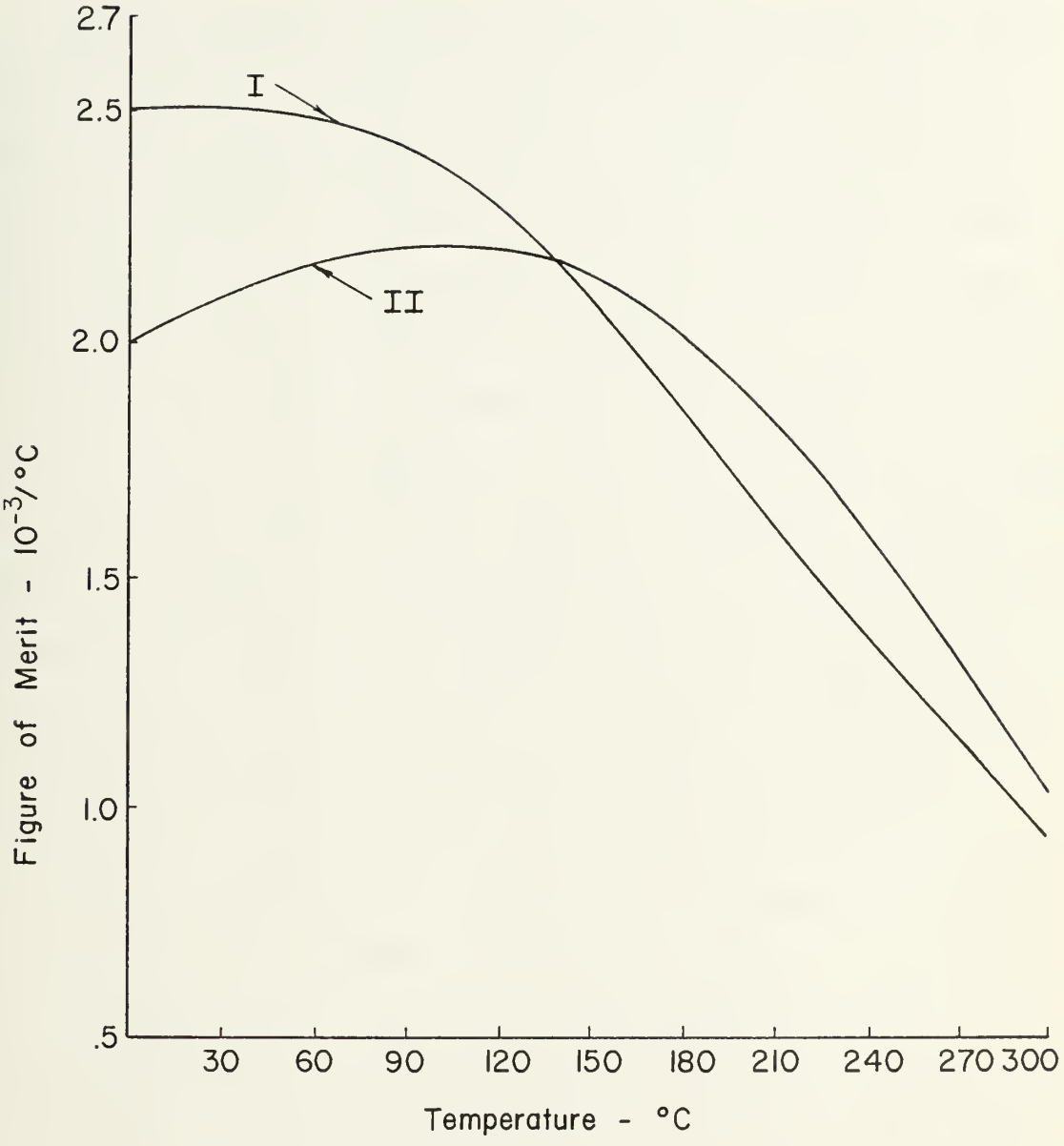

Figure 4.27 Figure of Merit of n-type:
(I) Bi_2Te_3(80m/o)/Bi_2Se_3(20m/o) and
(II) Bi_2Te_3(75m/o)/Bi_2Se_3(25m/o) Alloys

CHAPTER 5

SUMMARY

This paper presents a review of the thermoelectric materials most commonly employed in current radioisotope thermoelectric generator designs. The desirable characteristics of thermoelectric materials are first considered. It is shown that the best thermoelectric materials are those which possess large values of a performance parameter referred to as the figure of merit: $Z = \alpha^2\sigma/k$, where α is the Seebeck coefficient, σ the electrical conductivity, and k the thermal conductivity. Optimally doped semiconductors maximize the value of this parameter and result in more efficient generator performance than either metals or insulators. It is also explained why high mean atomic weight alloys of certain semiconductor elements and compounds generally perform better than other possible semiconductor materials. Operational considerations such as the temperature range over which the different materials should be employed and problems associated with oxidation and sublimation are discussed. The history of development of thermoelectric materials is reviewed. Semiconductor compounds of high mean atomic weight were first investigated as possible thermoelectric materials and later, alloys consisting of these compounds. Results of research efforts to develop thermoelectric materials with high figures of merit are summarized in tabular format.

Those thermoelectric materials which are presently the most commonly employed are reviewed individually. They are listed below according to the approximate temperature range over which they are normally employed:

A. High Temperature Applications (T_C-1000°C)

(1) n and p-type silicon (78a/o)/germanium (22a/o)

B. Intermediate Temperature Applications (T_C-600°C)

(1) n-type 2N and 3N lead telluride materials

(2) p-type 2P and 3P lead telluride materials

(3) p-type $AgSbTe_2$ (15m/o)/GeTe (85m/o)

C. Low Temperature Applications (T_C-300°C)

(1) n-type Bi_2Te_3 (75m/o)/Bi_2Se_2 (25m/o)

(2) n-type Bi_2Te_3 (80m/o)/Bi_2Se_3 (20m/o)

(3) p-type Sb_2Te_3 (75m/o)/Bi_2Te_3 (25m/o)

Dopants employed, fabrication techniques, and operational considerations such as sublimation suppression and electrode contacting are discussed for each material. Thermoelectric properties as a function of temperature (and time when possible) are presented graphically for each material also.

REFERENCES

1. Corliss, W. R. and D. G. Harvey. Radioisotopic Power Generation. Prentice Hall: Englewood Cliffs, New Jersey, 1964.

2. El-Wakil, M. M. Nuclear Energy Conversion. Intext Educational Publishers: New York, New York, 1971.

3. Rouklove, P. and V. Truscello. Thermoelectric Generators for Deep Space Application. NASA Technical Report 32-1495. Jet Propulsion Laboratory, California Institute of Technology, January 1971.

4. Raag, V. and V. Truscello. Status of Thermoelectric Power Conversion. Proceedings of the Sixth Annual Short Course on Thermoelectric Devices and Their Applications. University of Texas (Arlington), May 19-23, 1975.

5. Seebeck, J. Reports of the Prussian Academy of Sciences, 1822.

6. Peltier, M. Novelles Experiences Sur La Caloricité des Courans Electriques. Annales de Chemie et de Physique, Second Series, Volume 56, p. 371, 1834.

7. Thomson W. Phil. Transactions of the Royal Society, Volume 1, 1855.

8. Altenkirch, E. Über Den Nutzeffekt Der Thermosaüle. Physikalische Zeitschrift, Volume 10, p. 560, 1909; Electrochemical Refrigeration and Reversible Heating. Physikalische Zeitschrift, Volume 12, p. 920, 1911.

9. Heikes, R. R. and W. Ure, Jr. Thermoelectricity: Science and Engineering. Interscience Publishers: New York, New York, 1961.

10. Angrist, S. W. Direct Energy Conversion. Allyn and Bacon, Inc.: Boston, Massachusetts, 1971

11. Raag, V. Optimization of Thermoelectric Generators for Fixed Temperature and Fixed Heat Input Operations. Proceedings of the Sixth Annual Short Course on Thermoelectric Devices and their Applications. University of Texas (Arlington), May 19-23, 1975.

12. Fonash, S. J. Engineering Science 598 Lecture Notes. The Pennsylvania State University, University Park, Pennsylvania.

13. Raag, V. The Performance Characteristic of SiGe Alloys in Thermoelectric Applications. Proceedings of the Sixth Annual Short Course on Thermoelectric Devices and Their Applications. University of Texas (Arlington), May 19-23, 1975.

14. Wright, D. A. Thermoelectric Generation. In: Direct Generation of Electricity. K. H. Spring, ed. Academic Press: London, England, 1965.

15. Goldsmid, H. J. Applications of Thermoelectricity. Methuen and Company, Ltd.: London, England, 1960.

16. Kaye, J. and J. Welsh, eds. Direct Conversion of Heat to Electricity. John Wiley and Sons, Inc.: New York, New York, 1960.

17. Spring, K. H.,ed. Direct Generation of Electricity. Academic Press: London, England, 1965.

18. Goldsmid, H. J. Thermal Conduction in Semiconductors. Pergammon Press, 1961.

19. Summerfield, M., ed. Progress in Astronautics and Rocketry, Volume 3: Energy Conversion for Space Power. N. W. Snyder, ed. Academic Press: New York, New York, 1961.

20. Jasinski, R. J. and F. Wald. Study of Thermoelectric and Thermionic Power Conversion. Final Report, Contract N 00014-66-C-0147, Office of Naval Research, October 1967.

21. McGrew, J. W. A Report on the Properties and Performance of TAGS. Proceedings of the Intersociety Energy Conversion Engineering Conference, 1975.

22. Tubular Thermoelectric Module Development Program. Final Report WANL-PR(EEE)-058, Westinghouse Electric Corporation, March 1975.

23. Kelly, C. E. The MHW Converter (RTG). Proceedings of the Intersociety Energy Conversion Engineering Conference, 1975.

24. Telkes, M. J. Applied Physics, Volume 18, p. 1116, 1947.

25. Goldsmid, H. J. and R. W. Douglas. British J. Applied Physics, Volume 5, p. 386, 1954.

26. Ioffe, A. V. and A. F. Ioffe. Zhornal Tekhnicheskoi Fiziki, Volume 24, p. 1911, 1954.

27. Ioffe, A. V. and A. F. Ioffe. Akademiia Nauk SSSR.Doklady, Physics Section, Volume 98, p. 757, 1954.

28. Airapetyants, S. V. and B. A. Efimova. Zhornal Teknicheskoi Fiziki, Volume 28, p. 1768, 1958.

29. Ioffe, A. V., et al. Akademiia Nauk SSSR.Doklady, Physics Section, Volume 106, p. 981, 1956.

30. Rouklove, P. and V. Truscello. Thermoelectric Generators for Deep Space Application. NASA Technical Report 32-1495, Jet Propulsion Laboratory, California Institute of Technology, January 1971.

31. Carney, H. C. Comparison of Strontium-90 and Plutonium-238 Milliwatt Thermoelectric Generators. Proceedings of the Second International Symposium on Power from Radioisotopes, Madrid, 1972.

32. Raag, V. Thermoelectric Properties of SiGe Alloys as a Function of Time and Temperature. Memorandum No. 8, Contract 952808, Jet Propulsion Laboratory, California Institute of Technology, October 1970.

33. Raag, V. Research and Development of a SiGe Alloy. Final Report, NASA Contract NAS-5-3410, December 1963.

34. Dismukes, J. P., et al. Thermal and Electrical Properties of Heavily Doped Ge-Si Alloys up to 1300°K. J. Applied Physics, Volume 35, p. 2899, 1964.

35. Private Communication with Dr. V. Raag, Syncal Corporation, Sunnyvale, California.

36. Raag, V. The Time and Temperature Dependence of the Thermoelectric Properties of Silicon Germanium Alloy. Proceedings of the Inter-Society Energy Conversion Engineering Conference, 1975.

37. Hogarth, C. A. Materials Used in Semiconductor Devices. Interscience: New York, New York, 1965.

38. Baughman, R. J., et al. Preparation of Hot Pressed SiGe Ingots. Part I: Chill Casting of Se-Ge Alloys. Material Research Bulletin, Volume 9, No. 5, p. 685, 1974.

39. Pfann, W. G. Zone Melting. John Wiley and Sons: New York, New York, 1966.

40. Lefever, R. A., et al. Preparation of Hot Pressed SiGe Ingots. Part III: Vacuum Hot Pressing. Material Research Bulletin, Volume 9, No. 7, p. 864, 1974.

41. Nastoy, R. P. and E. L. Burgess. Precipitation of Dopants in SiGe Thermoelectric Alloys. J. Applied Physics, Volume 43, p. 2908, 1972.

42. Raag, V. The Time and Temperature Behavior of the Thermoelectric Properties of 78a/o Si/22a/o Ge Alloys. To be presented at the 1976 Intersociety Energy Conversion Engineering Conference.

43. Private Communication with Mr. D. Peterson, Global Thermoelectric Power Systems, Ltd., Bassano, Alberta, Canada.

44. Private Communication with Mr. N. B. Elsner, General Atomic Company, San Diego, California.

45. Hiser, B., et al. Thermoelectric Generator Design Manual, INSD-7089-1, Teledyne Isotopes, Timonium, Maryland.

46. Private Communication with Mr. R. Hannah, Teledyne Isotopes, Inc., Timonium, Maryland.

47. Elsner, N. B., et al. Radioisotope Space Power Generator Report. GA-A12848, General Atomic Company, San Diego, California, March 1974.

48. Elsner, N. B., et al. AEC Research and Development Report. GA-11005, Gulf General Atomic Company, San Diego, California, September 1972.

49. Waddoups, I. G. Effects of Load Conditions on Long Term Radioisotope Thermoelectric Generator Operation. SC-RR-70-854, Sandia Laboratories, Albuquerque, New Mexico, December 1970.

50. Goldsmid, H. J. and F. A. Underwood. Study of Orientation in Polycrystalline Bismuth Telluride Alloys. Advanced Energy Conversion, Volume 1, p. 297, 1968.

51. Gordyakova, et al. Investigation of Thermoelectric Properties of Solid Solution Bi_2Te_3-Bi_2Se_3. Soviet Physics-Technical Physics, Volume 3, p. 1, 1958.

52. Rosi, F. P., et al. Semiconducting Materials for Thermoelectric Power Generation. RCA Review, Volume 22, p. 82, 1961.

Thesis
V825 Vogt
160557
A review of thermo-electric materials used in radioisotope thermo-electric generators.